TECHNISCHE UNIVERSITÄT MÜNCHEN
Lehrstuhl für Humanbiologie

Diverse functions of Stat3 in intestinal epithelial cells during inflammation-associated and sporadic carcinogenesis

Julia Bollrath

Vollständiger Abdruck der von der Fakultät Wissenschaftszentrum Weihenstephan für Ernährung, Landnutzung und Umwelt der Technischen Universität München zur Erlangung des akademischen Grades eines

Doktors der Naturwissenschaften

genehmigten Dissertation.

Vorsitzender: Univ.-Prof. Dr. D. Haller
Prüfer der Dissertation: 1.   Univ.-Prof. Dr. M. Schemann
                               2.   Priv.-Doz. Dr. F. R. Greten
                               3.   Univ.-Prof. Dr. B. Küster

Die Dissertation wurde am 28.04.2010 bei der Technischen Universität München eingereicht und durch die Fakultät Wissenschaftszentrum Weihenstephan für Ernährung, Landnutzung und Umwelt am 03.10.2010 angenommen.

TABLE OF CONTENTS

1. Introduction

As the median survival of the population increases, the lifetime risk of developing cancer does as well. This development is further accelerated by changes in environmental and life-style derived factors which contribute to tumor development. Well-known predisposing factors include smoking as a risk-factor for the development of lung cancer, excessive UV-exposure as a risk-factor for the development of melanoma or an unbalanced nutrition leading to obesity which has been shown to increase the risk of developing different cancer types (Aggarwal et al., 2009b). Cancer development can be divided into three distinct steps (Hanahan and Weinberg, 2000), during the initiation step the cells acquire DNA mutations either spontaneously or by chemical or physical mutagens which lead to the inactivation of tumor suppressor genes or to the activation of oncogenes. To date there are different mutations known which predispose to the development of different cancer types. The initiated cells divide unregulated during tumor promotion due to a dysregulation in their genetic program governing proliferation and apoptosis. This promotion phase of tumorigenesis can be further accelerated by inflammatory cytokines. During recent years the significance of a proinflammatory tumor microenvironment has been recognized during tumor promotion, but as well as an initiating cause of cancer development (Grivennikov et al., 2010), for example in hepatocellular carcinoma (Schütte et al., 2009), gastric cancer (Chao & Hellmich, 2010) or colorectal cancer (Wu et al., 2009). In the last step of tumor progression the cells acquire additional mutations leading to invasion of surrounding tissue and possibly to metastasis. As general hallmarks of malignant cells different traits have been described: evasion from apoptotic signals, self-sufficiency in growth signals, insensitivity to anti-growth signals, limitless replicative potential, an increase in angiogenesis and tissue invasion and metastasis (Hanahan & Weinberg, 2000).

1.1 Role of the tumor microenvironment in cancer development

Growing evidence provides a link between inflammation and carcinogenesis, suggesting that not only chronic inflammation predisposes to the development of malignant disease, but also that genetic events causing neoplasia as well lead to the expression of inflammation-related programs establishing an inflammatory microenvironment. Therefore cancer-related inflammation has been proposed to be the seventh hallmark of cancer (Colotta et al., 2009).

The tumor microenvironment is composed of a heterogeneous mixture of cell types. This includes fibroblasts, cells of the innate immune system such as macrophages, neutrophils, natural killer (NK) cells, mast cells and dendritic cells (DC), as well as cells of the adaptive immune system, such as T-and B-cells; the mixture is completed by endothelial cells (deVisser et al., 2006).

The origin of fibroblasts in the tumor stroma is not yet clearly defined, these cells could result from epithelial to mesenchymal transition of tumor parenchyma, but could as well result from bone-marrow derived cells which are recruited from the circulation to the tumor microenvironment where they differentiate into fibroblast-like cells; resting fibroblast from the normal tissue could as well get activated at the tumor site (Spaeth et al., 2009). These tumor-associated fibroblasts have been shown to play an important role during tumor formation, growth and metastasis. For example in a study analyzing the correlation between the degree of tumor-associated fibroblast infiltration in colorectal cancer and the period of disease-free survival, a negative correlation for this marker could be shown (Tsujino et al, 2007).

Tumor-associated fibroblasts are a potent source of different cytokines, such as Interleukin (IL)-6, Vascular Endothelial Growth Factor (VEGF) and Transforming Growth Factor (TGF)-β (Silzle et al., 2004; Spaeth et al., 2009), thereby shaping the activation profile of other components of the tumor microenvironment. Furthermore they are responsible for the secretion of proteases such as matrix-metalloproteinases (MMP) 2 and 3, as well as pro-metastatic factors chemokine ligand C-C motif (CCL)-5 and chemokine ligand C-X-C motif (CXCL)-12/14, which have been shown to be important for the recruitment of bone-marrow derived cells and immune cells into the tumor (Östman and Augusten, 2009; Tsujino et al., 2007). In a recent study, loss of the tumor suppressor *Pten* specifically in stromal fibroblasts led to an acceleration of tumor initiation and promotion in a mouse model of mammary epithelial tumorigenesis by

regulation of the remodelling of the extracellular matrix, innate immune cell infiltration and angiogenesis (Trimboli et al., 2009).

The cells of the innate immune system can have favourable, but also unfavourable effects on tumor development. Tumor associated macrophages (TAMs) are mainly associated with tumor promoting effects (Solinas et al., 2009). They often represent together with T-cells the main class of tumor infiltrating immune cells (Sica et al., 2008) and are recruited to the tumor site by tumor cell derived CCL-2 and different other chemokines (Balkwill, 2004; Pollard, 2004; Mantovani et al., 2006). TAMs show a M2-like activation profile characterized by secretion of high amount of IL-1 and IL-6 and impaired antigen-presenting ability (Sica et al, 2008). Tumor cell invasion and metastasis are fueled by TAMs by secretion of different MMPs as well as by factors facilitating angiogenesis (Siveen und Kuttan, 2009). A high number of infiltrating TAMs in different tumor types has been associated with a poor prognosis (Murdoch et al., 2008).

Another cell type of the innate immune system whose activation profile is shaped by the tumor microenvironment, is represented by tumor associated neutrophils. In the presence of TGFβ signaling, neutrophils were shown to have an unfavourable effect on tumor growth and intra-tumoral CD8-T-cell activation (Fridlender et al., 2009). The blockade of this signaling pathway turned neutrophil infiltration of the tumor into a favourable event, illustrated by an influx of tumor-associated neutrophils which were more cytotoxic to tumor cells and secreted higher levels of proinflammatory cytokines (Fridlender et al., 2009). Neutrophils are recruited to the tumor environment mainly by CXCL-8 (Xie et al., 2001), as well as by CXCL-5 and 6 (Wislez et al., 2004; Gijsbers et al., 2005). They are involved in the generation of reactive oxygen species, which can lead to an increase in genomic instability, as demonstrated for *Tp53* mutations (Yu et al., 2002). Additionally neutrophils are believed to play a potent role in tumor angiogenesis by stimulating the tumor cells to secrete VEGF. Additionally they secrete Tissue Inhibitors of Metallo-Proteinase (TIMP)-free MMP 9 leading to the remodeling of the extra-cellular matrix and the release of bound pro-angiogenic factors VEGF and Fibroblast Growth Factor (FGF)-2 (Tazzyman et al., 2009).

DCs belong to the innate immune system, but represent together with macrophages and B-cells the class of antigen-presenting cells, thereby activating the cells of the adaptive immune system. Dendritic cells are the most potent antigen-presenting cells among the three groups and are responsible for the induction of adaptive anti-tumor immune

responses, but as well for the induction of tolerance to established tumors (Chaput et al., 2008). Traditionally the main role of tumor-associated DCs was believed to be the uptake of apoptotic tumor cells and the presentation of tumor associated-antigens to CD8$^+$ and CD4$^+$- T-cells, as well as the secretion of activating cytokines such as IL-12, IL-15 and IL-18 which lead to the activation and proliferation of natural killer cells (Ullrich et al., 2008). Quite recently it has been shown by different groups that a special subset of DC, called killer DCs, is capable of directly killing tumor cells (Chan and Housseau, 2007; Taieb et al., 2006). On the other hand, tumor-derived IL-10 was shown to modulate antigen-presentation by DC to induce anergy (Steinbrink et al., 1999) to tumor antigens. Differentiation of DC can as well be impaired by tumor-derived IL-6, leading to a predominant differentiation of monocytes into macrophages instead of DC (Chomarat et al., 2000).

NK cells, cytotoxic CD8$^+$ T-cells and T-helper cells are the main components of the anti-tumor immune response. NK cells can be directly activated by cell surface molecules and are not dependent on activation by antigen-presenting cells. For example the NKG2D receptor of human NK cells binds directly to the stably expressed proteins MICA/B which are upregulated in response to cellular stress as exerted by infection with *Mycobacterium tuberculosis*, but are as well upregulated in human lung, breast, prostate and colon carcinoma. This overexpression leads to recognition, secretion of Tumor Necrosis Factor α (TNFα), Interferon-γ (IFNγ) and other chemokines and direct killing of the cell (Backström et al., 2004). Natural killer cells recognize tumor cells by their down-modulated expression of Major Histocompatibility Complex (MHC) class-I which is sensed by the lack in binding of inhibitory NK-cell receptors to the MHC class-I complexes on the cancer cells (Purdy and Campbell, 2009). This downregulation of MHC class-I on the other hand leads to a lack of induction of cytotoxic T-lymphocytes (CTL) which depend on activating stimuli via MHC class-I either directly by tumor cells or by cross-presentation of tumor-derived antigens by antigen-presenting cells (Huang et al., 2007a). CTLs secrete IFNγ, perforin and granulysin upon activation, and can upregulate FasL expression on their cell surface leading to target cell apoptosis (Janssen et al., 2010).

Cells of the T-helper class can have different impacts on tumor development. Th1 cells whose differentiation is induced by IFNγ, IL-12 and IL-27, are associated with an anti-tumor immune response driven by the secretion of IFNγ and TNFα (Wan and Flavell, 2009). Shifting of the balance towards a Th2 responses by IL-4 and IL-25 leads to

secretion of IL-4, IL-5, IL-13 and IL-25, associated with a humoral immune response and a less potent anti-tumor immune response (Wan and Flavell, 2009). A fairly recently discovered T-helper cell subset, the Th17 cells, are induced by IL-6 and TGFβ, and have been implicated in autoimmune disease such inflammatory bowel disease (IBD), as well as in driving tumor growth (Wu et al., 2009), presumably by modulating Stat3 activation via IL-6 levels (Wang et al., 2009). Regulatory T-cells (Treg) are induced by TGFβ and IL-2, and are responsible for the secretion of IL-10 and TGFβ (Weiner, 2001; Stassen et al., 2004), thereby downregulating different components of the anti-tumor immune response.

The effect of the tumor microenvironment on tumor promotion is not solely determined by the cell types present, but mainly depends on the cytokines secreted by these cells (see Figure 1.1). Main tumor promoting cytokines include TNFα, IL-1, IL-6, IL-10, IL-17 and TGFβ, with TNFα, IL-1, IL-6 and IL-17 having a direct effect on tumor cell proliferation, while secretion of IL-10 and TGFβ has an adverse effect by suppression of the anti-tumor immune response.
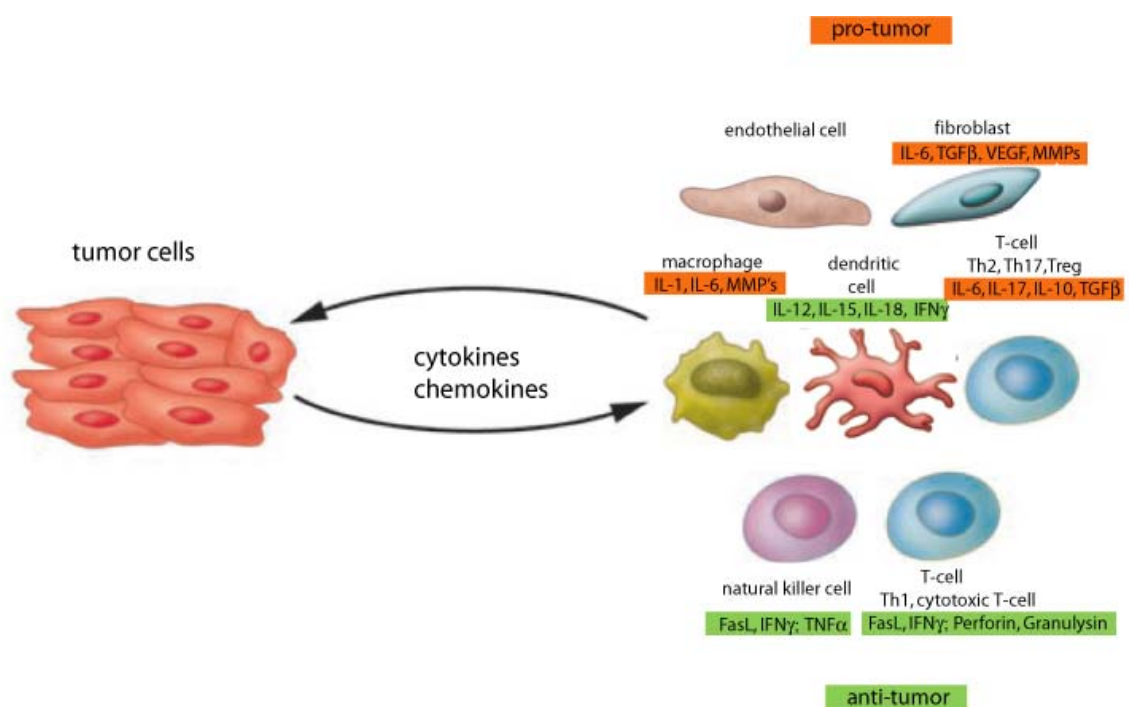
Figure 1.1: **The inflammatory tumor microenvironment, its cell types and the cytokines secreted. (adapted from Lin and Karin, 2007)** Tumor cells secrete different cytokines and chemokines, which then attract and/or activate cells of the tumor microenvironment. NK cells, Th1, cytotoxic T-cells as well as dendritic cells are associated with an anti-tumor immune response, while macrophages, Th2, Th17 and regulatory T-cells (Treg), fibroblasts and endothelial cells contribute to tumor promotion.

Interestingly, in the early stages of tumor development TGFβ has also been reported to have an inhibiting effect on tumor development in colitis-associated carcinogenesis by modulating IL-6 signaling (Becker et al., 2004).

On the other hand, IL-10 can as well have positive effects by dampening inflammation, thereby reducing the secretion of different other proinflammatory cytokines which are important in driving hyperproliferation of initiated cells. Cytokines important in driving the anti-tumor immune response include IL-12, IFNγ and TNF-Related Apoptosis Inducing Ligand (TRAIL).

Important signaling pathways in regulating cytokine secretion, but as well in regulating the intrinsic activation statuts of different cell types within the tumor microenvironment are represented by Nuclear Factor Kappa B (NF-κB) as well as the Signal Transducer and Activator of Transcription (Stat3) signaling pathway. NF-κB activation in macrophages leads to the secretion of IL-1β, TNFα and IL-6, which then in turn activate NF-κB and Stat3 signaling in intestinal epithelial cells (IEC) during colitis-associated cancer (CAC) (Greten et al., 2004). TNFα and IL-6 also play important roles in hepatocellular carcinogenesis (HCC). TNFα and lymphotoxin β promote tumor growth in mouse models of HCC (Pikarsky et al., 2004; Haybaeck et al., 2009). Ablation of IL-6 signaling leads to a reduction in tumorigenesis in an injury-dependent HCC model (Naugler et al., 2007). IL-10 activates the Stat3 signaling pathway in macrophages and deletion of IL-10 signaling leads to the development of spontaneous colitis (Takeda et al., 1999). IL-17 is expressed in a Stat3-dependent manner by T-cells and modulates IL-6 signaling leading to Stat3 activation in tumor cells (Wang et al., 2009). The diverse network regulated by Stat3 signaling in tumors has been illustrated by Kortylewski and colleagues (2009), who showed that Stat3 activation in tumor-derived macrophages leads to expression of IL-23. This inhibits *IL12p35* expression in tumor-associated DC and induces the transcription of the *Foxp3* gene in regulatory T-cells, leading to the secretion of immune suppressive IL-10. The results mentioned here represent only some examples which demonstrate the importance of the aforementioned signaling pathways in tumor cells, as well as in tumor infiltrating immune cells.

1.2 Inflammatory bowel disease as a predisposing factor for colorectal cancer development

Inflamatory bowel disease (IBD) comprises the two disease types of chronic intestinal inflammation: Crohn's disease (CD) and ulcerative colitis (UC). Both are characterized by persistent and recurrent inflammation of the gastrointestinal tract. In CD the inflammation is predominantly located to the terminal ileum and colon, but can as well localizes to any part of the gastrointestinal tract between mouth and anus, and can involve all layers of the tissue. Symptoms of UC often start from rectum then spreading across the whole mucosa to the proximal colon (Abraham & Cho, 2009). For CD and UC the causative factors are not well defined, it seems that a combination of genetically predisposing factors in combination with environmental factors leads to the development of these diseases. The notion of a genetic predisposition present in patients suffering from IBD is underlined by the findings that the risk of developing these diseases increases in people with a first–degree relative suffering from IBD (Baumgart and Carding, 2007).

Genetically predisposing factors for the development of IBD include alterations in genes of pattern recognition receptors, such as NOD mutations (Strober et al., 2008), genes governing the differentiation of Th17 lymphocytes or are involved in the IL-17 signaling pathway (Franke et al., 2010), autophagy and maintenance of epithelial barrier integrity (Van Limbergen, 2009). Environmental factors potentially modulating IBD include dietary factors, as well as smoking or the use of hormonal contraceptives. Another important role seems to be played by gut commensals colonizing the large intestine, as the distribution of bacterial species distinctly changes in patients suffering from IBD. A conclusive result on the relationship between bacterial colonization and the development of IBD remains to be established.

In IBD, T-cells were shown to be resistant to apoptosis leading to an expansion of the number of T-lymphocytes in the intestine of these patients. An expansion of effector as well as regulatory T-cell subsets can be observed, however more importantly the activation profile of these cells seems to differ significantly in IBD (Neurath and Finotto, 2009). Traditionally Crohn's disease has been associated with a cytokine milieu resembling a Th1 response, being dominated by the secretion of IFNγ. This view has recently been challenged by the discovery of a new subset of T-cells, the Th17 cells (Fujino et al., 2003; Kobayashi et al., 2008). The predominant cytokines secreted by antigen-presenting cells in Crohn's disease comprise IL-1β, IL-6 and IL-23, which can

induce the development of Th17 cells out of naive T-cells, and the latter two are potent inhibitors of regulatory T-cell formation (Brand, 2009). Furthermore, the secretion of IL-12 by antigen-presenting cells leads to the induction of
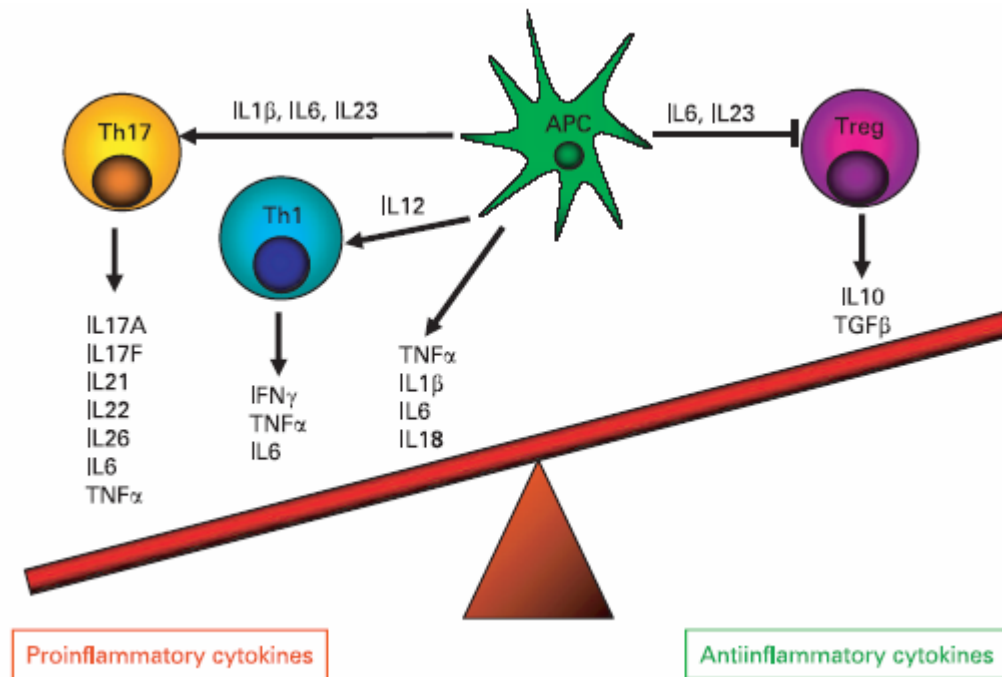
Figure 1.2.: The imbalance of pro- and anti-inflammatory cytokines in Crohn's disease (taken from Brand, 2009). In Crohn's disease an hypersecretion of the pro-inflammatory cytokines IL-1β, IL-6, IL-12 and IL-23 is secreted by antigen-presenting cell (APC) leading to a hyperactivated state of Th1 and Th17 cells while suppressing the activity of regulatory T-cells (Treg).

Th1 cells. These activated subsets of the adaptive as well as the innate immune system lead to an oversupply of proinflammatory cytokines such as IL-1, IL-6, IL-17a and f, IL-18, IL-21 and IL-23, as well as IFNγ and TNFα, whereas the secretion of the anti-inflammatory cytokines IL-10 and TGFβ is reduced (see Figure 1.2) (Brand, 2009). To date it seems that both subsets of activated T-cells play an important role in the development of Crohn's disease.

In UC, the dominating cytokines seem to be IL-5, IL-13 and TNFα which are associated with a Th2 dominated T-cell response. In a recent study IL-33, a member of the IL-1 cytokine family, was reported to be upregulated in patients with UC (Seidelin et al., 2010) and was shown to be able to raise a Th2-like response in immunocompetent cells. Treatment of IBD consists of an unspecific suppression of the immune system by administration of immune modulating drugs such as prednisone, azathioprine, TNFα-blocking antibodies and methotrexate (Baumgart, 2009). Severe cases may require surgical intervention. As IBD represents a chronical, non-curable disease, therapy aims at keeping the disease in a state of remission and early therapeutic intervention at times

of active outbreak of the disease. Research on new treatment options for IBD tries to find ways to modulate the immune response by administration of recombinant cytokines, such as IL-10 or cytokine blocking antibodies active against TNFα, IFNγ, IL-6R. Another strategy involves the modulation of the intestinal flora by administration of probiotic bacteria or even genetically modified bacterial strains (Neurath and Finotto, 2009).

IBD significantly impairs the life qualitiy, of the patient although fatale courses of the disease are rare and mostly caused by surgical complications. Patients suffering from IBD represent one of the groups with the highest risk of developing colon cancer, although this group only accounts for 1 % of all colorectal cancer cases which is due to a tight monitoring of IBD patients. Nonetheless, longstanding inflammation increases the risk of developing CRC to 20 % after 30 years (Eaden et al., 2001).

1.3 Colon cancer

Among human cancers, colon cancer was the third most common cancer type to be developed in the USA in 2009 (Jemal et al., 2009). Significant global variations in the distribution of colon cancer have been observed with higher rates in developed countries (USA, Europe, Oceania) and rising rates in Eastern Europe, resulting from growing "westernization" in these regions (Center et al., 2009). Risk factors for the development of colon cancer include smoking, physical inactivity, alcohol abuse and diet.

Colon cancer can be broadly classified into cases associated with a predeposition for the development of colon cancer, which include IBD and the hereditary syndromes: familial adenomatous polyposis (FAP) and hereditary nonpolyposis colorectal cancer (HNPCC), accounting for about 10 % of all colon cancer cases and sporadic cases which make up 90 % of all cases.

1.3.1 Molecular events in the development of colon cancer

The pathways leading to the development of sporadic, as well as colitis-associated colon cancer are similar. The initiation step of colon cancer is a result of genetic instability, which is mainly resulting from chromosomal instability (CIN) or microsatellite instability (MSI). Chromosomal instability, such as structural chromosomal instability (translocations, deletions, telomeric associations) or numerical instability, can be found in 85 % of all colon cancer cases and lead to abnormal segregation of the chromosomes during mitosis (Itzkowitz and Yio, 2004). This may lead to the inactivation of essential tumor suppressor genes, such as *Adenomatous Polyposis Coli* (*APC*). Mutations of *APC* can be found in 60 % of sporadic colorectal adenomas (Powell et al., 1992). *APC* was found to be mutated less frequently in UC-associated dysplasia and colitis-associated cancer cases, one study reported a mutation frequency of 30 % (Greenwald et al., 1992). The *KRAS* gene represents another frequently mutated gene in CIN tumors. Mutations were found in 47 % of sporadic adenomas larger than 1 cm (Vogelstein et al., 1988). For CAC mutation rates vary between 3 and 50 % (Fujii et al., 2002). The incidence for alterations in the tumor-suppressor gene *TP53* as well arise due to CIN and can be found in 50-80 % of human colorectal cancer cases (Fujii et al., 2002), as well as alterations of the TGFβ signaling pathway.

The second pathway leading to intestinal carcinogenesis is caused by microsatellite instability (MSI), which goes along with an inactivation of genes involved in mismatch-repair during DNA replication, such as *MSH2* and *MLH1*. This inactivation of DNA mismatch repair genes gives rise to DNA replication errors throughout the whole genome for example in microsatellite regions. These microsatellites represent DNA-repeat sequences of defined length, insertions or deletions within these microsatellites can lead to frameshift mutations. In colon cancer they can often lead to mutations in *TGFβRII*, *IGF2R* and *BAX* (Itzkowitz and Yio, 2004), while mutations concerning the WNT-signaling pathway play an inferior role in tumors resulting from MSI. This pathway accounts for about 15 % of CRC cases.

Apart from the CIN and MSI pathways a minor share of colonic tumors arises via alternative routes which are as well independent of mutations of the WNT signaling pathway, but can involve mutations in DNA-mismatch-repair enzymes. These tumors develop via the serrated pathway and often harbour mutations of the *KRAS* or *BRAF* gene.

1.3.2 Wnt signaling: a commonly hyperactivated pathway in colon cancer

The Wnt signaling pathway plays a key role in the development and tissue homeostasis of the intestine as well as in colon cancer (Funayama et al., 1995; Willert and Nusse, 1998; Arias et al., 1999; Polakis, 2000). Wnt signaling is initiated by binding of Wnt proteins to the extra-cellular domains of the Frizzled family of seven transmembrane receptors. Although hyperactivation of the Wnt pathway is a common finding in human carcinogenesis, an oversupply of Wnt ligands accounting for this hyperactivation has never been demonstrated. The activated Frizzled receptor recruits the protein Dishevelled to the membrane and mediates its phosphorylation (Axelrod et al., 1998; Lee et al., 1999). Dishevelled in turn disrupts the GSK-3β/Axin/APC complex, resulting in an inhibition of phosphorylation and targeting for degradation of β-Catenin (see Figure 1.3). Accumulation of β-Catenin in the cytoplasm finally leads to nuclear translocation and initiation of target gene transcription via TCF/LEF (Behrens et al., 1996). In colorectal cancer, hyperactivation of the Wnt signaling pathway commonly results from mutations in the *APC* gene. Stabilizing mutations in the *CTNNB1* gene have as well been described, but in a much smaller fraction of tumors mainly in the presence of MSI (Mirabelli-Primdahl et al., 1999).
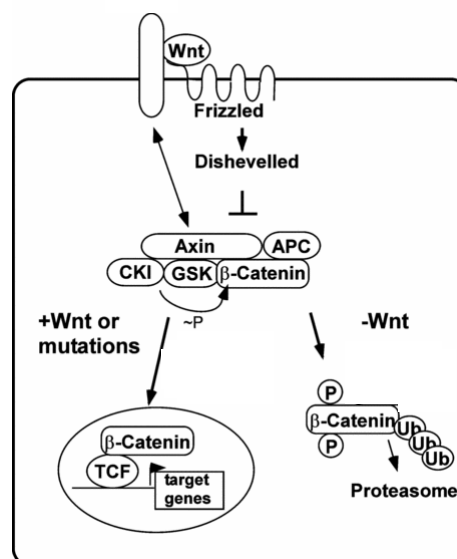
Figure 1.3.: The canonical Wnt signaling pathway (adapted from Behrens, 2005) Binding of Wnt protein to the extracellular domain of the Frizzled receptor leads to activation of Dishevelled, which disrupts the Axin/GSK/APC complex. This prevents phosphorylation of β-Catenin, which is the signal for its ubiquitinylation (Ub) and proteasomal degradation. Stabilized β-Catenin translocates to the nucelus and initiates TCF-dependent gene expression.

Interestingly, inactivating mutations of APC and activating mutations of the *CTNNB1* gene never seem to coexist in one tumor (Kolligs et al., 2002). It has been shown

recently that tumor formation via APC mutations is mainly exerted via c-Myc and deletion of this gene can inhibit the tumor formation (Sansom et al., 2007).

1.4 The Stat3 signaling pathway

1.4.1 Components and its functions

Stat3 was first identified in liver cells as a transcription factor involved in the acute phase response and has been shown to be induced by IL-6 (Wegenka et al., 1993). Since its discovery growing knowledge has evolved about its role in epithelial and immune cells under steady state and inflammatory conditions.

Induction of the Stat3 pathway can be achieved cell-type dependent by a variety of cytokines and growth factors. The main known activators of the pathway are cytokines of the IL-6 protein family (IL-6, IL-11, Leucocyte Inhibitory Factor (LIF), Oncostatin M (OSM), Ciliary Neutrophic Factor (CNTF) (Heinrich et al., 2003), members of the IL-10 protein family (Radaeva et al., 2004) and different growth factors (Hepatocyte Growth Factor (HGF), Epidermal Growth Factor (EGF), Platelet Derived Growth Factor (PDGF)) (see Figure 1.4). Activation of the Stat3 pathway occurs through di-or trimeric receptors. Members of the IL-6 cytokine family signal through gp130, which can associate with different cytokine specific subunits. Growth factors activate Stat3 in a gp130 independent way, relying on the expression of different growth factor receptors on the cells (e.g. EGFR, PDGFR).

Although expression of the IL-6 receptor subunit is restricted to hepatocytes, neutrophils, monocytes/macrophages and some lymphocytes, IL-6 signaling is activated in a variety of cell types. In cells not expressing the IL-6 receptor, signaling is initiated by a soluble form of the receptor which is either formed by proteolysis of the membrane-bound receptor (shedding) or by translation of an alternatively spliced form of the mRNA (Heinrich et al., 2003), this process is known as IL-6-trans signaling (Jones et al., 2001). A comparable mechanism has been shown for IL-11.

Dimerization of the different receptor types induced by ligand-binding leads to activation of receptor-associated Janus kinases (Jak1, Jak2, Tyk2) (Zhong et al., 1994). If two Jaks are brought into close proximity they are able to phosphorylate and thereby activate each other. Activation of the Jaks leads subsequently to phosphorylation of their major target Stat3 on a conserved tyrosine residue and to a lesser extent also to phosphorylation of Stat1. Phosphorylated Stat3 is able to dimerize over its SH2 domain

and is actively imported into the nucleus where it induces the transcription of target genes (Aggarwal et al., 2009a).

Tyrosine phosphorylation of Stat3 can also be achieved by non-receptor kinases, such as Src and Abl (Yu et al., 1995; Ilaria and Van Etten, 1996). Stat3 can also be phosphorylated on a serine-residue, while different kinases have been shown to mediate serine-phosphorylation of Stat3 (Jain et al., 1999; Aziz et al., 2007), the physiological role of it is not fully understood to date. Serine phosphorylation was suggested to be involved in the regulation of the duration and extent of the transcription of Stat3 target genes (Yokogami et al., 2000). These target genes include a vast diversity of genes controlling apoptosis, proliferation, angiogenesis and invasion (Alvarez and Frank, 2004).
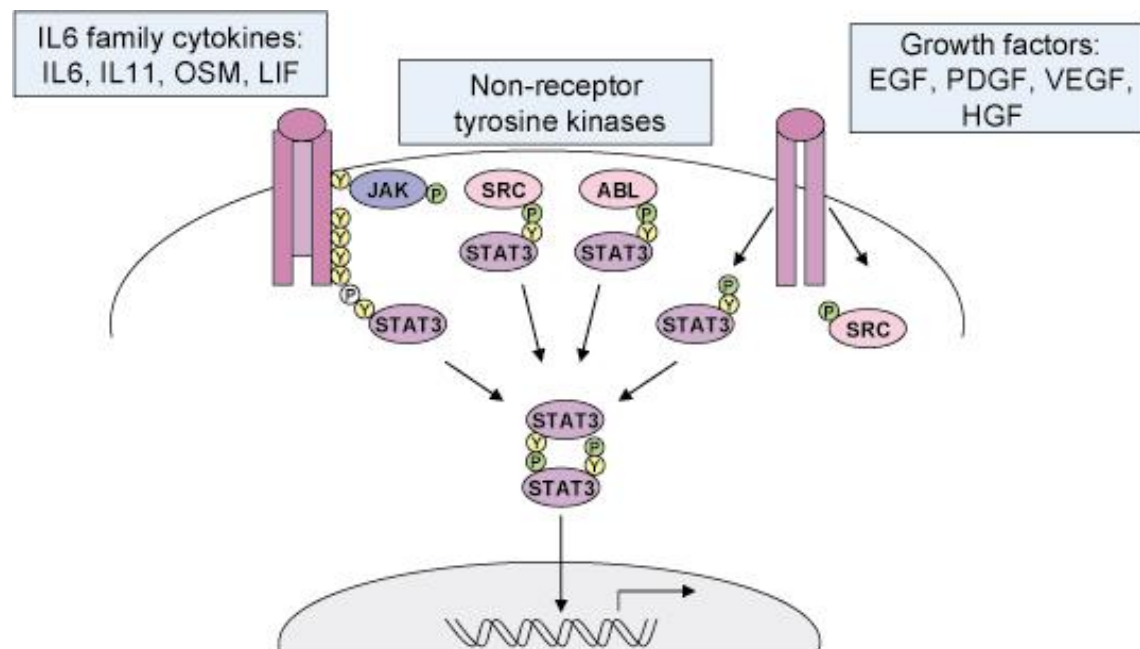
Figure 1.4: The Stat3 signaling pathway. Stat3 can be activated by different growth factors, non-receptor tyrosine kinases, as well as IL-6 family cytokines. Growth factors signal through dimerized cytokine receptors, whereas IL-6 family cytokines signal through hetero-trimers of gp130 and specific cytokine receptor subunits. This leads to phosphorylation of Stat3 at a tyrosine residue, which enables dimerization of the monomers. These translocate to the nucleus and initiate transcription of target genes.

Negative regulation of the Stat3 pathway occurs via different mechanisms: the phosphatase Shp2 is rapidly recruited to tyrosine-phosphorylated gp130, activated by its binding to the receptor and is able to dephosphorylate Stat3, gp130 and Jaks (Schaper et al, 1998). Suppressor of cytokine signaling 3 (Socs3) that is transcriptionally induced by Stat3 itself binds to the phosphorylated tyrosine residue of gp130 in a classical feedback

inhibitory manner (Lang et al., 2003). Furthermore Socs3 is also able to target the receptor and Jaks to the ubiquitin proteasome pathway. The other negative regulator of Stat3 signaling protein inhibitor of activated Stat3 (Pias3) carries out its function by binding to Stat3 and preventing its DNA association (Groner et al., 2008).

1.4.2 The Stat3 pathway in cancer development

Stat3 activation has been observed in a diverse set of human cancers, including haematological malignancies such as Hodgkin's disease, Non-Hodgkin's lymphoma and multiple myeloma, and solid tumors such as breast, prostate, lung, liver, pancreatic and colon cancer (Frank, 2007), although no activating mutations for the transcription factor itself could be identified. Constitutive activation of the pathway has been attributed for example to an oversupply of activating cytokines e.g. IL-6 in the case of colitis-associated carcinogenesis (Grivennikov et al., 2009), hyperactivation of Src-family kinases in breast carcinoma (Garcia et al., 2001), mutations in the gp130 receptor in hepatocellular carcinoma (HCC) (Rebouissou et al., 2009) or to impairment mutations in genes encoding negative regulators of Stat3 signaling e.g. Socs3 in lung cancer (He et al., 2003). Negative regulators of the Stat signaling pathways have as well been shown to be insufficiently induced due to promoter methylation in HCC and multiple myeloma (Yoshikawa et al., 2001; Galm, 2003), rendering even a weak phosphorylation signal to have a pronounced effect on gene expression. In the case of HCC, an infection with hepatitis C virus can be an initiating event and it could be shown that a core protein of the virus is able to mediate tyrosine phosphorylation of Stat3 by a yet unidentified mechanism (Hosui et al., 2003).

In 1999, Bromberg et al could demonstrate that expression of a constitutive active form of Stat3 (Stat3C) resulted in cellular transformation of immortalized fibroblasts, leading to anchorage-independent growth and tumor formation of these cells in nude mice. Since then important target genes of Stat3, which play a major role in tumor cell growth have been identified. It could be shown that Stat3 induces cell cycle progression by induction of CyclinD1/CyclinE (Sinibaldi et al., 2000) and c-Myc (Bowman et al., 2001) in v-Src transformed fibroblasts. Primary target genes of Stat3 leading to protection from apoptosis include Mcl1, Bcl-x, Bcl-2 and Survivin, which were shown to be regulated in different cell types. Apart from regulation of proliferation and apoptosis, activated Stat3 is also capable of regulating angiogenesis by controlling the expression of VEGF (Niu et al., 2002) and remodeling of the extracellular matrix by

regulating the expression of MMP-2 and -9 (Xie, 2004; Dechow et al., 2004). In an approach to identify the role of Stat3 in carcinogenesis, Stat3 target genes were identified by microarray expression analysis after transfection of fibroblasts cells with Stat3C. The expression of these target genes was then analyzed in various tumor data sets. Using this approach a genetic signature of 12 Stat3 target genes could be identified that were co-expressed in human cancers (Alvarez et al., 2005). These signature target genes revealed that activation of Stat3 can control all hallmarks of cancer cells necessary for malignant progression.

Stat3 signaling in tumor cells as well plays a role in shaping the tumor microenvironment. If tumor cells in which Stat3 signaling was disrupted were injected into mice, a tumor-specific T-cell dependent immune response could be shown (Wang et al., 2004). This was mediated by an increased expression of Rantes, IFNβ, IL-6 and TNFα by the tumor cells.

1.4.3 The Stat3 pathway in colon cancer

IL-6 plays together with IL-1 and TNFα a key role in driving acute inflammatory responses. A dysregulation of this signaling network has been shown to contribute to a diverse set of inflammatory conditions such as obesity and insulin resistance, inflammatory arthritis, sepsis and IBD. More recently an important role in driving different tumorigenesis, as well as in regulating the innate-adaptive immune response could be demonstrated.

In a mouse model of CAC, IL-6 were to be secreted by myeloid cells (Greten et al., 2004) in a NF-κB depending manner as well as by T-cells (Becker et al., 2004). When classical NF-κB signaling was genetically ablated, tumor number and size was reduced, presumably by a reduced IL-6 secretion by macrophages (Greten et al., 2004). This notion is supported by findings that loss of Socs3 expression during CAC leads to an increase in tumor number and size (Rigby et al., 2007). Colon cancer patients as well exibit elevated levels of IL-6 (Chung and Chang, 2003). The importance of IL-6-Stat3 signaling in sporadic colon carcinogenesis is underlined by experiments using mice with acitvating mutations in the APC gene. In mice lacking the Toll Like Receptor (TLR)-adaptor protein MyD88 decreased tumor numbers were observed, accompanied by a reduced expression of IL-6 (Rakoff-Nahoum and Medzhitov, 2007). Modulation of IL-6

trans-signaling can as well be achieved by T-cell specific overexpression of TGFβ and this leads to protection from CAC (Becker et al., 2004).

1.5 Mouse models of colon cancer

Mouse models are important tools for understanding the molecular events leading to the development of colorectal cancer, one can differentiate, between models mimicking colitis-associated colon cancer and sporadically occuring colon cancer.

The existing mouse models of inflammatory bowel disease all do not represent the full complexity of the human disease, but mimic different aspects of disease cause and progression, and only some of them lead to the development of CAC. Among them are the IL-10 knock-out mice, which show an increase in reactive T- and B-cells numbers, an upregulation in immunoglobulin secretion and aberrant expression of MHC-class II. This dysregulation of the activation state of immune cells is caused by an unbalanced secretion of TNFα and IL-12 and leads to the development of IBD and subsequently to the development of adenocarcinomas in the colon and rectum (Berg et al., 1996). In these mice a germfree housing protects from IBD and CAC development underlining the role of the enteric microflora in these disease. In a similar model the conditional ablation of the Stat3 signaling pathway in myeloid and lymphoid cells leads to a dramatic inflammatory response in the intestine and tumor formation at a similar frequency to that observed in human IBD patients. Interestingly these mice even develop invasive carcinomas driven by Stat3 activation in the colonic epithelium (Deng et al., 2010) The importance of the microflora for cancer development was as well unveiled by the Gpx1/Gpx2 mouse model, showing that oxidative stress contributes to inflammation and cancer development (Chu et al., 2004).

DSS-induced colitis relies on its toxicity to epithelial cells, which leads to a disruption of the epithelial barrier, allowing invasion of commensal microbiota into the lamina propria. The resulting inflammatory response resembles many features of human UC (Clapper et al., 2007) and is characterized by an upregulation of proinflammatory cytokines such as IL-2, IL-4 and IL-6. Repetitive administration induces a chronic colitis which in combination with the pro-carcinogen azoxymethane (AOM) leads to the development of adenomas in the distal colon with a penetrance of 100 % (Clapper et al., 2007). These adenomas exhibit nuclear β-Catenin translocation, which is also frequently observed in human CAC (Aust et al., 2001).

Hyperactivation of the Wingless (Wnt) signaling pathway by mutational modification of components of this pathway are proposed to be the initiating mutations in most sporadic colorectal cancer cases. Different *APC* mutant mice mimic these cases. These mice carry heterozygously an inactivating mutation of the *APC* gene and upon spontanous loss of the second functional copy of the *APC* gene develop multiple tumors predominantly in the small intestine and to a lesser extent in the large intestine. There are different mouse strains carrying different mutations of *APC* which all lead to the development of adenoma and occasionally also adenocarcinoma of the small intestine. The different mutations greatly vary in the number of tumors that are formed, the APC$^{\Delta716}$ mouse for example develops around 300 polyps (Oshima et al., 1997) whereas mice carrying the APC^{1638N} mutation only develop around 3-6 tumors (Smits et al., 1997). Quite recently a model of conditional ablation of APC function with the help of Cdx2-NLS-Cre recombinase has been established which limits adenoma/carcinoma formation to the large intestine and distal ileum (Hinoi et al., 2007).

Another mutation leading to the activation of the Wnt signaling pathway is represented by β-Catenin stabilizing mutations, which can as well been found in a subset of human colon tumors, that do not carry APC mutations. Depending on the promotor driving the expression of the mutant β-Catenin form, these mice develop between a few (calbindin promotor) and 700-3000 polyps (CK19 promotor) in the small intestine (Taketo and Edelmann, 2009).

2. Objective of this study

Among human cancers, colon cancer was the third most common cancer type to be developed in the USA and Europe in 2009. Although a big effort is made to improve the survival probability, the cumulative 5-year survival rate still remains as low as 50 %. One field in colorectal cancer research includes the effort to improve the diagnostic options, another big field aims at understanding the molecular events leading to colorectal carcinogenesis to improve therapeutic as well as preventive options. Known risk factors for the development of colon cancer include smoking, physical inactivity, alcohol abuse and diet. All these risk factors lead or can contribute to the establishment of an inflammatory environment which can promote or even initiate tumor growth.

Important pathways involved in the regulation of inflammation in immune cells as well as in epithelial cells include the Nuclear Factor Kappa B (NF-κB) as well as the Signal Transducer and Activator of Transcription 3 (Stat3) signaling pathway.

NF-κB regulates for example secretion of Interleukin (IL)-1β, Tumor Necrosis Factor α (TNFα) and IL-6 by activated macrophages. The Stat3 signaling pathway controls in immune cells mainly anti-inflammatory signals. In mice devoid of Stat3 signaling in macrophages, neutrophils as well as dendritic cells, this leads to a hyperactivation of the immune system and the development of spontaneous colitis.

During carcinogenesis, NF-κB has been shown to play a major role by protecting initiated cells from apoptosis in colitis-associated carcinogenesis (CAC) as well as in hepatocellular carcinogenesis (HCC). NF-κB activation in cells of the tumor microenvironment can lead to a secretion of IL-6, thereby activating the Stat3 signaling pathway. The role of Stat3 signaling in epithelial cells during colorectal carcinogenesis remains still ill defined. To address the function of Stat3 during different phases of tumor development as well as in sporadic and inflammation-associated cancer, we took advantage of mice carrying an intestinal epithelial cell (IEC)-specific deletion of Stat3 ($Stat3^{\Delta IEC}$) and employed different models: In a model for CAC, we exposed these mice to a mutagenic challenge by azoxymethane (AOM) administration followed by the repeated administration of dextrane-sulfate sodium in the drinking water to induce chronic inflammation, this leads to tumor formation in the distal colon within 12 weeks. To assess the role of Stat3 signaling during sporadic colorectal carcinogenesis, we crossed $Stat3^{\Delta IEC}$ mice to mice carrying an inducible mutation of the *Ctnnb* gene as a model for early tumor promotion during sporadic carcinogenesis.

3. Materials and Methods

3.1 Mice

3.1.1 Mouse models

CD11c-DTR (Jung et al., 2002)

The *CD11c-DTR* mouse constitutes a mouse model for the specific deletion of CD11c expressing cells. In order to generate these mice a transgene for the simian diphtheria toxin receptor was placed under the control of the *Itgax* (CD11c) promotor. This results in the expression of the receptor by CD11c expressing cells which are depleted upon intraperitoneal injection (i.p.) of diphtheria toxin (Merck) at a dosage of 4 ng/g bodyweigth in sterile PBS every second day.

Ctnnb$^{loxEx3/wt}$ (Harada et al., 1999)

These mice carry a mutant *Ctnnb* allele whose exon 3 is sandwiched by loxP sequences. When these mice are crossed to *villin-CreER^{T2}* mice, tamoxifen induced villin-Cre expression results in a truncated β-catenin protein, which lacks the serines and threonines encoded by exon 3, which are normally phosphorylated by glycogen synthase kinase 3 β (GSK3β) to target the protein for degradation. This leads to a stabilization of β-catenin protein specifically in intestinal enterocytes.

IFNγ$^{-/-}$ (Dalton et al., 1993)

A targeting vector containing a neomycin gene was introduced into exon 2 of the *IFNγ* gene, which introduces a termination codon after the translation of the first 30 amino acids and results in the expression of an immature protein.

IL6$^{-/-}$ (Kopf et al., 1994)

A targeting vector was designed to place a neomycin resistance cassette into the first coding exon (exon 2) of the *IL-6* gene, thus ablating the expression of a functional protein.

Socs3$^{flox/flox}$ (Yasukawa et al., 2003)

A targeting vector was designed to place *loxP* sites in intron 1 and the 3' untranslated region of exon 2 of the targeted *Socs3* gene. When these mice are crossed to *villin-CreER^{T2}* mice, tamoxifen induced villin-Cre expression results in the specific ablation of functional Socs3 protein in intestinal epithelial cells.

Stat3$^{flox/flox}$ (Takeda et al., 1998)

A targeting vector was designed leading to a floxed architecture of exon 21 of the *Stat3* gene. This results in the expression of a truncated protein lacking the phosphorylation sites necessary for activation of the transcription factor upon crossing with mice expressing Cre recombinase.

Villin-Cre (Madison et al., 2002)

Mice wich are hemizygous for this transgene express Cre recombinase under the direction of the mouse *villin* 1 promoter. Intercrossing with a strain containing a *loxP*-flanked sequence of interest leads to Cre-mediated recombination and tissue-specific deletion of the targeted sequence.

Villin-CreER^{T2} (El Marjou et al., 2004)

Transgenic mice bearing a tamoxifen dependent Cre recombinase expressed under the control of the *villin* promoter were created to perform targeted spatiotemporally controlled somatic recombination. In these mice a mutated ligand binding domain of the human estrogen receptor is fused to the Cre recombinase transgene leading to the inhibition of Cre expression in the absence of tamoxifen. Intercrossing with a strain containing a *loxP*-flanked sequence of interest leads to tamoxifen dependent Cre-mediated recombination and tissue-specific deletion of the targeted sequence.

3.1.2 LPS measurement

In order to measure the LPS level, serum was collected, diluted 1:4 with water and subsequently heated to 70°C for 10 min. Then the LPS-serum level was determined using the Limulus Amebocyte Lysate kit (Lonza) according to the manufacturer's instructions. This detection method is based on the fact that gram-negative infection of *Limulus polyphemus*, the horseshoe crab, results in intra-vascular protein coagulation. This coagulation is based on the activation of a proenzyme by endotoxin, which in turn

cleaves a colorless substrate into a peptide. This can be photometrically measured at 405-410 nm allowing the quantification of the endotoxin present in a given sample compared to a standard curve.

3.1.3 Bone marrow transplantation

Mice were subjected to whole body γ-irradiation of 9 grey, which represents a lethal dose. Bone marrow from a *CD11cDTR* donor mouse was isolated from femoral bones by flushing with sterile PBS. The total cell number was determined and adjusted to a concentration of $2*10^7$ cells/ml. 100 μl of this cell solution was injected into the tail vein of irradiated mice. The transplanted animals were kept on antibiotic water (1,4 mg/ml Ciprobay (Bayer)) for two weeks, followed by two more weeks on normal water to reconstitute.

3.1.4 Genotyping of mice

In order to genotype the mice tail samples were taken and lysed overnight in 95 μl tail lysis buffer supplemented with 5 μl Proteinase K (Qiagen) at 60°C. The enzymatic tissue digestion was stopped by heat inactivation at 95°C for 10 min. Samples were diluted with distilled water 1:10 and centrifuged for 10 min at 13200 rpm to remove insoluble parts. Supernatants were directly used for polymerase chain reaction (PCR).

General PCR reaction:	10x PCR buffer (Invitrogen)	2 μl
	50 mM MgCl$_2$ (Invitrogen)	0,6-0,8 μl
	100 mM dNTP Mix (Invitrogen)	0,4 μl
	20 pMol Forward Primer	0,5 μl
	20 pMol Reverse Primer	0,5 μl
	Taq Polymerase (5U/μl) (Invitrogen)	0,15 μl
	DNA	1,5 μl
	H$_2$O	14,15 μl

Tail lysis buffer:	1,5 M tris (pH 8,5)
	200 mM NaCl
	0,2% SDS
	5 mM EDTA

PCR conditions:	(35 cycles each, plus an initial denaturation period at 94°C for 5 min and a final elongation for 10 min at 72°C)

Ctnnb:

wt-PCR (2 mM MgCl$_2$)	94°C 30 s
	58°C 30 s
	72°C 30 s

β-catenin F: 5'-TTC CCA GTC CTT CAC GCA AG-3'

β-cateninwt R: 5'-GCA AGT TCC GCG TCA TCC T-3'

flox-PCR (1,5 mM MgCl$_2$)	94°C 30 s
	58°C 30 s
	72°C 60 s

β-catenin F: 5'-TTC CCA GTC CTT CAC GCA AG-3'

β-cateninflox R: 5'-CTG AAT GAA CTG CAG GAC GA-3'

CD11cDTR: (2 mM MgCl$_2$)	94°C 30 s
	62°C 60s
	72°C 60 s

CD11cDTRwt: 5'-F CAA ATG TTG CTT GTC TGG TG-3'

CD11cDTRwt R: 5'-GTC AGT CGA GTG CAC AGT TT-3'

CD11cDTRtg F: 5'-GGG ACC ATG AAG CTG CTG CCG-3'

CD11cDTRtg R: 5'-TCA GTG GGA ATT AGT CAT GCC-3'

Cre: (2 mM MgCl$_2$)	94°C 30 s
	58°C 30 s
	72°C 30 s

Cre F: 5'-ACC TGA AGA TGT TCG CGA TTA TCT-3'

Cre R: 5'-ACC GTC AGT ACG TGA GAT ATC TT-3'

IFNγ: (2 mM MgCl$_2$)   94°C 30 s

58°C 30 s

72°C 30 s

IFNγwt F: 5'-CTG AAT GAA CTG CAG GAC GA-3'

IFNγko F: 5'-AGA AGT AAG TGG AAG GGC CCA GAA G-3'

IFNγ R: 5'-AGG GAA ACT GGG AGA GGA GAA ATA T-3'

IL6: (2 mM MgCl$_2$)   94°C 30 s

61°C 60 s

72°C 60 s

IL6 F: 5'-TTC CAT CCA GTT GCC TTC TTG G-3'

IL6wt R: 5'-TTC TCA TTT CCA CGA TTT CCC AG-3'

IL6ko R: 5'-CCG GAG AAC CTG CGT GCA ATC C-3'

Stat3: (2 mM MgCl$_2$)   94°C 30 s

58°C 30 s

72°C 30 s

Stat3 F: 5'-CCT GAA GAC CAA GTT CAT CTG TGT GAC-3'

Stat3 R: 5'-CAC ACA AGC CAT CAA ACT CTG GTC TCC-3'

Socs3: (2 mM MgCl$_2$)   94°C 30 s

58°C 30 s

72°C 30 s

Socs3 F: 5'-GCG GGC AGG GGA AGA GAC TGT CTG GGG TTG-3'

Socs3 R: 5'-GGC GCA CGG AGC CAG CGT GGA TCT GCG-3'

3.1.5 Mouse treatment

AOM injections/DSS administration

In order to induce colonic tumor formation mice were injected with AOM (Sigma) i.p. at a dose of 10 mg AOM per kg bodyweight of the mice. AOM was dissolved in sterile 0,9% sodium chloride to a concentration of 0,5 mg/ml. Dextran sulfate sodium (DSS, MP Biomedicals) was dissolved in the drinking water at concentrations between 2,5 and 3,5% (w/v).

Tamoxifen administration

In order to induce Cre expression in the *Cre-ER^{T2}* model mice were administered 1 mg tamoxifen (Sigma) per day dissolved in 100 µl 10% ethanol/90% sunflower oil mixture for 5 consecutive days by oral gavage.

α-CD8/4 antibody administration

Recombinant CD8 (clone 2.43) and CD4 (clone GK1.5) was kindly provided by Dr. J. Gamrekelashvili and PD Dr. T. Greten (MHH Hannover). Mice received on 3 consecutive days 150 µg antibody in 100 µl sterile PBS by i.p. injection, followed by the administration of tamoxifen for 5 days. After the tamoxifen administration the mice were again injected for 3 consecutive days with 150 µg of antibody. Then mice were injected every 7 days for 3 consecutive days. This treatment results in depletion of CD8^{+}/CD4^{+} cells.

α-AsialoGM1 antibody administration

20 µl of α-AsialoGM1 antibody (Wako) dissolved in 180 µl of sterile PBS was injected i.p. on the first day of tamoxifen gavage. This injection was repeated every 4 days, resulting in depletion of AsialoGM1 expressing cells, a surface marker mainly present on natural killer cells.

3.1.6 Sacrifice of mice

1,5 h before they were sacrificied the mice were injected i.p. with 75 mg/kg bromodesoxyuridine (BrdU, Sigma) in PBS. BrdU represents an analogue of the base thymidine and can be incorporated in the DNA of proliferating cells instead of thymidine. The incorporation of BrdU and thereby the proliferating cells can subsequently be identified by immunohistochemical staining.

Depending on the purpose, the colon and the small intestine as well as other organs were removed after the sacrifice of the animals. The different parts of the intestine were flushed with PBS to remove feces.

In order to process the different parts of the intestine for histological analysis it was cut open longitudinally and rolled to form a "swiss roll" (Moolenbeek and Ruitenberg, 1981). These as well as whole organs were incubated overnight in 4% paraformaldehyde (Electron Microscopy Science) in PBS at 4°C, dehydrated (Leica ASP 300 S) and embedded in paraffin.

For the molecular biological analysis whole parts of intestinal mucosa were snap frozen in liquid nitrogen and stored at -80°C until further use. To isolate intestinal epithelial cells (IEC) the cleaned intestines were cut into small pieces and incubated gently shaking in 7,5 ml HBSS (Invitrogen) supplemented with 30 mM EDTA (Fluka) for 10 min at 37°C. Subsequently, the solution was vigorously vortexed for 30 s and then put on ice. The supernatant containing the detached epithelial cells was removed and transferred to a new falcon tube, which was centrifuged at 1500 rpm for 10 min at 4 °C. The pellet was resuspended in PBS and transferred to Eppendorf tubes. After another centrifugation step (5000 rpm, 5 min, 4°C), the supernatant was removed, the pellets were snap frozen in liquid nitrogen and stored at -80°C.

For fluorescence activated cell sorting (FACS) analysis spleen and mesenteric lymph nodes were removed and mechanically minced between two glass slides in PBS. The suspended cells were poured over a cell strainer (40 μm, BD Falcon) and the resulting single cell suspension was centrifuged at 1200 rpm at 4°C for 5 min. The pellet was resuspended in 1 ml of red blood cell lysing buffer (Sigma) and incubated at RT for 5 min. 10 ml of PBS were added to dilute the buffer and the cell suspension was again centrifuged at 1200 rpm at 4°C for 5 min. The pellet was resuspended in FACS buffer and kept on ice until stained for FACS analysis.

FACS buffer: 5% FCS (Biochrom)

                        2 mM EDTA

                        PBS (Invitrogen)

3.1.7 T-cell stimulation and intracellular staining for Fluorescence Activated Cell Sorting (FACS)

For FACS analysis cells were divided into 96-well plates with plate-bound α-CD3 antibody (1 μg/ml, clone 145-2C11, ebioscience), centrifuged at 1200 rpm for 5 min at 4°C and resuspended in RPMI (Gibco) supplemented with 10% FCS (Biochrom) and 1 μg/ml α-CD28 antibody (clone 37.51, eBioscience). Cells were incubated for 48 h in a 37°C incubator at 5% CO_2. Then the medium was changed to RPMI containing golgi plug (1:1000, IFN-γ staining kit, BD) and incubated for another 6 h. If the cells had not been stimulated with α-CD3/CD28 antibody, stimulation was carried out using phorbol 12-myristate 13-acetate (PMA, Sigma) at a concentration of 20 ng/ml and ionomycin (Sigma) at a concentration of 1 μg/ml in RPMI supplemented with 10% FCS for 6 h. In this case the golgi plug was directly applied while stimulating the cells (1:1000). After either stimulation step the cells were centrifuged at 1200 rpm for 5 min at 4°C, washed once with FACS buffer, and then centrifuged again. Cells were resuspended in α-CD16/CD32 (BD) blocking antibody at a dilution of 1:100 in FACS buffer on ice for 10 min. The cells were centrifuged at 1200 rpm for 5 min at 4°C and washed once with FACS buffer. Subsequently, the cells were dissolved in antibody dilutions of required cell surface antibodies (α-CD4-FITC: clone H129.19, BD; α-CD8-APC: clone 53-6.7, eBioscience; α-CD11c-FITC: clone HL3, BD) in FACS buffer at a dilution of 1:200 and incubated on ice for 10 min. Cells were washed twice with FACS buffer and then resuspended in fixation/permeabilization buffer (IFNγ staining kit, BD). After an incubation for 30 min at 4°C the cells were washed twice with washing buffer (IFN-γ staining kit, BD) and resuspended in α-IFNγ–PE (BD) antibody or α-IL-12-PE (BD) diluted at 1:100 in washing buffer. The cells were again incubated for 30 min at 4 °C and then washed once with washing buffer, and once with FACS buffer. Then the cells were analysed on a FACS Calibur (BD).

3.2 Histology

3.2.1 Haematoxylin & Eosin staining (H&E)

H&E staining was performed for a general examination of the tissue and the organs. Therefore, 3 μm thick cuts of paraffin embedded tissues were made, mounted on adherent glass slides (Thermo Scientific), and left to dry overnight at room temperature. The paraffin cuts were deparaffinized two times for 10 min in xylol (X-TRA Solv, Medite) and rehydrated in descending dilutions of ethanol (100%, 96%, 80%, 70%, 50%) in which the slides were incubated for 2 min each. Finally, the cuts were incubated for 5 min in PBS. The tissue was stained for 1 min in a ready-to-use haematoxylin solution (Vector Laboratories) and was washed twice with distilled water. Afterwards the tissue was stained for 10 s in a 3% eosin (Sigma) solution in water (acidified with 10 drops acetic acid per 100 ml) and again washed twice with distilled water. Dehydration occurred in ascending dilutions of ethanol (50%, 70%, 80%, 96%, 100%, 2 min each) and was terminated by incubating the tissue for 5 min in xylol. Finally the tissue was air dried and covered with cover slips with the help of mounting medium (Vector Laboratories).

3.2.2 Alcian Blue staining

The preparation of tissue cuts and deparaffinization, rehydration and dehydration were carried out as described for H&E staining. After the rehydration, the slides were incubated for 20 min in a 1% alcian blue (Sigma) solution dissolved in 3% acetic acid. Then the slides were washed in distilled water and counterstained with ready-to-use nuclear fast red (Vector Laboratories) for 1 min. After an additional wash in PBS, the tissue was dehydrated and embedded with mounting medium.

3.2.3 Azure Eosin staining

The preparation of tissue cuts, deparaffinization and rehydration was carried out as described for H&E staining. After the rehydration, the slides were incubated for 2 hours in a 0,05% azure II (Sigma)/0,01% eosin in water (acidified with 10 drops acetic acid per 100 ml). Subsequently, slides were washed twice with distilled water and dehydrated for 1 min in 96% and 100% ethanol each, followed by a 5 min incubation in

xylol. Finally, the tissue was dried and covered with cover slips with the help of mounting medium.

3.2.4 Immunohistochemical staining (IHC)

Tissue cuts were deparaffinized and rehydrated as described for the H&E staining. For antigen retrieval, the cuts were heated for 20 min in a microwave in a sodium citrate buffer (antigen unmasking solution, Vector Laboratories). Slides were washed 3 times for 5 min in PBS. In order to block endogenous peroxidases, slides were incubated for 10 min with 3% H_2O_2 (Sigma) and again washed 3 times with PBS. The unspecific binding of the antibody was blocked for 30 min with 3% BSA (Sigma)/PBS plus avidin-block (2 drops per ml, vector), then the first antibody was applied (for dilutions see table 3.1) in 3% BSA/PBS plus biotin-block (2 drops per ml, Vector Laboratories). At the end of the incubation time, the slides were washed 3 times for 5 min each in PBS. Secondary biotinylated antibody (Vector Laboratories) was applied in a dilution of 1:1000 in 3% BSA/PBS for 1 hour, followed again by 3 washing steps in PBS. Then the slides were incubated for 30 min with ABC complex (of avidin dehydroxygenase and biotinylated horseradish peroxidase, Vector Laboratories), which has been prepared out of 2 drops of solution A and 2 drops of solution B in PBS 30 min prior to use and incubated at 4°C. For the DAB (3,3'-diaminobenzidine) colour reaction, 2 drops of buffer were mixed with 4 drops of DAB and 2 drops of peroxidase (DAB Kit, Vector Laboratories) in 5 ml of distilled water. This solution was then applied on the slides for 30 s- 10 min. Counterstaining was carried out by incubation with haematoxylin for 1 min. The slides were washed, dehydrated, and embedded as described for the H&E staining

Table 3.1: First antibodies used in IHC

Antibody	Company	#	Working Dilution
BrdU	Amersham Bioscience	RPN 201	1:400
CD3	Dako	IS503	undiluted
cleaved Caspase 3	Cell signaling	9661	1:300
Cyclin B1	Santa Cruz	752	1:300
phospho-Histone H3	Cell signaling	9701	1:100
Interferon-γ	R&D	BAF 485	1:50
Mbl2	R&D	AF 2208	1:50
Reg3β/PAP	Algül et al., 2007		1:100
phospho-Stat3	Cell signaling	9145	1:100
Survivin	Cell signaling	2808	1:400

3.2.5 TUNEL staining (TdT-mediated dUTP-biotin nick end labeling)

TUNEL is a staining to label apoptotic cells with a fluorescent dye. It is based on the DNA fragmentation in apoptotic cells which is identified by the terminal deoxynucleotidyl transferase. This enzyme adds dUTP, which is labeled with a fluorescent marker to the nicked DNA, thus marking the cell.

The staining was carried out with the commercial Kit ApoAlert DNA-Fragmentation Assay (Clontech) using the protocol for PFA-fixed, paraffin embedded samples. Tissue cuts were deparaffinized and rehydrated as described for the H&E staining. Samples were incubated for 5 min with a 0,85% sodium chloride solution, followed by washing with PBS. Subsequently, the samples were fixed in 4% paraformaldehyde in PBS for 15 min, washed again and incubated for 5 min with a 20 µg/ml proteinase K solution. The tissue was washed 3 times with PBS and then incubated with the equilibration buffer for 15 min, directly followed by application of the enzyme/nucleotide mix in equilibration buffer (30 µl equilibration buffer, 3 µl nucleotide mix, 0,33 µl TdT enzyme per slide) onto the slides. The reaction was carried out at 37°C in the dark for one hour. The enzymatic reaction was terminated by incubation in 2x SCC buffer for 15 min at room temperature in the dark, followed by two washes with PBS. The tissue was embedded in DAPI containing conservation medium (ProLong Gold, Invitrogen) and stored at 4°C in the dark.

3.3 RNA analysis

3.3.1 RNA-isolation from epithelial cells or tissue

The RNeasy Mini Kit (Qiagen) was used to isolate total RNA from epithelial cells or tissue. Epithelial cell pellets were directly lysed in RLT buffer + 1% β-mercaptoethanol by pipetting vigorously up-and down. To ensure complete homogenization of the lysate it was applied to a QIAshredder column (Qiagen) and the following steps were carried out by using the flow-through. Total intestinal tissue was as well placed in RLT buffer + 1% β-mercaptoethanol followed by mechanical disruption of the tissue (Polytron PT 1200 E). The resulting lysates or the flow-through in the case of RNA isolation from epithelial cells were mixed with an equal amount of 70% ethanol and applied to the column. After the centrifugation at maximum speed for 30 s and the removal of the flow-through, the column-bound RNA was washed once with buffer RW1 followed by

2 washes with buffer RPE. The flow-through was removed again and the column was centrifuged at maximum speed for an additional 2 min to remove residual buffer. 30 µl of RNase-free water was applied directly on the column and the RNA was eluted into a clean tube by centrifugation at maximum speed for 1 min. The RNA was stored at -80°C until further use.

3.3.2 cDNA synthesis

For cDNA synthesis, the concentration and purity of RNA was determined. Generally 1 µg of RNA was used for cDNA synthesis. First, the RNA was incubated with 1 µl of OligodT (50 µM, Invitrogen) and 1 µl of dNTP-mix (10 mM each, Invitrogen) in a final volume of 11 µl filled up with RNase-free water at 65°C for 5 min. Then the mix was incubated on ice for 2 min and 7 µl of the mastermix consisting of 4 µl 5x buffer, 1 µl DTT (0,1 M), 1 µl RNaseOUT (40 units/µl, Invitrogen) and 1 µl SuperscriptII (200 units/µl, Invitrogen) were added. The mix was briefly centrifuged and incubated at 50°C for 60 min. The resulting cDNA was diluted 1:4 with RNase-free water and stored at -20°C.

3.3.3 Realtime (RT) -PCR

The RT-PCR was carried out on a StepOnePlus Real Time PCR system (Applied Biosystems) using the appropriate primers (see table 3.2) and the SYBR Green MasterMix (Roche). The primers were designed with the software Primerexpress 1.0 and used as a primermix with a final concentration of 20 mM of each primer. For a single well 12,5 µl of SYBR-Green MasterMix was first diluted with 9,5 µl of distilled water, then 0,5 µl of cDNA as well as 2,5 µl of primermix were added. The samples were analyzed on the standard program: 50°C for 2 min, 10 min 95°C, followed by 40 cycles of 95°C for 30 s and 60°C for 1 min. The results were analyzed using the StepOne Software v2.0.2 and normalized according to the expression observed for the house keeping gene *Cyclophilin*. This was done using the equation $2^{\Delta CT_{Cyclophilin} - \Delta CT_{targetgene}}$.

Table 3.2: Primer sequences of RT-PCR primers employed

Primer	Sequence
Bcl-x F	GGT CGC ATC GTG GCC TTT
Bcl-x R	TCC GAC TCA CCA ATA CCT GCA T
C2TA F	GAC AGA GCG CCA GCT AGC C
C2TA R	CTC TCC TGG TCG CCT GCA
CD4 F	GAG GCT CAG ATT CCC AAC CA
CD4 R	GCA GCA AGC GCC TAA GAG AG
CD8 F	CGT GGT GGT GCA TGC CT
CD8 R	CCT CGA ACT CAGAGA TCC GC
CD11c F	AAC AGA GGT GCT GTC TAC ATA TTT CAT G
CD11c R	TGC TGA AAT CCT CTG GCT GG
Cdc2 F	TCG CAT CCC ACG TCA AGA
Cdc2 R	GTT TGG CAG GAT CAT AGA CTA GCA
cMyc F	AAC TAC GCA GCG CCT CCC
cMyc R	ATT TTC GGT TGT TGC TGA TCT GT
Cox-2 F	CAG CCA GGC AGC AAA TCC T
Cox-2 R	CTT ATA CTG GTC AAA TCC TGT GCT CA
Cryptdin F	CAG CCA GGA GAA GAG GAC CAG
Cryptdin R	TAG CAT ACC AGA TCT CTC AAC GAT TC
Cxcl9 F	GAACGGAGATCAAACCTGCC
Cxcl9 R	TCTTTTCCCATTCTTTCATCAGC
Cyclin B F	ACT TCA GCC TGG GTC GCC
Cyclin B R	ACG TCA ACC TCT CCG ACT TTA GA
Cyclin D1 F	CCC TGA CAC CAA TCT CCT CAA C
Cyclin D1 R	GCA TGG ATG GCA CAA TCT CCT
Cyclin E F	ATG TGG CCG TGT TTT GCA
Cyclin E R	GGT CTG ATT TTC CGA GGC TGA
Cyclophilin F	ATG GTC AAC CCC ACC GTG T
Cyclophilin R	TTC TGC TGT CTT TGG AAC TTT GTC
F4/80 F	CTT TGG CTA TGG GCT TCC AGT C
F 4/80 R	GCA AGG AGG ACA GAG TTT ATC GTG
Foxp3 F	TAG GAG CCG CAA GCT AAA AGC
Foxp3 R	TCC TTG TTT TGC GCT GAG AGT
GBP F	TCTAAAGAGCCTGGTGCAGACC
GBP R	CTCTATCTGGGCCAAAGTCAGC
Gr1 F	GCA ATG CAG CAG TTC CCA CT
Gr1 R	ATT GAA TGG ATC ATC AGA GAA AGG TC
Hsp70 F	GGT CTC AAG GGC AAG CTC AG
Hsp70 R	CGT GTT GGA GTC CAG CCA G
ICAM-1 F	GCA GTC CGC TGT GCT TTG A
ICAM-1 R	CTC CGG AAA CGA ATA CAC GGT
IDO F	AGCTGCCCGACGCATACA

31

IDO R	AGCTGCCCGTTCTCAATCAG
IFNγ F	TTA CTG CCA CGG CAC AGT CA
IFNγ R	AGT TCC TCC AGA TAT CCA GAA AGA GA
IL-1β F	GTG GCT GTG GAG AAG CTG TG
IL-1β R	GAA GGT CCA CGG GAA AGA CAC
IL-2 F	AGC AGG ATG GAG AAT TAC AGG AAC
IL-2 R	TGT GGC CTG CTT GGG C
IL-4 F	ACA GGA GAA GGG ACG CCA T
IL-4 R	GAA GCC CTA CAG ACG AGC TCA
IL-6 F	ATG GTA CTC CAG AAG ACC AGA GGA
IL-6 R	GTA TGA ACA ACG ATG ATG CAC TTG
IL-10 F	GGT TGC CAA GCC TTA TCG GA
IL-10 R	ACC TGC TCC ACT GCC TTG CT
IL-11 F	CTG CAC AGA TGA GAG ACA AAT TCC
IL-11 R	GAA GCT GCA AGA TCC CAA TG
IL-12p35 F	CAC GCT ACC TCC TCT TTT TG
IL-12p35 R	CAG CAG TGC AGG AAT AAT GTT
IL-12p40 F	AAA CCA GAC CCG CCC AAG AAC
IL-12p40 R	AAA AAG CCA ACC AAG CAG AAG ACA G
IL-13 F	AGG ACC CAG AGG ATA TTG CAT G
IL-13 R	GGG AGG CTG GAG ACC GTA G
IL-17A F	AAG TGA GCT CCA GAA GGC CC
IL-17A R	TCA TTG CGG TGG AGA GTC C
IL-17F F	CCA GGG TCA GGA AGA CAG CA
IL-17F R	CCC TCC GAA GGA CCA GGA
MPa2 F	CCG TAC AGG GAA GTC CTA TTTGAT
MPa2 R	ACG GTG GAG CCC AGA GG
Muc2 F	TCG CCC AAG TCG ACA CTC A
Muc2 R	GCA AAT AGC CAT AGT ACA GTT ACA CAG C
OAS F	CAA GGT GGT GAA GGG TGG C
OAS R	TCA AAG CTG GTG AGA TTG TTA AGG
p21 F	ATT CAG AGC CAC AGG CAC CAT
p21 R	TCT CCG TGA CGA AGT CAA AGT T
RegIIIβ/PAP F	CTC CTG CCT GAT GCT CTT AT
RegIIIb/PAP R	TTG TTA CTC CAC TCC CAT CC
SOCS1 F	CCG TGG GTC GCG AGA AC
SOCS1 R	AAG GAA CTC AGG TAG TCA CGG AGT A
STAT1 F	GAC CCT GCA GCA GAT CCG T
STAT1 R	GGT CGG GCT CAT AGG TGA ATT
Survivin F	CCT GCA CCC CAG AGC GAA T
Survivin R	AGA AAA AAC ACT GGG CCA AAT CAG
Synaptophysin F	TTC GTG AAG GTG CTG CAG TG
Synaptophysin R	TCT CCG GTG TAG CTG CCG

TGTP F	AGG TGC AGC CCC CAC TG
TGTP R	TCA CGT TGG GAA GCT TTG G
TNFα F	ACT CCA GGC GGT GCC TAT G
TNFα R	GAG CGT GGT GGC CCC T
Usp18 F	TTC GTC CAG CCC AAA GAG TTA
Usp18 R	GGC AGA TGA GTC AGC TTC AGA AC

3.3.4 RNA microarray analysis

The RNA microarray analysis was carried out by probing the Affymetrix Gene ST GeneChip (~ 28.000 genes) with RNA from epithelial cells isolated as described above. The nalysis was carried out using the SAM 3.0 software (significance analysis of microarray).

3.4 Protein analysis

3.4.1 Epithelial cell lysis for protein lysates

Epithelial cell pellets were lysed in 200 µl ice cold protein lysis buffer by mechanical homogenization with a micro-pistill. In order to ensure a complete lysis, homogenates were incubated on ice for 10 min. Finally, homogenates were centrifuged at 13200 rpm at 4°C for 10 min to pellet cell debris on the bottom of the tube. Lysates were stored at -80°C.

Protein lysis buffer (1x):   50 mM tris (pH 7,5) (Roth)

                        250 mM NaCl (Sigma)

                        30mM EDTA

                        30 mM EGTA (Sigma)

                        25 mM sodiumpyrophosphate (Sigma)

                        1% triton-X 100 (Sigma)

                        0,5% NP40 (Sigma)

                        10% glycerol (Merck)

                        1 mM DTT (Sigma)

                        50 mM β-glycerophosphate (Sigma)

                        25 mM sodium fluoride (Sigma)

                        5 mM sodium orthovanadate (Sigma)

                        2 nM PMSF (Sigma)

1 tablet of complete-protease inhibitor cocktail tablets (Roche)/50 ml

3.4.2 Immunoblot analysis

For immuoblot analysis, acrylamide gels (8 to 12 %) were casted using the "BioRad Mini Protean Gel System" (BioRad). In order to assess the protein concentration, 2µl of the lysates were mixed with 1 ml of 1:5 diluted BioRad protein assay, which was measured quantitatively in a spectrophotometer (BioRad SmartSpec Plus) at a wavelength of 595 nm. In comparison with a BSA standard curve, the protein concentration of the lysates was determined, 50 µg of protein were adjusted to a volume of 24 µl by filling up with protein lysis buffer, and 8 µl of 4x Laemmli buffer was added. The samples were heated to 95°C for 5 min, cooled down on ice, briefly centrifuged and loaded onto the gel. The gel was run at 120 volt in 1x running buffer.

Gel 8-15%:	2-3,75 ml 40% acrylamide (Merck)
	5,5-3,75 ml distilled water
	2,5 ml stacking/resolving gel buffer
	62,5 µl/50 µl 10% APS (Sigma)
	12,5 µl/5 µl TEMED (Sigma)
Stacking gel buffer:	1,5 M tris (pH 8,8)
	0,4% (w/v) SDS (Fluka)
Resolving gel buffer:	0,5 M tris (pH 6,8)
	0,4% (w/v) SDS
Laemmli buffer:	200 mM tris (pH 6,8)
	40% (v/v) glycerol
	8% (w/v) SDS
	0,4% (w/v) bromphenole blue (Sigma)
	5% (v/v) β-mercaptoethanol (Sigma)
Running buffer (10x):	9,5 M glycine (Roth)
	0,25 M tris
	35 mM SDS

The gel was blotted for 60 min at 350 mA onto a PVDF membrane (Immobilon P, Zefa Laborservice), after activation of the membrane for 15 s in methanol, in transfer buffer. The Mini Trans-Blot Cell system (BioRad) was used for the transfer

Transfer buffer stock (10x): 9,5 M glycine

0,25 M tris

Transfer buffer: 100 ml transfer buffer stock

200 ml methanol (Merck)

700 ml distilled water

After the transfer the membrane was washed briefly in PBS-T followed by a 30 min incubation in PBS-T+ 5% (w/v) skim milk (Fluka) to block unspecific binding of antibody. This was then followed by incubation with the primary antibody overnight (for antibodies and dilutions, see table 3.3). The membrane was washed 3 times for 5 min with PBS-T, followed by incubation with a 1:3000 diluted HRP-labeled secondary antibody (α-rabbit/α-mouse/α-goat, GE Healthcare) in PBS-T+ 5% (w/v) skim milk for 1 h. The membrane was washed again 3 times for 5 min with PBS-T. For detection, the membrane was incubated for 5 min with ECL solution (Super Signal West Pico or Super Signal West Femto, Thermo Scientific), briefly dried between two Whatman papers and incubated with a X-ray film (Thermo Scientific) between 10 s and 10 min. Development of the film was done using the Hyperprocessor (Amersham Bioscience).

PBS-T: PBS (Invitrogen)

0,1 % (v/v) TWEEN 20 (Sigma)

Table 3.3: Antibodies employed in western blot

Antibody	Company	#	Dilution	First Antibody in
β-Actin	Sigma	A4700	1:1000	3 % skim milk/PBS-T
Bak	Santa Cruz	832	1:500	3 % skim milk/PBS-T
Bax	BD Pharmingen	554106	1:500	3 % skim milk/PBS-T
Bcl-2	BD Pharmingen	610539	1:1000	3 % skim milk/PBS-T
Bcl-xL	BD Pharmingen	556499	1:1000	5 % BSA/PBS-T
Caspase 9	Cell Signaling	9504	1:1000	5 % BSA/PBS-T
Fas	Santa Cruz	1024	1:500	3 % skim milk/PBS-T
Hsp70	Stressgen	SPA-810	1:500	3 % skim milk/PBS-T
Mbl2	R&D	AF 2208	1:50	5 % BSA/PBS-T
Mcl-1	Santa Cruz	819	1:500	3 % skim milk/PBS-T
phospho-Stat3	Cell Signaling	9145	1:200	5 % BSA/PBS-T
Stat1	Santa Cruz	346	1:1000	3 % skim milk/PBS-T
Stat3	Santa Cruz	482	1:500	3 % skim milk/PBS-T
Survivin	Cell Signaling	2808	1:1000	3 % skim milk/PBS-T

3.4.3 Kinase assay

The kinase assay is a method which is used to determine the activity of a defined kinase within a protein lysate. To do so the kinase is immunoprecipitated with an antibody and then incubated with a recombinant substrate of the kinase together with radioactively labelled ATP. This leads to radioactive labelling of the substrate, which can be visualized on a X-ray film after the separation of the different proteins via polyacrylamide gel electrophoresis, and blotting of the proteins on a membrane.

Firstly, 15 µl of Sepharose ProteinA beads (GE Healthcare) per sample were washed 3 times with 100 µl of protein lysis buffer. Between the washing steps the beads were centrifuged at 2000 rpm for 2 min and the supernatant was discarded. Subsequently, beads were resuspended in 50 µl of protein lysis buffer, to which 1 µl of specific antibody (α-Cdc2, sc-54; α-Cdk4, sc-163, Santa Cruz) and 200-300 µg of total protein lysate were added. The volume was adjusted to a total of 500 µl with protein lysis buffer. For immunoprecipitation this mixture was incubated while being rotated for 4 hours or overnight at 4°C. Following this, the beads were washed twice with 500 µl protein lysis buffer, resuspended in 500 µl 1x kinase assay buffer and incubated while being rotated for 20 min at 4 °C. The samples were centrifuged again at 2000 rpm for 2 min and resuspended in 15 µl 2x kinase assay buffer. 15 µl of the mastermix consisting of 1 µg substrate (RB (Santa Cruz) for Cdk4, Histone H1 (Boehringer) for Cdc2), 10 mM ATP-solution, 0,5 µl [γ-32P]-ATP (Perkin Elmer) per sample were added and

incubated for 20 min at 37°C. To stop the kinase activity 7 µl of Laemmli buffer per sample were added and the samples were heated for 5 min to 95°C. After the centrifugation at 13000 rpm for 5 min to pellet the beads, 20 µl per sample were loaded on a 10 %polyacrylamide gel. The gel was run and the proteins were subsequently blotted on a PVDF membrane as described for immunoblot analysis. Signal detection occurred overnight by autoradiography at -80°C.

Kinase assay buffer (10x):   0,25 M HEPES (pH 7,5) (Invitrogen)

1,5 M NaCl

0,25 M β-glycerophosphate

0,1 M $MgCl_2$ (Fluka)

ATP-solution: 100 mM tris (pH 7,5)

10 mM ATP (Roche)

50 mM $MgCl_2$

10 mM DTT (Sigma)

3.5 Mutation analysis for *Ctnnb* mutations

To isolate DNA from paraffin embedded tissues, we used a laser capture microscope (Nikon Eclipse TE200). The paraffin tissue cuts were mounted on special slides for microdissection (membrane slides for microdissection, Medite), dried over night and H&E stained as described above without the final dehydration and embedding steps. Adenomas and intraepithelial neoplasias were identified with the help of the microscope and cut out using the laser. From these tissues, DNA was isolated using the Qiamp DNA Micro Kit (Qiagen) according to the manufacturer's protocol. In brief, the tissue was lysed in proteinase K containing buffer overnight at 56°C, the DNA was bound to a column, repeatedly washed, and eluted in distilled water. We designed primers specific for exon 3 of the mouse *Catnb1* gene, containing restriction sites for EcoR1. The PCR was carried out using approximately 5-10 ng of genomic DNA isolated from the tumors as a template as well as the specific primers at an annealing temperature of 60°C using Taq polymerase (Invitrogen). The PCR products were analysed on a 1,5% agarose gel, the specific band was cut out and cleaned up using the Qiaquick Gel Extraction Kit (Qiagen). The PCR products as well as 2 µg of the cloning vector pBluescript II KS+ were digested by adding 2 µl of EcoR1 buffer and 20 units of EcoR1 enzyme (New

England Biolabs) in a total volume of 20 µl for 1 h at 37°C. The cloning vector was additionally dephosphorylated by adding 2 µl of calf intestinal phosphatase (CIP, New England Biolabs) to the restriction sample and incubating it for another 20 min at 37°C. The vector as well as the PCR products were purified using the Qiaquick Gel Extraction Kit and ligated using 400 units of the T4 ligase (Invitrogen) in a total volume of 20 µl overnight at 4°C. For the transformation 100 µl of XL-1 bacteria were thawed on ice, 2 µl of the ligation was added and the bacteria were incubated on ice for 30 min. Heat shock was performed at 42°C for 45 s in a water bath, subsequently the bacteria were incubated for 2 min on ice and 1 ml of LB-broth was added. Cells recovered at 37°C for 1 h. Finally, the bacteria were plated on agar plates containing 100 µg/ml ampicillin (Sigma) and incubated overnight at 37 °C.

βcatex3 F: 5'-GCG AAT TCG CTG ACC TGA TGG AGT TGG A-3'

βcatex3 R: 5'-GCG AAT TCG CTA CTT GCT CTT GCG TGA A-3'

LB-broth and agar plates: 10 g tryptone (BD)

5 g yeast extract (BD)

10 g NaCl

1 l distilled water

15 g agar-agar (Roth) for plates

Single colonies were inoculated in 2 ml of LB-broth containing 100 µg/ml ampicillin and incubated overnight while shaking at 37 °C. Plasmid DNA was isolated using the Qiaprep Spin Miniprep Kit (Qiagen), therefore 2 ml of the overnight culture were transferred into an Eppendorf tube and centrifugung it at 13200 rpm for 10 min. The supernatant was discarded and the pellet was resuspended in buffer P1. By addition of buffer P2 cells were lysed, buffer P3 was added and the precipitate was pelleted by centrifugation at 13200 rpm for 10 min. The supernatant was loaded onto the column and the column-bound DNA was washed 2 times with buffer RPE. The column was dried by 2 min centrifugation and DNA was eluted with 50 µl of buffer EB. The inclusion of the PCR product into the vector was verified by the restriction analysis and

the vector insert was sequenced (GATC Biotech, Konstanz) using M13 primers and compared to the unmutated sequence.

M13 F: 5'-TGT AAA ACG ACG GCC AGT-3'

M13 R: 5'-CAG GAA ACA GCT ATG ACC-3'

3.6 Statistics

Counting of proliferation and apoptosis was carried out in a blinded fashion. Results are expressed including their standard error, significances were calculated by Student's T-test, p-values $\leq 0,05$ were considered to be significant. *$\leq 0,05$; **$\leq 0,01$; ***$\leq 0,001$.

4. Results

4.1 Intestinal epithelial cell (IEC)-specific ablation of Stat3 does not induce any overt phenotype in unchallenged animals

In order to clarify the role of Stat3 signaling in intestinal epithelial cells during colitis-associated tumorigenesis, we crossed *Stat3* floxed mice (Takeda et al., 1998) to *villin cre* transgenic mice (called in the following *Stat3^ΔIEC*). This results in excision of exon 21 of the *Stat3* gene leading to the expression of a truncated protein lacking the site of tyrosine phosphorylation which is important for the activation of the transcription factor. We confirmed ablation of full-length Stat3 protein in all epithelial lineages by immunoblot analysis of isolated intestinal epithelial cells (IEC) from the small and large intestine (Figure 4.1 A). IEC-specific Stat3 deficiency does not induce any overt phenotype, mice bred normally and *Stat3^ΔIEC* mice were born at a normal Mendelian ratio.
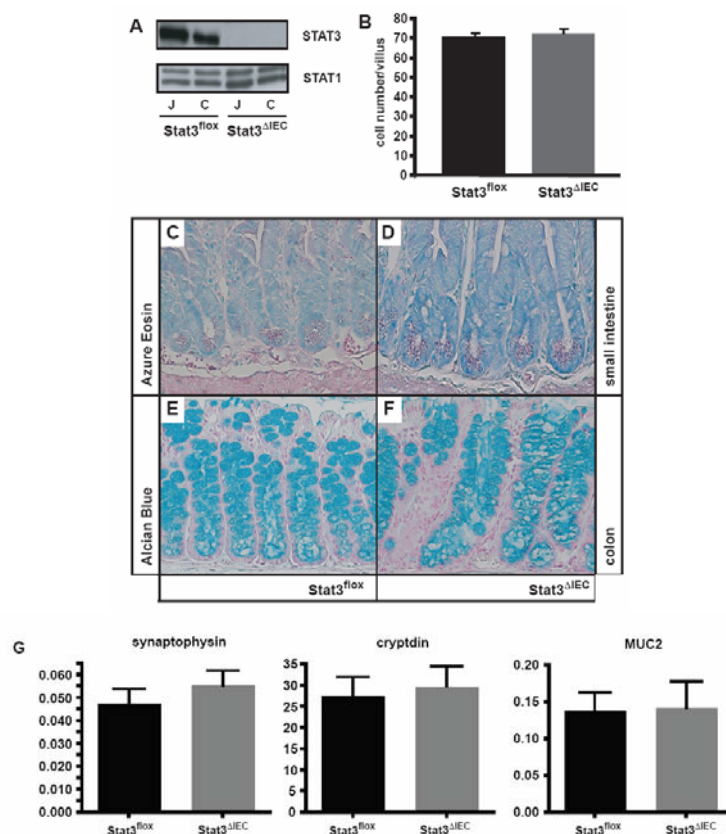
Figure 4.1: Lack of Stat3 in IEC does not affect basal proliferation rate or intestinal differentiation.
(A) Immunoblot analysis of Stat3 and Stat1 protein expression in IEC isolated from jejunum (J) or colon (C) from *Stat3^flox* and *Stat3^ΔIEC* mice. (B) Cell number per villus in unchallenged *Stat3^flox* and *Stat3^ΔIEC*. (C,D) Azure Eosin staining on sections of small intestine of *Stat3^flox* and *Stat3^ΔIEC* mice indicating the presence of normal numbers of Paneth cells. (E,F) Alcian Blue staining on colon sections of *Stat3^flox* and *Stat3^ΔIEC* mice indicating the presence of normal numbers of goblet cells. (G) Relative mRNA expression of markers for neuroendocrine (*synaptophysin*), Paneth (*cryptdin*) and goblet cells (*MUC2*) in IEC isolated from of *Stat3^flox* and *Stat3^ΔIEC* mice.

Stat3^ΔIEC mice were healthy and fertile, and showed no differences in the development of the intestine concerning the cell numbers per villus (Figure 4.1 B) as well as the differentiation of the enterocytes into the different lineages shown here by an Azure Eosin (Figure 4.1 C &D) staining demonstrating equal differentiation of Paneth cells in small intestine of *Stat3^flox* and *Stat3^ΔIEC* mice and by an Alcian Blue staining demonstrating equal differentiation of goblet cells in large intestine of *Stat3^flox* and *Stat3^ΔIEC* mice (Figure 4.1 E & F). Normal differentiation of epithelial precursors into the intestinal lineages was further confirmed by analysis of the relative mRNA expression levels of *synaptophysin*, c*ryptdin* and *MUC2* as markers for the presence of neuroendocrine, Paneth and goblet cells (Figure 4.1 G).

4.2 Lack of Stat3 in IEC protects from tumor formation in a mouse model of CAC

In order to analyze the role of Stat3 during colitis-associated carcinogenesis, we exposed *Stat3^flox*, *Stat3^ΔIEC* and *gp130^Y757F* mice to the CAC challenge. *Gp130^Y757F* animals carry a mutated cytokine receptor subunit resulting in an exaggerated Stat1 and Stat3 activation in response to ligand binding (Jenkins et al., 2005; Tebbutt et al., 2002). Experiments using *gp130^Y757F* mice, were carried out in collaboration with Dr. T. Phesse and other group members of the working group of Prof. M. Ernst (Ludwig Institute for Cancer Research, Melbourne) and are displayed here with his permission. In response to the CAC challenge, all *Stat3^flox* mice showed formation of 2-6 tubular adenomas in the distal colon while *Stat3^ΔIEC* mice were almost completely protected from tumor formation (Figure 4.2 A). Only 2 out of 8 *Stat3^ΔIEC* animals developed two tumors, which were significantly smaller than the average tumors in *Stat3^flox* mice (Figure 4.2 A, B, C & D). In accordance with the results observed in *Stat3^ΔIEC* mice, the *gp130^Y757F* mice exhibited an increase in tumor frequency and size (Figure 4.2 A, B & E). To examine the reasons for the observed differences in tumor size and number, we determined the intra-tumoral proliferation rate (Figure 4.2 F) by staining for BrdU incorporation. We observed a reduction in the epithelial proliferation in *Stat3^ΔIEC* mice while *gp130^Y757F* mice exhibit an increase of 25 % compared to the proliferation rate determined for *Stat3^flox* mice. Reciprocally, TUNEL analysis revealed an increase in apoptosis in tumors occurring in *Stat3^ΔIEC* mice (Figure 4.2 H) compared to tumors in *Stat3^flox* and *gp130^Y757F* mice (Figure 4.2 G & I).
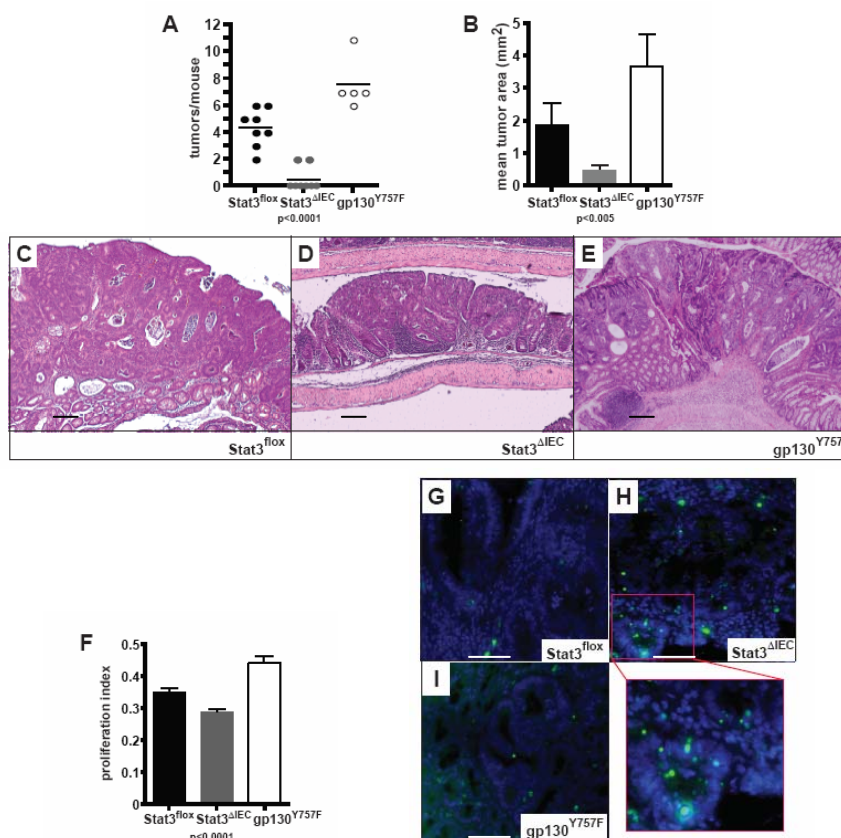
Figure 4.2: Stat3 is essential for colitis-associated tumor development. (A, B) Tumor incidence (A) and mean tumor size (B) in $Stat3^{flox}$, $Stat3^{\Delta IEC}$ and $gp130^{Y757F}$ mice after completion of the colitis-associated cancer (CAC) challenge on day 84. **(C, D, E)** Haematoxylin and Eosin (H&E)-stained sections of colons from mice at the end of the CAC challenge (day 84) showing representative adenomatous polyps protruding into the colonic lumen in $Stat3^{flox}$, $Stat3^{\Delta IEC}$ and $gp130^{Y757F}$ mice. Scale bars= 200 μm. **(F)** BrdU proliferation index of epithelial cells in polyps protruding into the lumen of $Stat3^{flox}$, $Stat3^{\Delta IEC}$ and $gp130^{Y757F}$ mice. **(G, H, I)** Assessment of apoptosis by TUNEL staining of tumors from $Stat3^{flox}$ (G), $Stat3^{\Delta IEC}$ (H) and $gp130^{Y757F}$ (I) mice on day 84 of the CAC challenge. Scale bars= 100 μm. A magnified view of the boxed area from the $Stat3^{\Delta IEC}$ mouse in (H) confirms that the TUNEL-positive signals originate primarily from epithelial cells. Note that CAC-dependent tumor incidence in $gp130^{Y757F}$ animals was compared to that in wildtype littermate controls, which showed tumor incidence and size comparable to $Stat3^{flox}$ mice and were therefore omitted from the graphs. Data are mean ± SEM. Differences between groups were analyzed by one-way ANOVA.

The results obtained with the direct Stat3 loss-of-function ($Stat3^{\Delta IEC}$) and the indirect Stat3 gain-of-function ($gp130^{Y757F}$) model indicate a dose-dependent relationship between epithelial Stat3 activation and colonic tumor incidence and growth in the CAC model. Although $Stat3^{\Delta IEC}$ mice exhibited a reduction in tumor frequency and size, these mice suffered from more severe mucosal inflammation accompanied by an increased tissue damage in response to the CAC challenge (Figure 4.3 B-F).
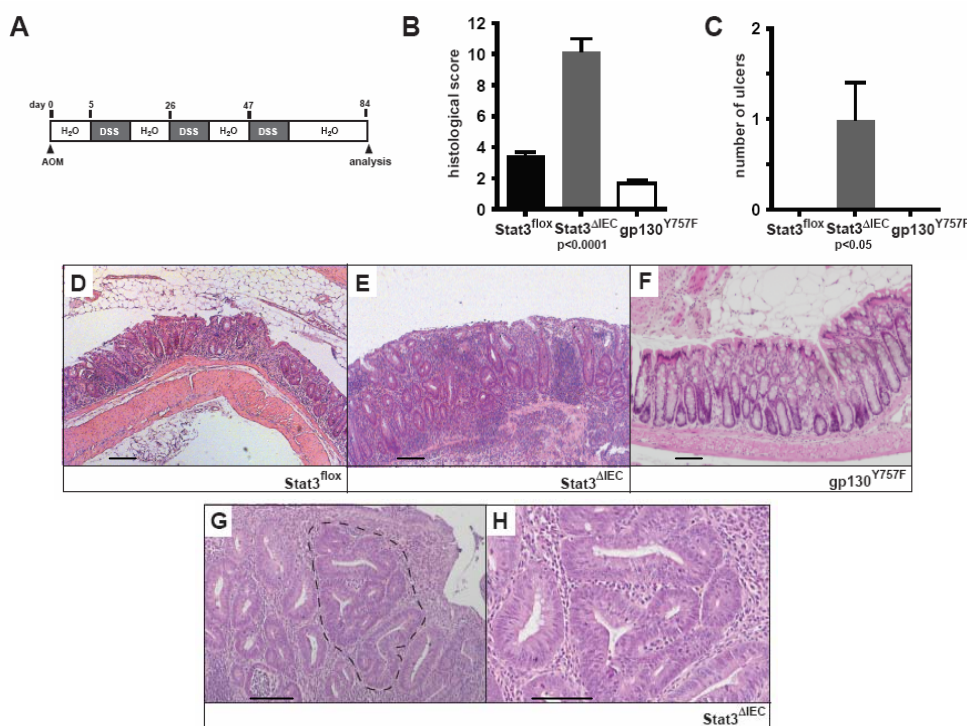
Figure 4.3: Increased epithelial damage and infiltration of inflammatory cells in *Stat3^ΔIEC* mice after completion of the CAC challenge. (A) Schematic representation of the CAC model. **(B, C)** Histological damage (B) and number of ulcers (C) in *Stat3^flox*, *Stat3^ΔIEC* and *gp130^Y757F* mice analyzed on day 84 of the CAC model. Data are mean ± SEM, n=8. **(D, E, F)** Representative H&E-stained sections demonstrating varying degrees of inflammation in mice of the indicated genotypes. Scale bars= 200 μm. **(G, H)** Representative H&E-stained sections of mulitfocal flat low-grade intraepithelial neoplasia (indicated by dashed line) frequently found in *Stat3^ΔIEC* mice at the end of the CAC challenge (G) as well as a larger magnification of this tumor precursor (H). Scale bars= 100 μm.

Scoring of mucosal tissue damage revealed an increase in *Stat3^ΔIEC* mice, while *gp130^Y757F* mice were more protected from mucosal damage in response to DSS treatment (Figure 4.3 B, D-F) compared to wildtype mice. This result was as well illustrated by the presence of ulcers only in *Stat3^ΔIEC* mice (Figure 4.3 C) at the endpoint of the CAC regimen. To determine if this increase in mucosal damage was due to the initial mutagenic challenge by administration of AOM, the regimen was carried out without the injection of AOM and the animals were sacrificed on day 84 of the model. This treatment as well resulted in an increased mucosal damage and ulcer number (Figure 4.4 A-D) in *Stat3^ΔIEC* compared to *Stat3^flox* mice. These results confirm that the more severe inflammation observed in *Stat3^ΔIEC* animals is independent of AOM treatment in *Stat3^ΔIEC* mice illustrating the protective function of Stat3 during colitis.
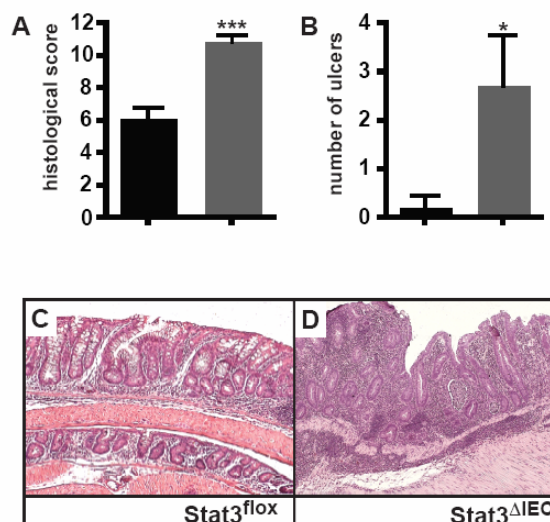
Figure 4.4: Stat3 protects from chronic DSS-induced colitis. (A,B) Histological damage (A) and ulcer number (B) in *Stat3^flox* and Stat3^ΔIEC mice analyzed on day 84 after 3 cycles of DSS in analogy to the CAC challenge, but without prior AOM injection. Data are mean ±SEM; n≥7; ***p<0.001, *p<0.05 by t-test. **(C,D)** Representative H&E-stained sections.

AOM is a pro-carcinogen which is metabolically activated, leading to missense mutations for example in exon 3 of *Ctnnb*. These mutations can lead to stabilization and nuclear translocation of β-Catenin, thereby activating the Wnt/ β-Catenin pathway (Greten et al., 2004). These mutations initiate the formation of colonic flat low-grade intraepithelial neoplasias in the CAC model which subsequently progress into tubular adenomas in *Stat3^flox* mice. *Stat3^ΔIEC* animals seldomly develop these advanced tubular adenomas at the end of the CAC regimen, instead these mice displayed numerous low-grade intraepithelial neoplasias at the end of the model (Figure 4.3 G, H). We hypothesized that these lesions represent initiated cells with stabilizing *Ctnnb* mutations which did not progress. To verify the early premalignant state of these lesions, we performed laser capture microdissection from these intraepithelial neoplastic lesions from six different animals as well as from advanced tubular adenomas from six *Stat3^flox* mice and isolated epithelial cell DNA. We performed a mutation analysis on exon 3 of the *Ctnnb* gene, as this is the important genetic region for phosphorylation and subsequent degradation of the protein. In both analyzed groups we found activating mutations confirming that the intraepithelial neoplasias in *Stat3^ΔIEC* mice represent early tumor precursors which leads to the conclusion that Stat3 is an important modulator of Wnt signaling–initiated tumorigenesis in CAC.

4.3 Stat3 is an essential factor for the protection of enterocytes from apoptosis during early tumor promotion

It was described previously that ablation of IKKβ in IEC reduces the tumor incidence by increasing IEC-apoptosis, thereby modulating the early stages of tumor promotion (Greten et al., 2004). To assess the molecular mechanisms of the increase in apoptosis (Figure 4.2 H) in the few tumors present in $Stat3^{\Delta IEC}$ mice, we examined the apoptosis rate at an early time point of the CAC regimen. We injected $Stat3^{flox}$ and $Stat3^{\Delta IEC}$ mice with AOM and sacrificed them 3 days after starting the DSS administration, which corresponds to day 8 of the CAC model (Figure 4.5 A). Activation of the Stat3 signaling pathway occurs in IEC in response to DSS treatment predominantly in the luminal enterocytes at this time point, as revealed by immunohistochemical staining for phospho-Stat3 (Figure 4.5 B) and is absent in epithelial cells of $Stat3^{\Delta IEC}$ mice (Figure 4.5 C). Efficient induction of apoptosis was confirmed by immunhistochemical staining for cleaved Caspase 3, as well as by TUNEL staining (Figure 4.5 D-G). Enhanced apoptosis in $Stat3^{\Delta IEC}$ mice is accompanied by cleavage of Caspase 9, which remains uncleaved in $Stat3^{flox}$ mice, as visible in an immunoblot analysis of lysates of colonocytes from $Stat3^{flox}$ and $Stat3^{\Delta IEC}$ mice (Figure 4.5 H). In Stat3 proficient mice immunoblot analysis for Bcl-X$_L$, Survivin, Hsp70, Mcl-1 and Fas revealed an induction of expression of these proteins in AOM and DSS treated compared to untreated mice. This induction was absent in colonic lysates from $Stat3^{\Delta IEC}$ mice for the anti-apoptotic proteins Bcl-X$_L$, Survivin and Hsp70. This is consistent with previous results showing that *Bcl-x*, *Survivin* and *Hspa1a* (encoding Hsp70) can be transcriptionally induced by Stat3 (Yu and Jove, 2004).
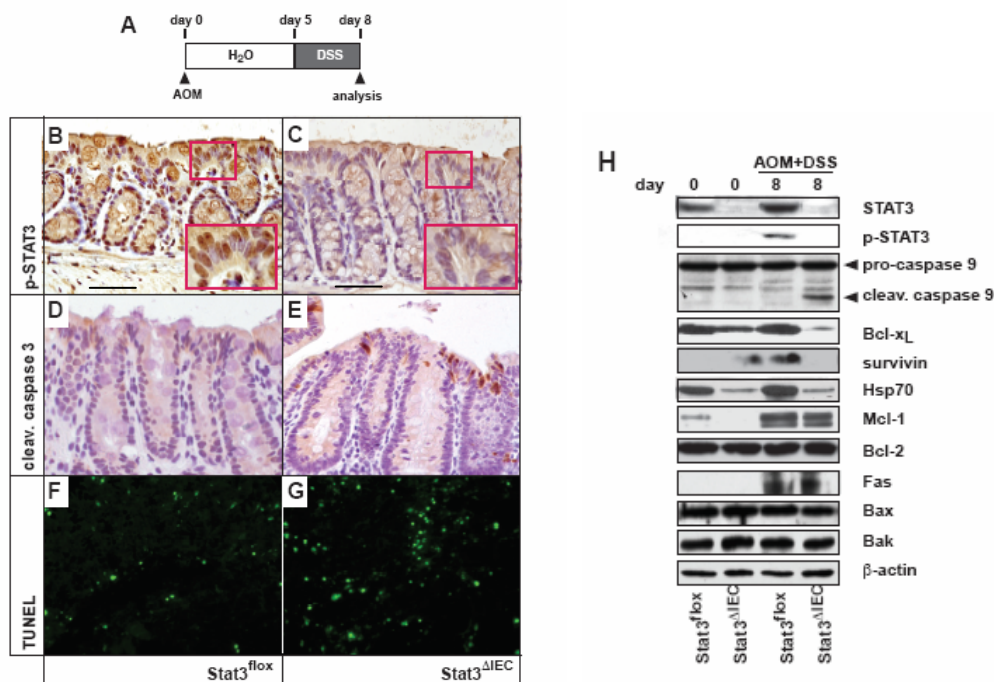
Figure 4.5: Loss of Stat3 in intestinal epithelial cells sensitizes enterocytes to apoptosis early after AOM and DSS administration. (A) Schematic representation of the early steps in the CAC challenge that result in maximal apoptotic response on day 8 of the CAC regimen. (B-G) Immunohistochemical analysis of phospho-Stat3 (B, C), cleaved Caspase 3 (D, E) and TUNEL staining (F, G) of colons from *Stat3^{flox}* mice (B, D, F) and *Stat3^{ΔIEC}* mice (C, E, G). Insets in (B) and (C) demonstrate nuclear localization of phoshpo-Stat3 in *Stat3^{flox}* mice (B) that is absent in *Stat3^{ΔIEC}* mice (C). Scale bars= 100 µm. (H) Immunoblot analysis for the indicated proteins in lysates prepared from isolated enterocytes from *Stat3^{flox}* and *Stat3^{ΔIEC}* mice at day 0 and day 8 of the CAC challenge.

The expression of other presumed Stat3 regulated genes such as *Mcl-1* and *Bcl-2* remained unchanged compared to *Stat3^{flox}* mice. The pro-apoptotic proteins Bax and Bak were constitutively expressed in unchallenged, as well as in challenged *Stat3^{flox}* and *Stat3^{ΔIEC}* mice. These results imply that the increase in the apoptotic response in *Stat3^{ΔIEC}* mice is rather dependent on an impaired induction of Bcl-x_L, Survivin and Hsp70 expression than on differential regulation of Bcl-2, Mcl-1, Bak and Bax.

4.4 *Stat3^{ΔIEC}* mice develop more severe acute colitis in response to DSS treatment and show an impaired wound healing response

DSS-induced apoptosis leads to a disruption of the intestinal epithelial barrier and thereby to a translocation of commensal bacteria into the lamina propria. This puts immune cells present in the lamina propria in contact with commensal bacteria and leads to the initiation of an inflammatory response. Upon termination of the DSS treatment the colonic epithelium starts to regenerate and inflammation resolves. This process of mucosal regeneration represents a wound-healing response which mainly involves hyperproliferation of the epithelial cells to restore normal crypt architecture in

response to the secreted inflammatory cytokines by immune cells. Termination of the inflammatory reaction is achieved by restoration of the epithelial barrier and upregulation of immune-suppressive cytokines. We hypothesized that $Stat3^{\Delta IEC}$ mice would develop more acute colitis in response to the more severe apoptotic response in these animals. This could be confirmed by the body weight curve during the first cycle of AOM/DSS administration, $Stat3^{\Delta IEC}$ mice loose significantly more body weight than $Stat3^{flox}$ mice (Figure 4.6 A) and also show an impairment in regaining their initial body weight after termination of the DSS treatment. This delay in the induction of the healing phase is also visible in H&E stained sections from mice sacrificed 5 days after termination of the DSS treatment (corresponding to day 15 of the CAC model). $Stat3^{\Delta IEC}$ clearly show a widespread destruction of the epithelial architecture
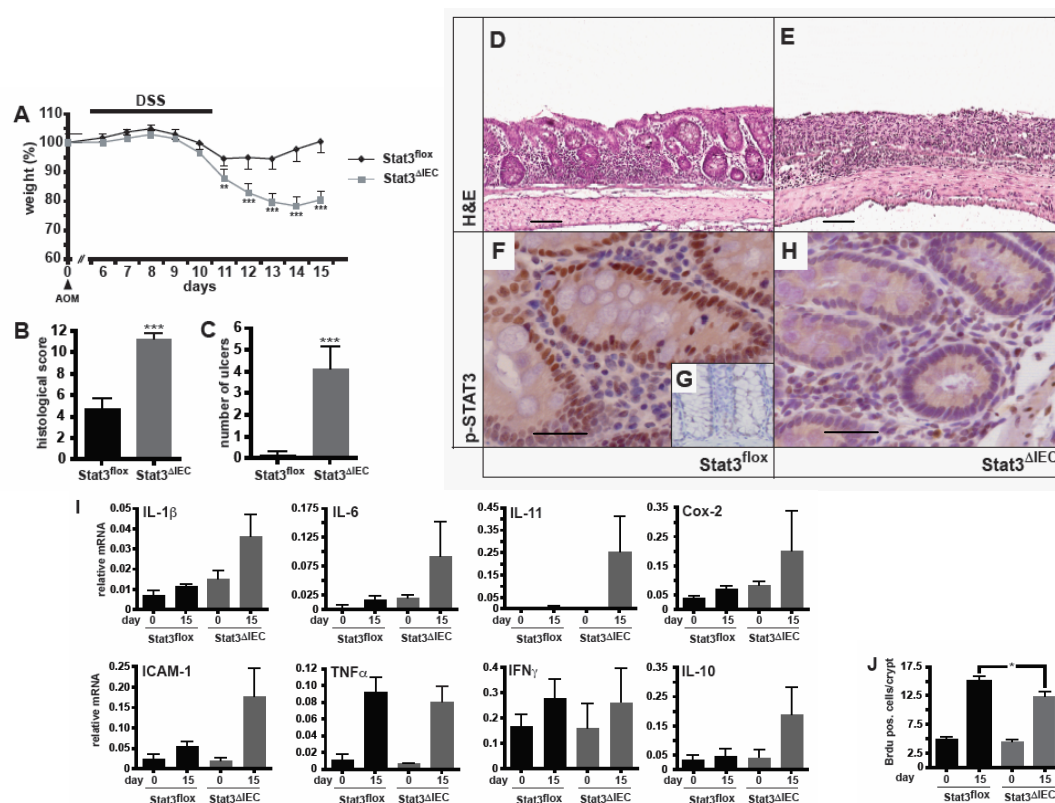

Figure 4.6: $Stat3^{\Delta IEC}$ **mice develop more acute ulcerative colitis during the CAC regimen and show impaired mucosal wound healing. (A)** Changes in body weight of $Stat3^{flox}$ and $Stat3^{\Delta IEC}$ mice during the first cycle of acute DSS-induced colitis. Five days after AOM treatment, mice were administered 3,5 % DSS in the drinking water for 5 days, followed by a 5 day recovery phase on normal drinking water. All mice were sacrificed and analyzed on day 15 of the CAC regimen. Data are mean ± SEM, n≥7; **p<0,01;***p<0,001 by t-test. **(B, C)** Histological damage (B) and number of ulcers (C) in $Stat3^{flox}$ and $Stat3^{\Delta IEC}$ mice analyzed at day 15 of the CAC model. Data are mean ± SEM; n≥7;***p<0,001 by t-test. (D-H) Representative H&E- stained sections **(D, E)** and immunohistochemical analysis of phospho-Stat3 **(F, G, H)** of colons from $Stat3^{flox}$ (D and F) and $Stat3^{\Delta IEC}$ mice (E and H) at day 15 of the CAC model or in an unchallenged $Stat3^{flox}$ mouse. Scale bars=100 µm. **(I)** Relative expression levels of mRNAs encoding for the indicated cytokines determined from whole colonic mucosa of $Stat3^{flox}$ and $Stat3^{\Delta IEC}$ mice at day 15 of the CAC model and analyzed by real-time PCR. Data are mean ± SEM, n≥3. **(J)** BrdU proliferation index in colonic enterocytes of $Stat3^{flox}$ and $Stat3^{\Delta IEC}$ mice on day 0 and day 15 of the CAC challenge. Data are mean ± SEM, n≥7; *p<0,05 by t-test.

(Figure 4.6 B & E) which is replaced by large areas of inflammatory cells and large numbers of ulcerations (Figure 4.6 C) compared to *Stat3^flox* mice which show a more preserved epithelial structure (Figure 4.6 D & E). We confirmed activation of the Stat3 signaling pathway by immunohistochemical staining for phospho-Stat3 which revealed positive staining in *Stat3^flox* colonocytes (Figure 4.6 F) which is absent in *Stat3^ΔIEC* and untreated *Stat3^flox* mice (Figure 4.6 H & G). Consistent with the more severe inflammation in *Stat3^ΔIEC* mice in response to the increased epithelial damage, the mRNAs encoding IL-1β, IL-6, IL-11, Cox-2, ICAM-1 and IL-10 were elevated in the colonic mucosa compared to *Stat3^flox* mice (Figure 4.6 I) while TNFα and IFN-γ levels were equally elevated in *Stat3^ΔIEC* and *Stat3^flox* mice compared to untreated animals of the same genotypes. BrdU incorporation studies revealed an impairment in proliferation at this time point in *Stat3^ΔIEC* mice (Figure 4.6 J). To address the question whether these changes in the expression of inflammatory cytokines are mediated by or lead to changes in the composition of the inflammatory cells in the lamina propria of these mice, we measured the expression levels of mRNAs coding for different cell surface markers or transcription factors as a mean to assess the number of different cell types present. We measured the mRNA coding for CD4, CD8, Foxp3 and CD11c representing the relative presence of T-helper, cytotoxic, regulatory T-cells and dendritic cells within the lamina propria of *Stat3^flox* and *Stat3^ΔIEC* mice on day 15 of the CAC model. These did not reveal any differences between the two genotypes (Figure 4.7).
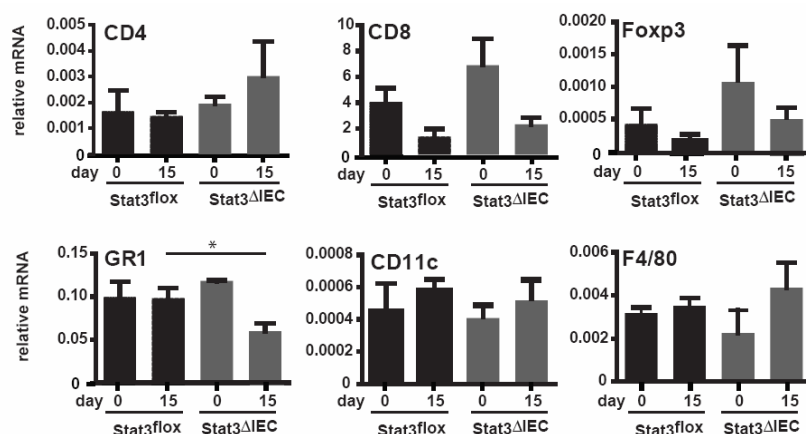

Figure 4.7: Loss of Stat3 in IEC leads to a reduction in Gr1+ expression in the lamina propria after DSS treatment. Relative expression levels of cell surface markers of different immune cell subsets from whole colonic mucosa of *Stat3^flox* and *Stat3^ΔIEC* mice at day 15 of the CAC model analyzed by real-time PCR. Data are mean ± SEM, n≥3. *p<0,05 by t-test.

The expression of the mRNA encoding the surface marker Gr1, representing neutrophils within the lamina propria, was significantly decreased in $Stat3^{\Delta IEC}$ mice after DSS treatment, while the expression level of the mRNA coding for F4/80 as a marker for the presence of macrophages was insignificantly upregulated (Figure 4.7) on day 15 of the model.

4.5 Stat3 controls cell cycle progression by regulating key factors at G1/S and G2/M phase transition

To analyze the target genes involved in the hyperproliferative response in tumors of the $gp130^{Y757F}$ mice (Figure 4.2 F), we isolated RNA of IEC at day 12 of the CAC model (Figure 4.8 A), at the height of the proliferative response elicited in response to the DSS treatment, and performed quantitative PCR analysis for the expression of mRNAs encoding the cell-cycle regulating proteins Cyclin D1, Cyclin D2, Cyclin E, c-Myc, Cdc2, Cyclin B and p21 (Figure 4.8 B). We observed a marked increase in the expression of the mRNA encoding the G1/S phase proteins Cyclin D1 and c-Myc, while the expression of the mRNAs encoding Cyclin D2 and Cyclin E remained unaltered between $gp130^{Y757F}$ mice and wildtype animals. Looking at the G2/M phase proteins Cyclin B1 and Cdc2, a transcriptional increase was observed.
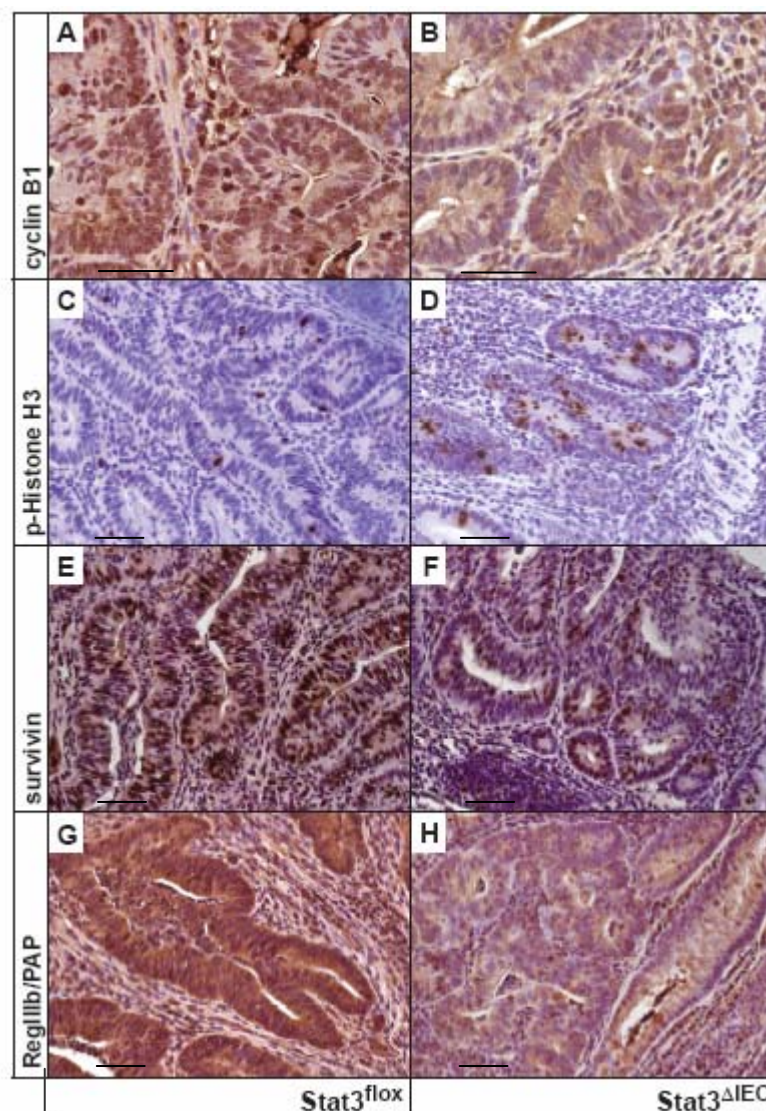
Figure 4.8: Stat3 controls expression of G1/S and G2/M regulators. (A) Schematic representation of the initial steps of the CAC challenge that results in maximal proliferative response on day 12 of the CAC regimen. (B) Expression of the cell-cycle and apoptosis regulators in isolated IEC of wildtype (wt, black bars) and $gp130^{Y757F}$ mice (white bars) before or at day 12 of the CAC challenge. Relative expression levels of mRNAs were determined by real-time PCR. Data are mean ± SEM. (C) Immunoblot analysis of Cyclin D1 and immunocomplex kinase assay of Cdk4 and Cdc2 prepared from isolated IECs of wt, $gp130^{Y757F}$ and $Stat3^{\Delta IEC}$ mice before or at day 12 of the CAC challenge. (D) Relative expression levels of mRNAs encoding c-Myc and p21 in $Stat3^{flox}$ (black bars) and $Stat3^{\Delta IEC}$ mice (grey bars) at day 12 of the CAC challenge. Data are mean ± SEM.

This suggests a stimulatory effect of Stat3 for transition from G1 into S-phase and G2 into M-phase and is consistent with the downregulation of the mRNA coding for the Cdk inhibitor p21^{cip}. To confirm this effect on protein level, we performed immunoblot analysis of Cyclin D1 and immunocomplex kinase assay of Cdk4 and Cdc2 on protein lysates prepared from wildtype, $gp130^{Y757F}$, $Stat3^{flox}$ and $Stat3^{\Delta IEC}$ mice on day 12 of the regimen. This revealed an increase in Cyclin D1 protein expression in $gp130^{Y757F}$ mice and a lack in induction of expression in $Stat3^{\Delta IEC}$ mice (Figure 4.8 C), as well as a more pronounced kinase activity for Cdk4 and Cdc2 in $gp130^{Y757F}$ mice compared to an impaired induction in $Stat3^{\Delta IEC}$ mice.

Figure 4.9: Loss of Stat3 induces a mitotic arrest in preneoplastic lesions. (A-H) Immunohistochemical analysis of Cyclin B1 (A and B), phospho-Histone H3 (C and D) , Survivin (E and F), RegIIIb/PAP (G and H) in tumors from $Stat3^{flox}$ (A, C, E, G) and intraepithelial neoplasias found in Stat3$^{\Delta IEC}$ mice (B, D, F, H) at the end of the CAC model on day 84. Scale bars= 100 μm.

This result was accompanied by an impaired induction of c-Myc and a lack in downregulation of the mRNA encoding p21 (Figure 4.8 D) in $Stat3^{\Delta IEC}$ mice, further underlining our findings that the expression of these are dependent on the extent of Stat3 activation. Meanwhile, a strong nuclear expression of Cyclin B1 in the epithelial components of the AOM-induced tumors in $Stat3^{flox}$ mice was almost completely absent from the polyp precursors in $Stat3^{\Delta IEC}$ mice, as visible in an immunohistochemical analysis of paraffin sections from day 84 of the model (Figure 4.9 A & B). Intraepithelial neoplastic lesions from $Stat3^{\Delta IEC}$ mice showed an accumulation of the M-phase cell cycle marker phospho-Histone H3 (Figure 4.9 D) compared to the adenomas formed in $Stat3^{flox}$ mice (Figure 4.9 C). This strongly suggests that lack of Stat3 in AOM-mutagenized IEC leads to a mitotic growth arrest and the persistence of the polyp

precursors without progression into adenomas as shown in Stat3 proficient mice. Finally, we wished to analyze whether the anti-apoptotic response observed in Stat3-proficient mice during the early phase of DSS challenge would persist throughout the phase of maximal wound healing. We could verify this by analyzing the mRNA expression levels of the anti-apoptotic proteins Bcl-x_L and Survivin which were transcriptionally induced in wildtype mice in response to DSS treatment and which showed a significant increase in expression in $gp130^{Y757F}$ mice (Figure 4.8 B). At this time point a more pronounced induction of the mRNA of *RegIIIb/PAP* was noted. Expression of RegIIIb/PAP and Survivin was strongly decreased in intraepithelial neoplastic lesions from *Stat3$^{\Delta IEC}$* mice (Figure 4.9 F, H), while adenomas from Stat3-proficient mice showed a highly induced expression of these proteins (Figure 4.9 E, G) on day 84 of the CAC model.

4.6 The hyperproliferative effect in $gp130^{Y757F}$ mice is dependent on non-haematopoietic cells and is induced by IL-6, as well as by IL-11

Gp130^{Y757F} mice show an enhanced hyperproliferative response to DSS administration, this was confirmed by BrdU incorporation studies after one cycle of DSS administration (Figure 4.10 A, B). We took advantage of this finding to verify that the hyperproliferative response in these animals is dependent on hyperactivation of the signaling pathway in the epithelial cell compartment and not in the haematopoietic compartment. Therefore we performed reciprocal bone-marrow transplantation, challenged these animals with one cycle of DSS and determined the change in BrdU positive epithelial cells in colonic crypts compared to wildtype animals. *Gp130^{Y757F}* mice exhibited an increase of about 70% more BrdU-positive cells compared to wildtype animals. This value remained between 60 and 70% for $gp130^{Y757F}$ mice receiving bone-marrow either from wildtype or $gp130^{Y757F}$ mice, it was only reduced to a value of about 20% in wildtype animals receiving bone-marrow from $gp130^{Y757F}$ mice (Figure 4.10 C). This indicates that the hyperproliferative response in $gp130^{Y757F}$ mice mainly results from hyperactivation of the pathway in the epithelial cell compartment. Previous work using the $gp130^{Y757F}$ mice in a mouse model of inflammation-associated gastric cancer demonstrated that rather IL-11 than IL-6 signaling drove tumorigenesis (Ernst et al., 2008), while IL-6 has been proposed to play this role in the CAC model (Becker et al., 2004). We therefore wished to examine if IL-11 as well contributes to the hyperproliferative response observed in colonocytes of $gp130^{Y757F}$ mice. To address this question, we generated $gp130^{Y757F}/Il11r^{-/-}$ and $gp130^{Y757F}/Il6^{-/-}$ double mutants, as well

as triple mutant $gp130^{Y757F}/Il11r^{-/-}/Il6^{-/-}$ mice. While double mutant mice showed no significant reduction in their hyperproliferative response to DSS treatment compared to $gp130^{Y757F}$ mice, triple mutant mice lacking IL-6 as well as IL-11 signaling exhibited a significant reduction in BrdU-positive IECs after DSS challenge (Figure 4.10 D), suggesting a redundant activity for these two cytokines in eliciting a gp130/Stat3-dependent proliferative mucosal response. To address the question which cell type is mainly responsible for the secretion of these cytokines in the colonic mucosa in response to DSS challenge, we transplanted bone-marrow from mice carrying a transgene for the expression of the diphtheria toxin receptor under the control of the CD11c promoter, enabling the targeted deletion of these cells by multiple injections of the toxin. After DSS administration on day 6, the expression of the mRNA encoding for IL-11 was markedly reduced in the colonic mucosa of animals depleted for CD11c positive cells, while the mRNA encoding for IL-6 showed only a slight reduction compared to levels in wildtype animals (Figure 4.10 E). This implies that dendritic cells which most highly express the cell surface marker CD11c are the main producers of IL-11 in response to DSS challenge and that these cells as well contribute to IL-6 production.
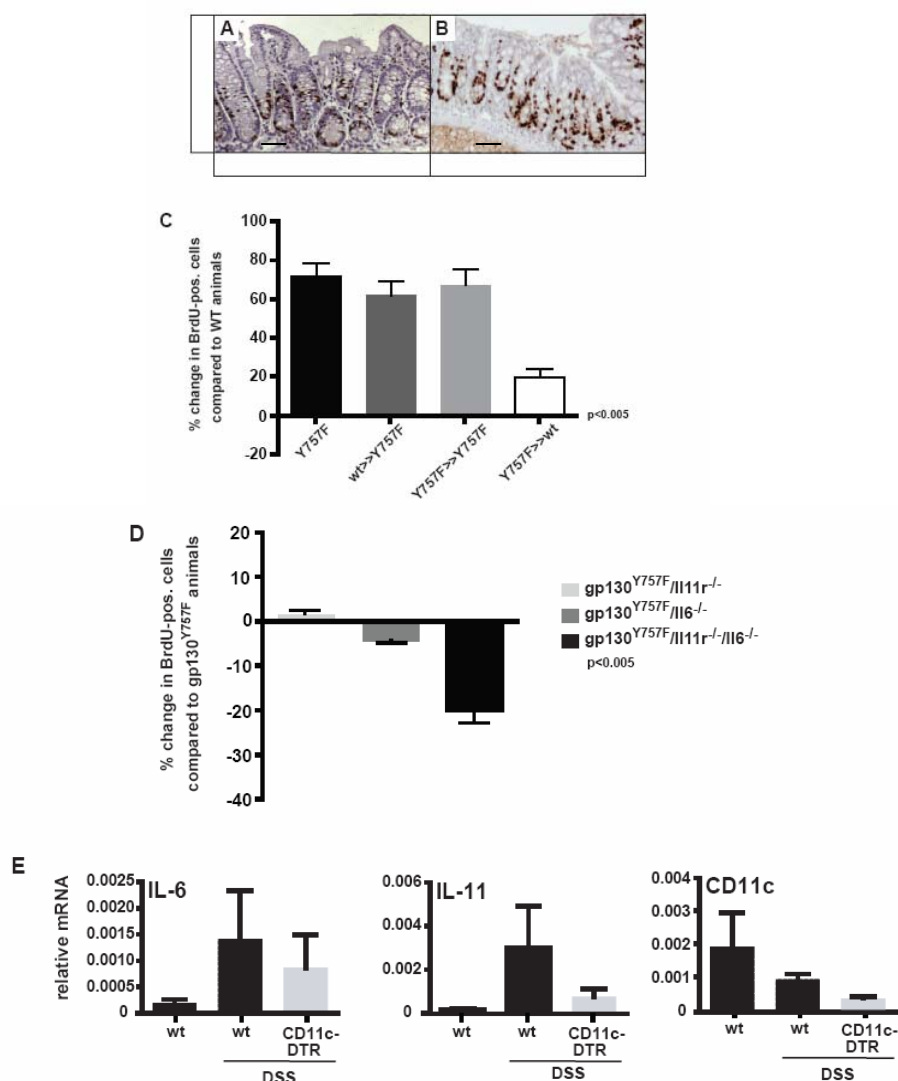
Figure 4.10: The hyperproliferation observed in *gp130^Y757F* mice during DSS-induced colitis is mediated by non-haematopoietic cells and is dependent on IL-6 as well as on IL-11.
(**A, B**) BrdU incorporation in colonic crypts of wildtype (A) and *gp130^Y757F* (B) mice after one cycle of DSS-induced colitis, 1 day after termination of DSS administration. Scale bars = 100 μm. (**C**) Relative change of BrdU incorporation in colonic crypts of *gp130^Y757F* mice or respective bone marrow-transplanted mice compared to wildtype mice after one cycle of DSS-induced colitis (wt >>Y757F indicates wildtype bone marrow transplanted into *gp130^Y757F* recipient mice). (**D**) Relative change in BrdU incorporation in colonic crypts of *gp130^Y757/Il11r^-/-*, *gp130^Y757F/Il6^-/-*, and *gp130^Y757F/Il11r^-/-/Il6^-/-* compound mutants compared to single-mutant *gp130^Y757F* mice after one cycle of DSS-induced colitis. BrdU-positive cells were only determined in well-orientated crypts. Data are average of 15 crypts/mouse, n≥5. Data are mean ± SEM. Differences between genotypes were analyzed by one-way ANOVA. (**E**) Relative expression levels of mRNAs for IL-6 and IL-11 in total tissue of unchallenged wildtype mice, DSS-treated wildtype mice and DSS-treated mice depleted of CD11c-positive cells were determined by real-time PCR. Data are mean ± SEM.

4.7 Lack of Stat3 prolongs survival in a model of sporadic intestinal carcinogenesis

β-Catenin activation and thereby hyperactivation of the Wnt signaling pathway is thought to be an early event during sporadic intestinal carcinogenesis. To address the question if Stat3 as well plays a role during sporadic intestinal carcinogenesis, we crossed *Stat3^flox^* mice to mice carrying a floxed *Ctnnb1* allele together with a tamoxifen-inducible *villin Cre*. Activation of the Cre recombinase upon tamoxifen gavage leads to excision of exon 3 of the *Ctnnb1* gene, resulting in the expression of a stabilized protein which fails to undergo GSK3β-mediated proteolysis (Harada et al., 1999). Thereby β-Catenin becomes constitutively activated in all epithelial cell lineages resulting in an almost complete loss of differentiated absorptive enterocytes and to an expansion of highly proliferative cells (Figure 4.12 B & D). Due to this hyperproliferative effect and loss in IEC function, single mutant *villin CreER^T2^/Ctnnb^loxEx3/wt^* (called *β-cat ^c.a.^*) show a medium survival of 23 days, whereas double mutant mice for β-Catenin and Stat3 (*β-cat^c.a.^Stat3^ΔIEC^*) exhibit a medium survival of 31 days (Figure 4.11 A). Interestingly mice of both genotypes revealed no overt histological differences at time of death (Figure 4.11 B-E).
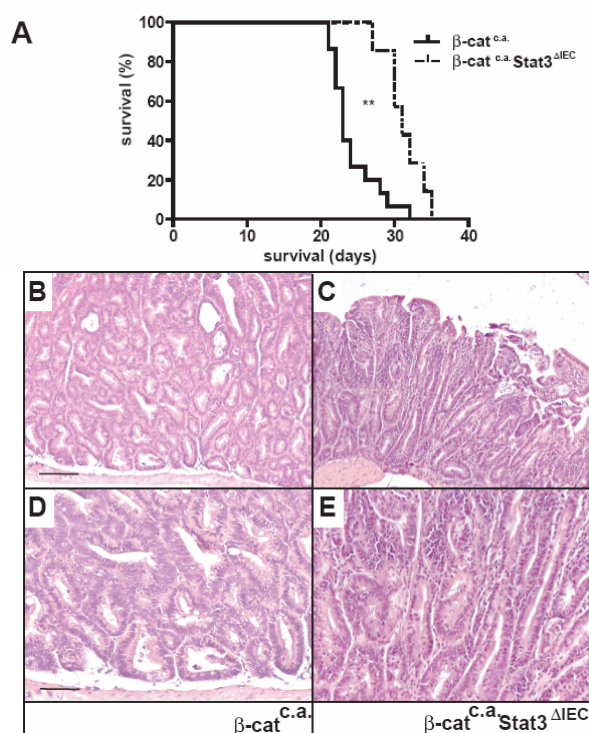
Figure 4.11: Lack of Stat3 in intestinal epithelial cells leads to prolongation of survival after conditional activation of β-Catenin by tamoxifen administration. (A) Kaplan-Meier survival curve of *β-cat^c.a.^* (n= 15) and *β-cat^c.a.^ Stat3^ΔIEC^* (n= 7) animals**. **p<0,01 by log rank test. (B-E)** Representative H&E stained sections from small intestine of *β-cat^c.a.^* (B, D) and *β-cat^c.a.^ Stat3^ΔIEC^* (D, E) animals at time of death. Scale bars (B)= 100 μm , (D)= 50 μm.

As we observed changes in the proliferation rate and induction of apoptosis in colonic epithelial cells in our CAC model, we wanted to address if these mechanisms as well account for the survival advantages after tamoxifen induced β-Catenin activation in *β-cat*$^{c.a.}$*Stat3*^{ΔIEC} animals. As we could not observe any histological differences at time of death, we carried out our analysis at an earlier time point. We chose day 15 after tamoxifen gavage, 5 days before the death of the first *β-cat*$^{c.a.}$ animal. The proliferation rate at this time point did not reveal any differences between *β-cat*$^{c.a.}$ and *β-cat*$^{c.a.}$*Stat3*^{ΔIEC} animals (Figure 4.12 I, E-F), but histologically we observed distinct differences between the two genotypes. *β-cat*$^{c.a.}$ animals as well as *β-cat*$^{c.a.}$*Stat3*^{ΔIEC} animals show hyperproliferation and villus elongation (Figure 4.12 A, C, E), additionally in the latter group of mice the villi are highly infiltrated by leukocytes (Figure 4.12 B, D).
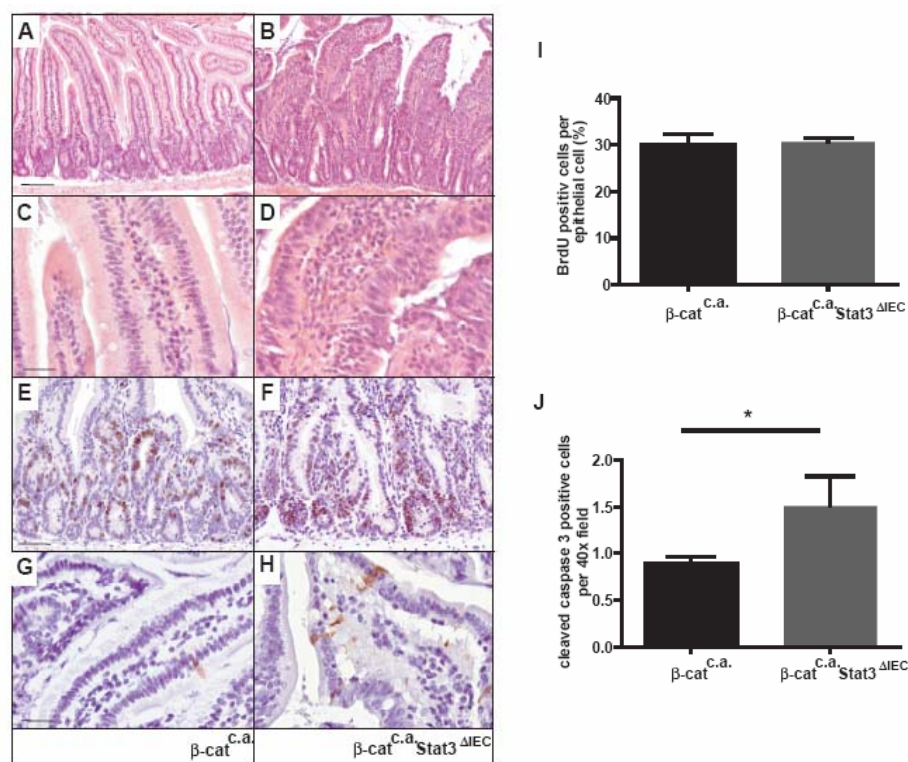
Figure 4.12: **IEC-specific ablation of Stat3 does not lead to changes in proliferation rate after induction of β-Catenin activation but leads to an increase in apoptotic cell number on day 15 after administration of tamoxifen.** **(A-D)** Representative H&E stained sections from duodenum of *β-cat*$^{c.a.}$ (A, C) and *β-cat*$^{c.a.}$*Stat3*^{ΔIEC} (B, D) animals on day 15 after tamoxifen administration showing infiltration of leukocytes in villi of *β-cat*$^{c.a.}$*Stat3*^{ΔIEC} animals. Scale bars (A)= 100 μm, (C)= 50 μm. **(E, F)** BrdU incorporation in epithelial cells in *β-cat*$^{c.a.}$ (E) and *β-cat*$^{c.a.}$*Stat3*^{ΔIEC} (F) animals on day 15 after tamoxifen administration. Scale bar= 50 μm **(G, H)** Cleaved Caspase 3 staining on sections of *β-cat*$^{c.a.}$ (G) and *β-cat*$^{c.a.}$*Stat3*^{ΔIEC} (H) animals on day 15 after tamoxifen administration. Scale bar= 25 μm. **(I)** BrdU proliferation index of IEC from *β-cat*$^{c.a.}$ and *β-cat*$^{c.a.}$*Stat3*^{ΔIEC} animals on day 15 after tamoxifen administration. **(J)** Quantification of apoptotic IEC in *β-cat*$^{c.a.}$ and *β-cat*$^{c.a.}$*Stat3*^{ΔIEC} animals by staining for cleaved Caspase 3 on day 15 of the model; n=6 of each genotype, 20 fields per animal, *p<0,05 by t-test.

Furthermore, determination of the apoptosis rate by staining for cleaved,and thereby activated, Caspase 3 revealed a significant increase in apoptotic cells especially in the villus region of *β-cat^{c.a.}Stat3^{ΔIEC}* animals compared to *β-cat^{c.a.}* animals (Figure 4.12 G, H, J). To elucidate the molecular reasons for the increase in the apoptosis rate in *β-cat^{c.a.}Stat3^{ΔIEC}*, we performed quantitative PCR analysis for the previously identified target genes of Stat3, which we found to be responsible for the increased apoptosis in colonocytes of *Stat3^{ΔIEC}* in response to DSS treatment. Surprisingly the mRNAs encoding Bcl-x_L, Survivin and Hsp70 showed no significant regulation between wildtype, *Stat3^{ΔIEC}*, *β-cat^{c.a}*, *β-cat^{c.a.}Stat3^{ΔIEC}* mice on day 15 of the model (Figure 4.13 A), although there seemed to be a slight downregulation in the expression of the mRNA encoding for Survivin in *Stat3^{ΔIEC}* and *β-cat^{c.a.}Stat3^{ΔIEC}* animals. To confirm Stat3 activation in epithelial cells we performed immunoblot analysis of lysates from IEC on day 15 of the model, which showed activation of Stat3 by phosphorylation in *β-cat^{c.a.}*, which was absent in lysates of *β-cat^{c.a.}Stat3^{ΔIEC}* animals (Figure 4.13 B). A low level of Stat3 phosphorylation was as well observable in lysates from IEC of wildtype animals. Immunoblot analysis for total Stat3 expression level confirmed absence of protein expression in *Stat3^{ΔIEC}* and *β-cat^{c.a.}Stat3^{ΔIEC}*.
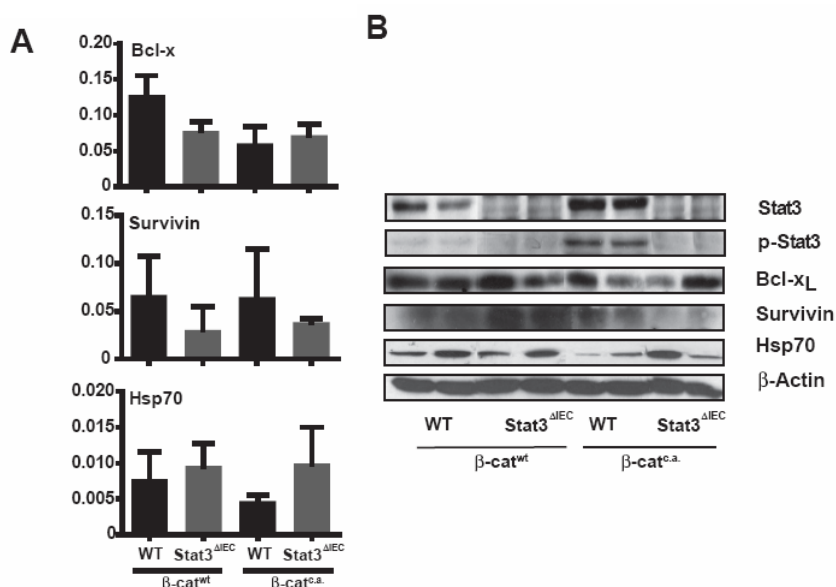
Figure 4.13: Molecular analysis of Stat3 target genes involved in regulation of apoptosis. (A) Relative expression levels of mRNA of apoptosis-related Stat3 target genes analyzed by real-time PCR. Data are mean ± SEM, n≥4. **(B)** Immunoblot analysis for the indicated proteins in lysates prepared from isolated small intestinal enterocytes from wildtype, *Stat3^{ΔIEC}*, *β-cat^{c.a}* and *β-cat^{c.a.}Stat3^{ΔIEC}* on day 15 after administration of tamoxifen.

Levels of Bcl-x_L and Hsp70 were not significantly downregulated in *β-cat^{c.a.}Stat3^{ΔIEC}* compared to *β-cat^{c.a.}* animals although expression of both proteins seemed to be slightly

downregulated compared to wildtype and $Stat3^{\Delta IEC}$ animals. Expression of Survivin showed an increase in $Stat3^{\Delta IEC}$ animals compared to wildtype animals and a decrease in $\beta\text{-}cat^{c.a.}Stat3^{\Delta IEC}$ compared to $\beta\text{-}cat^{c.a.}$ on day 15 of the model (Figure 4.13 B). Equal loading of protein amounts was confirmed by probing with α-β–actin antibody.

4.8 Survival advantage is not dependent on cell autonomous changes in proliferation or induction of apoptosis in IEC, but on activation of haematopoietic cells

As expression analysis of different Stat3 target genes which could hold responsible for the increase in apoptosis observed in $\beta\text{-}cat^{c.a}$ $Stat3^{\Delta IEC}$ mice only revealed a minor downregulation in the expression of Survivin compared to $\beta\text{-}cat^{c.a}$ animals, we wished to further elucidate the molecular mechanisms responsible for the prolongation in survival in $\beta\text{-}cat^{c.a}$ $Stat3^{\Delta IEC}$ animals. Therefore we isolated RNA from $\beta\text{-}cat^{c.a}$ and $\beta\text{-}cat^{c.a}$ $Stat3^{\Delta IEC}$ duodenal enterocytes on day 15 of the model and performed a RNA-Microarray analysis. Out of 28.000 analyzed genes 128 were upregulated ≥ 2,5 and 177 genes were downregulated ≤ 0,5 in $\beta\text{-}cat^{c.a}Stat3^{\Delta IEC}$ compared to $\beta\text{-}cat^{c.a}$ animals. Among the upregulated genes, 23 % were involved in the regulation of immune response and inflammation, while only 5 % and 1 % were found to be involved in the regulation of apoptosis and cell cycle control respectively (Figure 4.14 A). The other upregulated genes could be grouped in the regulation of metabolism, transcription, signal transduction, proteolysis, DNA repair and adhesion. Interestingly, in $Stat3^{\Delta IEC}$ animals 195 genes were as well ≥ 2,5 upregulated and 340 genes were ≤ 0,5 downregulated. Among the upregulated genes, only 6 % were involved in the regulation of the immune response and inflammation. The biggest groups of genes included genes regulating metabolism (15 %) and transcription (13 %), while a minor share of the upregulated genes could be grouped into transport, proteolysis, signal transduction and adhesion regulating genes (Figure 4.14 A). The biggest group of upregulated genes in the $\beta\text{-}cat^{c.a}Stat3^{\Delta IEC}$ include several genes involved in regulation of immune recognition (such as *C2TA*) and IFNγ-inducible genes (such as *Socs1, Cxcl9, TGTP*), we verified the upregulation of some of these by quantitative real-time PCR analysis (Figure 4.14 B) which also revealed an insignificant upregulation of most of these genes in $Stat3^{\Delta IEC}$ animals compared to wildtype mice.
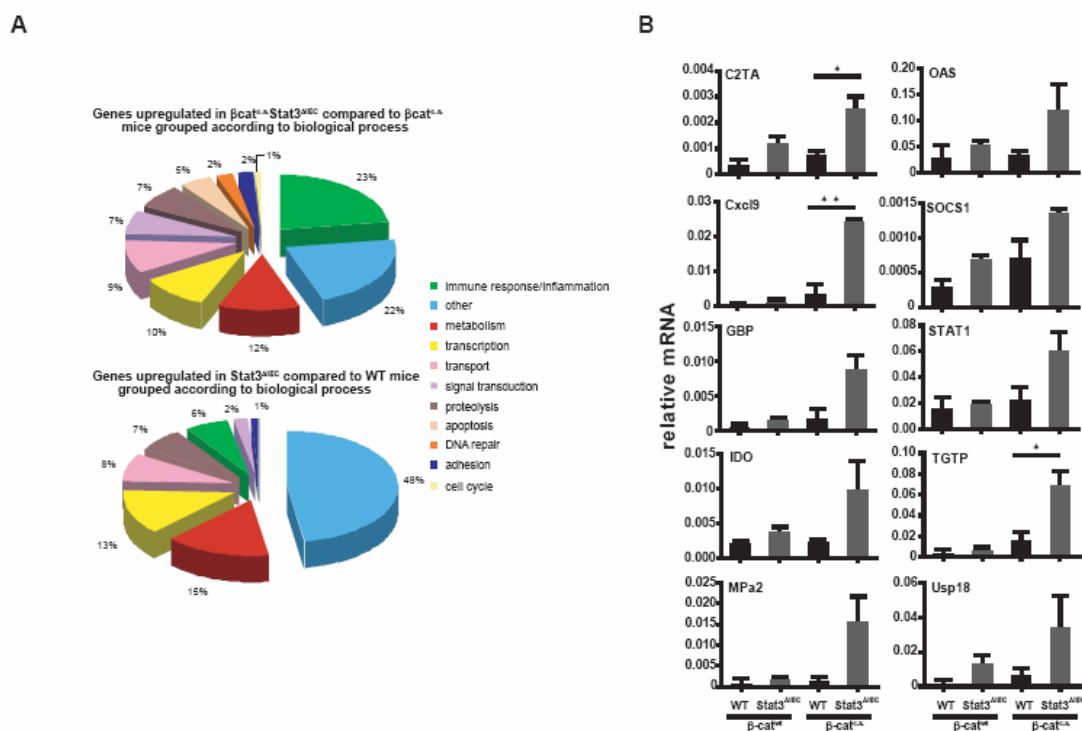
Figure 4.14: RNA-Microarray analysis of IEC of *β-cat$^{c.a}$Stat3^{ΔIEC}* animals reveals an induction of immune response/inflammation regulating genes. **(A)** Genes upregulated in *β-cat$^{c.a}$Stat3^{ΔIEC}* compared to *β-cat$^{c.a}$* animals and in *Stat3^{ΔIEC}* compared to wildtype animals on day 15 grouped according to biological process. **(B)** Relative expression levels of mRNA encoding for immune response and IFNγ induced target genes in IEC analyzed by real-time PCR on day 15 of the model. Data are mean ± SEM, n≥4. *p<0,05, **p<0,01 by t-test.

We verified upregulation of IFNγ expression in the lamina propria of *β-cat$^{c.a}$Stat3^{ΔIEC}* on day 15 by isolation of RNA from total tissue and subsequent quantitative real-time PCR analysis (Figure 4.15 A). We as well checked the mRNA expression of different other inflammatory cytokines such as IL-2, IL-4, IL-6, IL-10, IL-12 p35, IL-12p40, IL-13, IL-17 a and f (Figure 4.15A and data not shown) and found only the mRNA encoding IL-6 to be as well significantly upregulated in *β-cat$^{c.a}$Stat3^{ΔIEC}* animals. IFNγ secretion was verified by immunohistochemical staining of paraffin sections (Figure 4.15 B-F) and revealed positive cells in the lamina propria and predominantly in cells infiltrating the villus epithelium of *β-cat$^{c.a}$Stat3^{ΔIEC}* animals which were only seldom observable in *β-cat$^{c.a}$* animals (Figure 4.15 D-F). Occasionally positive stained cells were visible infiltrating the lamina propria and the villus epithelium of *Stat3^{ΔIEC}* animals (Figure 4.15 C).
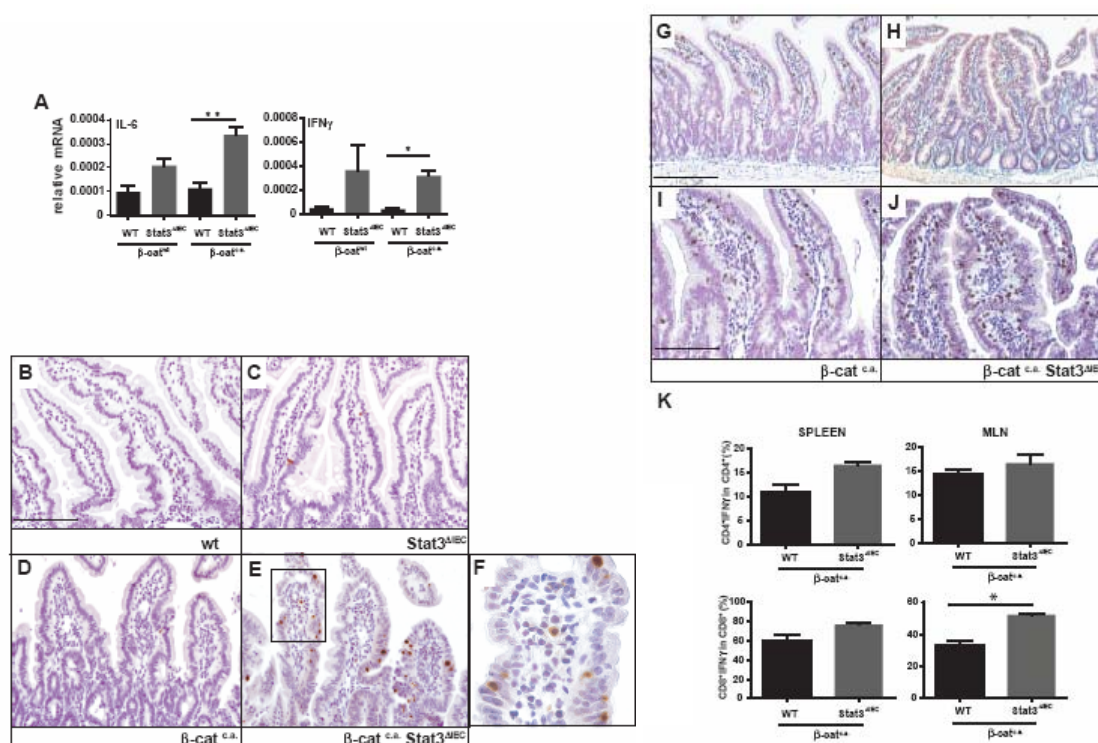
Figure 4.15: Intestinal epithelial deletion of Stat3 leads to IFNγ secretion in the lamina propria on day 15 after β-Catenin activation by tamoxifen administration. (A) Relative expression levels of mRNA encoding for IL-6 and IFNγ in the lamina propria in animals of the indicated genotype on day 15 of the model analyzed by real-time PCR. Data are mean ± SEM, n ≥4. *p<0,05, **p<0,01 by t-test. (B-F) Immunohistochemical analysis of IFNγ in sections of wildtype (B), *Stat3^ΔIEC* (C), *β-cat^c.a*(D), *β-cat^c.a.Stat3^ΔIEC* animals. (F) Magnified view of inset in (E). Scale bar= 100 µm. (G-J) Immuohistochemical analysis of CD3 in sections of *β-cat^c.a*(G&I) and *β-cat^c.a.Stat3^ΔIEC* animals (H&J). Scale bar (G)= 100 µm, (I)= 50 µm. (K) FACS analysis of T-cells isolated from spleen and mesenteric lymph node (MLN) of *β-cat^c.a* and *β-cat^c.a.Stat3^ΔIEC* animals on day 15 of the model, stimulated for 48 hours with CD3/CD28 antibody and co-stained for CD4/CD8 expression together with IFNγ expression. *p<0,05 by t-test.

IFNγ is mainly produced by activated Th1-polarized CD4^{+} T-cells, CD8^{+} cytotoxic T-cells, as well as by activated natural killer cells (Bach, 1997; Young & Hardy, 1990), although it can also be secreted by different antigen-presenting cell types (Frucht, 2001). To analyze which cell type is responsible for the IFNγ secretion in *β-cat^c.a Stat3^ΔIEC*, we performed CD3 immunohistochemical staining which showed a high increase in lamina propria infiltrating CD3^{+} cells (Figure 4.15 G-J). To test the activation status of the T-cells, we isolated total splenic cells and mesenteric lymph node cells of *β-cat^c.a* and *β-cat^c.a Stat3^ΔIEC* on day 15 of the model, which revealed a significant increase in IFNγ producing CD8^{+}-positive cells in the mesenteric lymph nodes (MLN) of *β-cat^c.a Stat3^ΔIEC* animals, as well as an insignificant increase in splenic CD4^{+}, IFNγ producing cells (Figure 4.15 K). This raised the hypothesis that activated T-cells are the source of the IFNγ in the lamina propria of *β-cat^c.a Stat3^ΔIEC* animals. To test this and to find out if the prolongation of survival observed in *β-*

cat^{c.a}Stat3^{ΔIEC} animals depended on IFNγ secretion, we depleted CD4^+ as well as CD8^+-positive cells in *β-cat^{c.a}Stat3^{ΔIEC}* animals by intra-peritoneal administration of α-CD8 and α-CD4 antibody. This revealed complete reduction of survival to the same level of *β-cat^{c.a}* animals treated with α-CD8 or α-CD4 antibody (Figure 4.16 A). *β-cat^{c.a}* animals treated with α-CD8 antibody as well showed a significant, but much less sustained reduction in survival compared to untreated *β-cat^{c.a}* animals.
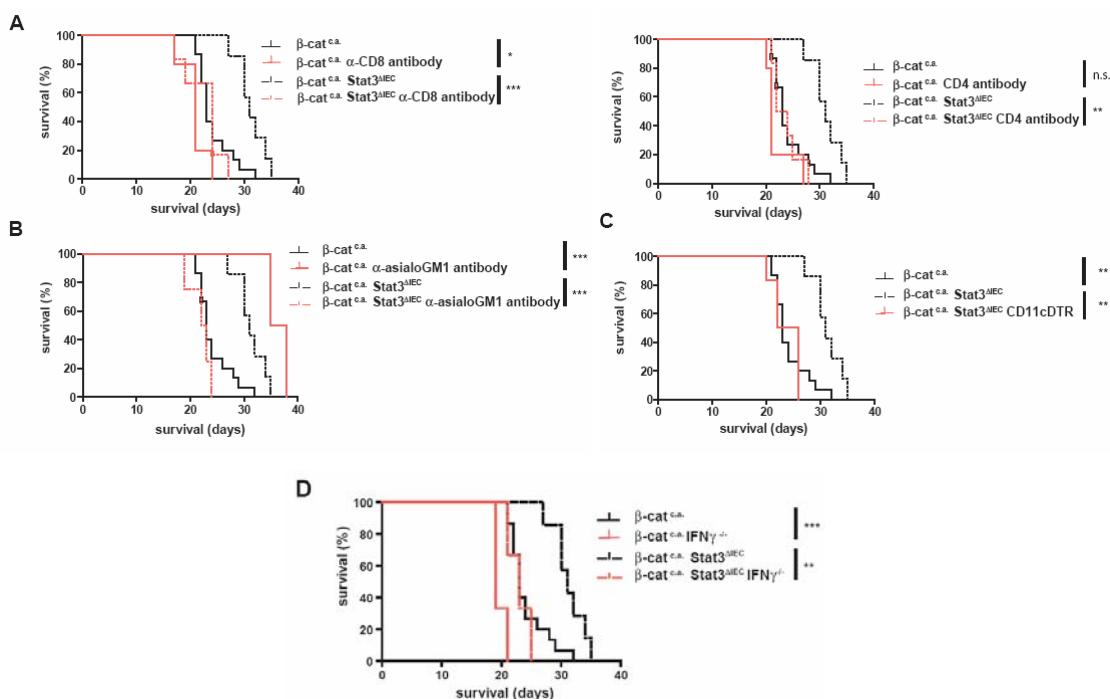
Figure 4.16: Survival advantage in *β-cat^{c.a}Stat3^{ΔIEC}* animals relies on CD4^+ and CD8^+ T-cells, NK-cells as well as CD11c^+ cells. (A) Kaplan-Meier survival curve of *β-cat^{c.a.}* and *β-cat^{c.a.} Stat3^{ΔIEC}* animals untreated (black lines) and treated with α-CD8/α-CD4 (n≥5) (red lines) antibody. **(B)** Kaplan-Meier survival curve of *β-cat^{c.a.}* and *β-cat^{c.a.} Stat3^{ΔIEC}* animals untreated (black lines) and treated with α-asialoGM1 (red lines) (n≥ 4) antibody to deplete natural killer cells. **(C)** Kaplan-Meier survival curve of *β-cat^{c.a.}* and *β-cat^{c.a.} Stat3^{ΔIEC}* animals untreated (black lines) and *β-cat^{c.a.}Stat3^{ΔIEC}* transplanted with bone marrow of *CD11cDTR* animals (n= 6) and treated diphtheria toxin (DT) (red line) to deplete CD11c^+ cells. **(D)** Kaplan-Meier survival curve of *β-cat^{c.a ·}* (n≥7), *β-cat^{c.a.} Stat3^{ΔIEC}* (n≥7), *β-cat^{c.a}IFNγ^{/-}* (n≥3) and *β-cat^{c.a.}Stat3^{ΔIEC}IFNγ^{/-}* (n≥3) mice.*p<0,05, **p<0,01, ***p<0,001 by log-rank test.

These results indicate that IFNγ production by activated CD8^+- and CD4^+-cells is an important factor for the prolongation in survival of *β-cat^{c.a}Stat3^{ΔIEC}* animals. Furthermore, natural killer cells also seem to play an important role in this phenomenon as depletion of these cells by administration of α-asialoGM1 antibody as well completely reduces the survival time of *β-cat^{c.a}Stat3^{ΔIEC}* animals to the level of untreated *β-cat^{c.a}* animals. Curiously, depletion of these cells in *β-cat^{c.a}* animals prolongs the survival of these animals significantly (Figure 4.16 B). To test if the immune cell activation in the *β-cat^{c.a}Stat3^{ΔIEC}* animals constitutes an adaptive immune

response which is dependent on antigen presentation by dendritic cells, we performed bone marrow transplantation of *CD11cDTR* animals into *β-cat^{c.a}Stat3^{ΔIEC}* animals and depleted CD11c⁺ cells by intra-peritoneal administration of diphtheria toxin every second day. This reduced survival of *β-cat^{c.a}Stat3^{ΔIEC}* animals to the level of *β-cat^{c.a}* mice (Figure 4.16 C), illustrating the important role of CD11c⁺ cells for the immune activation in *β-cat^{c.a}Stat3^{ΔIEC}* animals. The dependence of the survival advantage observed in *β-cat^{c.a}Stat3^{ΔIEC}* mice on IFNγ production was further confirmed by *β-cat^{c.a}Stat3^{ΔIEC}IFNγ^{-/-}* mice, which as well show a median survival comparable to *β-cat^{c.a}* mice (Figure 4.16 D). *β-cat^{c.a}IFNγ^{-/-}* even show a significant, but much less sustained reduction in survival compared to *β-cat^{c.a}* animals.

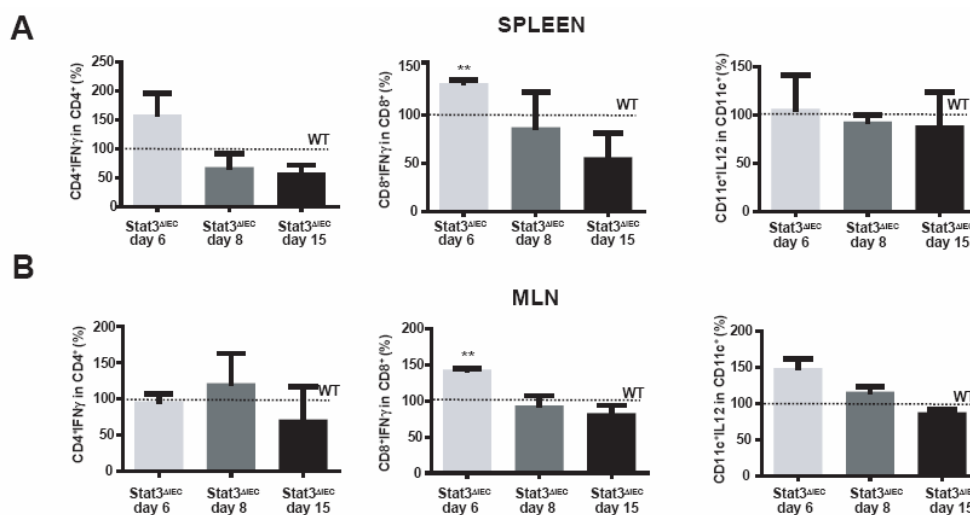**Figure 4.17: Immune cell activation is as well observable in *Stat3^{ΔIEC}* animals, but only on day 6 after tamoxifen administration. (A-B)** FACS analysis of T-cells isolated from spleen (A) and mesenteric lymph node (MLN) (B) of wildtype and *Stat3^{ΔIEC}* animals on day 6, 8 and 15 of the model, stimulated for 6 hours with PMA/Ionomycin and co-stained for CD4 or CD8 expression together with IFNγ expression and CD11c together with IL-12 expression. Depicted are 4 animals per experiment and genotype compared to the matching wildtype animals.

RNA microarray analysis and mRNA expression analysis of different immune and inflammation induced genes revealed induction of these genes in *β-cat^{c.a}Stat3^{ΔIEC}* mice, but as well to a lesser extent in *Stat3^{ΔIEC}* mice (Figure 4.14 A & B). Therefore we wished to analyze if the immune activation observed in *β-cat^{c.a}Stat3^{ΔIEC}* was as well present in *Stat3^{ΔIEC}* mice on day 15. At this time point we could not show any increase in the activation status of CD4⁺, CD8⁺ and CD11c⁺ (Figure 4.17 A & B) neither in spleen nor in MLN compared to wildtype animals. Therefore we looked at different time-points of the model and could show on day 6 after tamoxifen administration a significant increase in IFNγ secretion by CD8⁺ cells after PMA and Ionomycin

stimulation in MLN and spleen. At the same time point as well occurred an insignificant increase in IL-12 secretion by CD11c^{+} cells in MLN and in IFNγ secretion by CD4^{+} cells in spleen. This effect was not observable when looking on IFNγ and IL-12 expression on day 8 of the model. Having shown a predominantly CD8-driven IFNγ-secretion in *Stat3^ΔIEC* as well as in *β-cat^c.a Stat3^ΔIEC* animals, we wished to investigate the cause of the immune activation in these animals.

4.9 What is causing the immune activation in *β-cat^c.a Stat3^ΔIEC* animals?

IL-10 knock-out animals suffer from a barrier defect which leads to translocation of commensals into the lamina propria and possibly to activation of the immune system, therefore we hypothesized that this could as well be true in *Stat3^ΔIEC* and *β-cat^c.a Stat3^ΔIEC* animals, thereby causing an immune response in these animals. Therefore we measured the LPS-level in serum of *Stat3^ΔIEC* on day 6, the time-point of the observed immune activation (Figure 4.18 A), but could not show any differences between wildtype and *Stat3^ΔIEC* animals. Additionally, we gavaged *Stat3^ΔIEC* with FITC-Dextran and collected blood serum 4 hours later on day 6 of the model to address the same question. Here again we could not show any differences between the two groups (data not shown). This makes a barrier defect as the causing factor for the immune activation in these animals unlikely, although it is possible that the defect is not pronounced enough to be measured by the methods employed here. Among the genes most highly upregulated in *β-cat^c.a Stat3^ΔIEC*, as well as in *Stat3^ΔIEC* animals in our RNA-microarray analysis, we found the gene encoding for the complement protein Mannose-binding lectin (Mbl2). This protein is most commonly known for its role in serum to opsonize bacteria for removal by the innate immune system (Ip et al., 2009) .
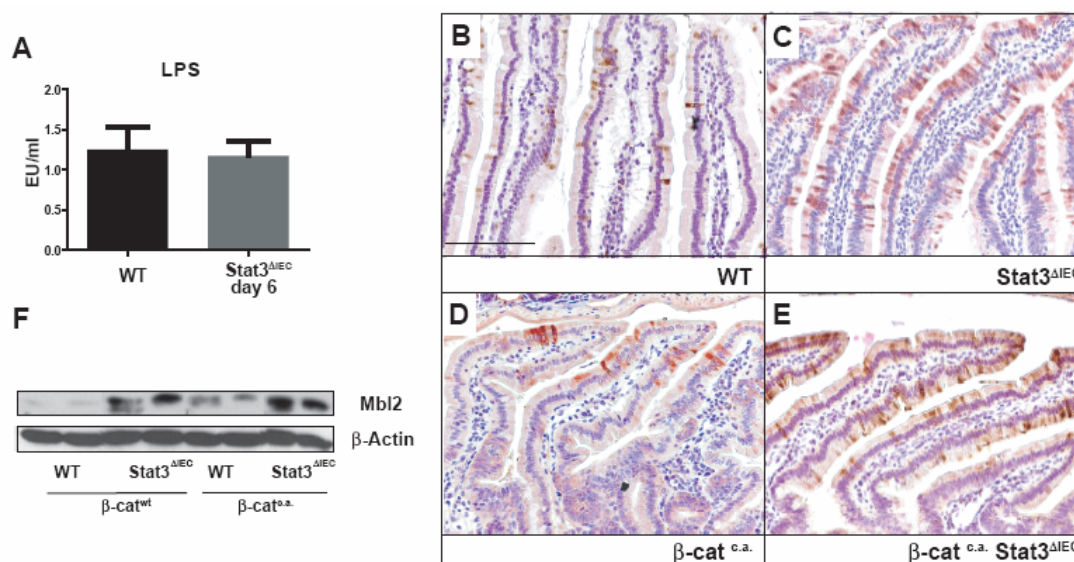
Figure 4.18: *Stat3^ΔIEC* **animals do not show an increase in serum LPS levels, but exhibit an increased expression of the complement protein Mannose-binding lectin (Mbl2). (A)** LPS level in serum of wildtype and *Stat3^ΔIEC* on day 6 as determined by LAL assay. **(B-E)** Immunohistochemical analysis of Mbl2 in sections of wildtype (B), *Stat3^ΔIEC* (C), *β-cat^c.a* (D) and *β-cat^c.a Stat3^ΔIEC* (E) animals. Magnified view of inset. Scale bar= 50 μm. **(F)** Immunoblot analysis for the indicated proteins in lysates prepared from isolated small intestinal enterocytes from wildtype, *Stat3^ΔIEC*, *β-cat^c.a* and *β-cat^c.a Stat3^ΔIEC* on day 15 after administration of tamoxifen.

In recent years, it has as well been implicated in the targeting of apoptotic cells for removal by phagocytic cells (Pittoni and Valesini, 2002), specifically to macrophages and DC which lead to a secretion of pro-inflammatory cytokines by these cells *in vitro* (Nauta et al., 2004). We could verify upregulation of Mbl2 expression *β-cat^c.a Stat3^ΔIEC*, as well as in *Stat3^ΔIEC* by immunohistochemical staining and immunoblot analysis (Figure 4.18 B-E, F). To check for an apoptotic event in unchallenged *Stat3^ΔIEC*, we performed immunohistochemical analysis for cleaved Caspase 3 on different time points before the observed immune activation on day 6 in these animals and could show that loss of full-length Stat3 protein in response to genetic recombination due to tamoxifen treatment induces a short-lived apoptotic trigger in epithelial cells on day 3 of the model (Figure 4.19 A-C, D) that resolved already on day 4 of the model. Ablation of full-length Stat3 at this early time-point could be verified by immunoblot analysis (Figure 4.19 E). In *β-cat^c.a* animals epithelial cell apoptosis takes place regularly in response to hyperactivation of the Wnt pathway as revealed by immunohistochemical analysis on day 15 of the model (Figure 4.12 G, J). We propose that epithelial cell apoptosis at an early time point of the model in *Stat3^ΔIEC* and *β-cat^c.a Stat3^ΔIEC* animals constitutes an immunogenic event either by itself or in conjunction with the overexpression of the complement protein Mbl2 and leads to priming of adaptive immune cells.
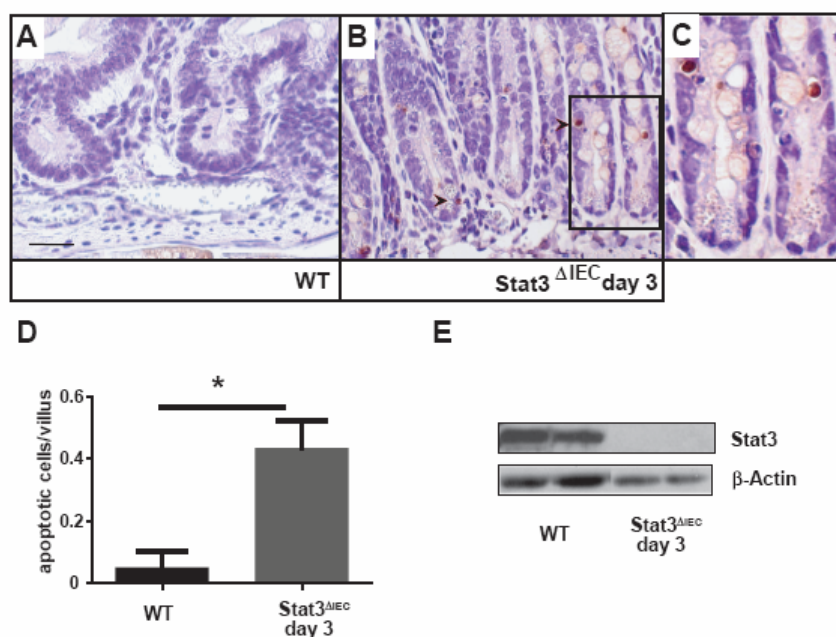
Figure 4.19: Apoptosis on day 3 in IEC of *Stat3ᴬᴵᴱᶜ* animals could be the reason for the immune activation in these animals. (**A-C**) Immunohistochemical analysis of cleaved Caspase 3 in sections of wildtype (A) and *Stat3ᴬᴵᴱᶜ* (B) animals. (C) Magnified view of inset in (B). Scale bar= 25 μm. (**D**) Quantification of apoptotic IEC in wildtype and *Stat3ᴬᴵᴱᶜ* animals by staining for cleaved Caspase 3 on day 3 of the model; n=6 of each genotype, 20 fields per animal, *p<0,05. (**E**) Immunoblot analysis for the indicated proteins in lysates prepared from isolated small intestinal enterocytes from wildtype and *Stat3ᴬᴵᴱᶜ* on day 3 after administration of tamoxifen.

4.10 What are the factors responsible for hyperactivation of the Stat3 signaling pathway in *β-cat^{c.a}* animals?

Finally, to address the question how activation of the Stat3 signaling pathway is achieved in this model, we crossed *β-cat^{c.a}* to *IL-6^{-/-}* knock-out mice, expecting to
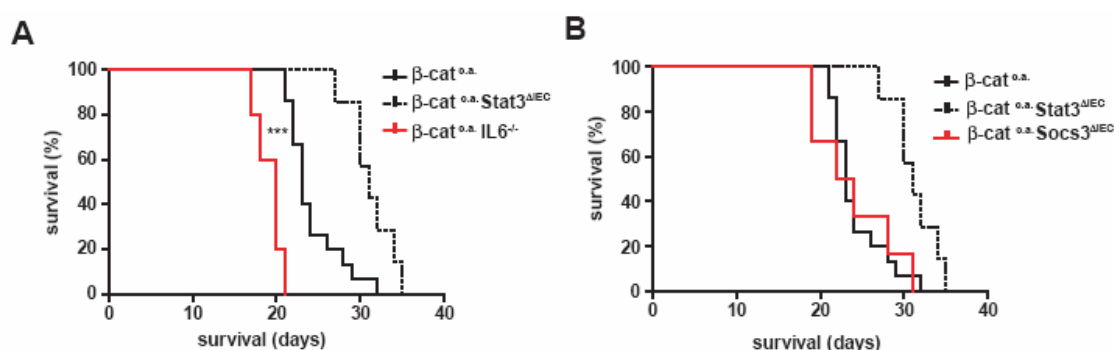

Figure 4.20: Hyperactivation of the Stat3 pathway is not induced via the IL-6/gp130 signaling pathway. (**A**) Kaplan-Meier survival curve of *β-cat^{c.a.}*, *β-cat^{c.a.}IL6^{-/-}* (n= 5) and *β-cat^{c.a.} Stat3ᴬᴵᴱᶜ* animals. ***p<0,001 by log-rank test (**B**) Kaplan-Meier survival curve of *β-cat^{c.a.}*, *β-cat^{c.a.}Socs3ᴬᴵᴱᶜ* (n= 6) and *β-cat^{c.a.} Stat3ᴬᴵᴱᶜ* animals.

achieve a similar prolongation in survival as in *β-cat^{c.a}Stat3ᴬᴵᴱᶜ* animals as IL-6 proved to be a major cytokine inducing signaling via this pathway in the CAC model. Surprisingly, ablation of IL-6 did not prolong survival in the *β-cat^{c.a}* model, but even

significantly reduced survival to a small extent (Figure 4.20 A). This fits to the result that IEC-specific ablation of the gp130 binding inhibitor Socs3 did not reduce survival of *β-cat$^{c.a}$* mice (Figure 4.20 B).

5. Discussion

Both the NF-κB and the Stat3 signaling pathway is aberrantly activated in inflammation as well as in different cancer types. In a mouse model of CAC, NF-κB activation in IEC has been shown to protect these cells from apoptosis (Greten et al., 2004). Therefore, ablation of IKKβ in IEC leads to a reduction in tumor number. Ablation of the same molecule in myeloid cells showed an impact on tumor number and size presumably by a reduced secretion of cytokines inducing the Stat3 signaling pathway. These results and others suggest that IL-6 family cytokines provide one of the missing links between inflammation and cancer (Ernst et al., 2008; Naugler and Karin 2008; Park et al., 2010). Stat3 plays a central role in the activation regulation in inflammatory cells by mediating signaling through pro-inflammatory cytokines. It constitutes a main factor in the differentiation of naive T-cells towards the Th17 subset driven by IL-6 and TGFβ (Nishihara et al., 2007). Additionally it mediates anti-inflammatory responses through IL-10, which is an important factor for immune suppression in the intestine. IL-10 knock-out animals, which lack this anti-inflammatory response, develop spontaneous enterocolitis which progresses into adenocarcinoma (Kühn et al., 1993; Berg et al., 1996). Targeted deletion of Stat3 in macrophages and neutrophils as well leads to spontaneous enterocolitis driven by a polarized Th1 immune response (Takeda et al., 1999; Alonzi et al., 2004). The dampening role for the Stat3 signaling pathway is as well important in the regulation of dendritic cell activation, as deletion in these cells leads to a hyperactivation of the immune response and the development of ileocolitis (Melillo et al., 2010). These findings are just some examples to illustrate the unique role that Stat3 plays in inflammatory cells. In our experiments, we wanted to address the role played by Stat3 in IEC during intestinal carcinogenesis.

As a main finding of our experiments we could demonstrate that ablation of Stat3 in IEC during steady-state conditions does not induce any overt phenotype, while in a colitis-associated carcinogenesis model as well as in a sporadic model of intestinal carcinogenesis, deletion of Stat3 in IEC modulated tumor development. Surprisingly, the mechanisms accounting for these differences in tumor formation differed fundamentally between the two models.

5.1 Stat3 signaling in CAC

5.1.1 Stat3 regulates apoptosis and cell-cycle progression of IEC during CAC

In the CAC model, deletion of IKKβ in IEC leads to an increase of apoptosis which is caused by the impaired induction of the anti-apoptotic protein Bcl-x$_L$. This constitutes a common finding between IEC-specific ablation of IKKβ as well as Stat3. Additionally, lack of Stat3 signaling results in an impaired induction of Hsp70 and Survivin. This is in accordance with the observation that pharmacological inhibition of IKKβ results in a reduced phosphorylation of Stat3, as well as in an impaired induction of Hsp70 in mice during acute colitis (Eckmann et al., 2008). It has been shown that Hsp70 is an important anti-apoptotic factor for IEC (Sikora and Grzesiuk, 2007) and protects from DSS-induced colitis (Tanaka et al., 2007). The anti-apoptotic protein Survivin has been shown to carry out a dual function as it has as well an important function during cell cycle regulation (Altieri, 2008). In untransformed cells, it is expressed in the G2/M phase at the spindle (Li et al., 1998) and is phosphorylated in association with Cdc2 (O'Connor et al., 2000). Knock-down with the help of small-interfering RNAs induces cell cycle arrest in human colorectal cancer cells (Rödel et al., 2005). Indeed, we could verify an impact of Stat3 signaling on epithelial cell proliferation in the tumors developed in response to the CAC regimen, as well as in the colonic epithelium directly in response to DSS treatment. In contrast, NF-κB signaling in myeloid cells, but not in IEC during the CAC model, influences epithelial cell proliferation presumably due to a reduction in the production of pro-inflammatory cytokines (Greten et al., 2004). These results suggest how myeloid NF-κB and epithelial Stat3 signaling together shape the tumor microenvironment and thereby promote tumor growth during CAC. The observed reduction in epithelial cell proliferation in Stat3 deficient animals in response to the CAC regimen was caused by a reduced expression of Cyclin B1, Cyclin D1, c-Myc and decreased kinase activity of Cdc2 and Cdk2. Cyclin D1 and c-Myc constitute known Stat3 target genes (Masuda et al., 2002; Kiuchi et al., 1999), while Cyclin B1 and Cdc2 have been associated with G2/M phase arrest after Stat3 inhibition by cucurbitacin (Liu et al., 2008; Su et al., 2008).

5.1.2 Stat3 signaling in IEC as a central factor in mucosal wound-healing

The animals lacking Stat3 expression showed a higher degree of epithelial damage in response to the CAC regimen as marked by the increase in epithelial ulcer formation and the weight development of these animals in response to acute DSS treatment. This more severe mucosal damage is not dependent on the initial mutagenic challenge by AOM injection, as Stat3 deficient animals as well show a higher degree of mucosal damage and a higher number of ulcers if AOM is omitted from the regimen. Hsp70 expression has been shown to be an important factor for epithelial balance protection after DSS-induced colitis (Tanaka et al., 2007) and is induced in an IKKβ dependent manner in the colonic mucosa (Eckmann et al., 2008). The lack of Hsp70 induction could account for the increased epithelial damage in Stat3 deficient animals. An increase in epithelial damage could as well be observed in IKKβ deficient mice in response to DSS (Greten et al., 2004). These mice also exhibit an increase in apoptosis due to a strong reduction in Bcl-x_L expression. In this model, epithelial cell proliferation remained unchanged between control and IKKβ deficient animals. On the other hand, in an in *vivo* wound-healing assay, in which wounds were induced by biopsy forceps and healing was monitored via endoscopic recording of the sizes of the wounds, Stat3 deficient animals as well showed a delayed healing response (Pickert et al., 2009). This indicates that the impaired induction of proliferation does play a role in the wound-healing defect observed in Stat3 deficient animals, as this experiment is independent of the induction of apoptosis. Another factor in the impaired mucosal wound healing response in the Stat3 deficient mice is the lack in induction of epithelial Reg3β/PAP expression. Reg3β/PAP is upregulated during acute pancreatitis, but also in DSS colitis and IBD in response to IL-6 and IFNγ (teVelde et al., 2007) and in 60% of human colorectal cancers (Macadam et al., 2000). It is presumably involved in the regulation of cell cycle progression in human colorectal carcinoma (Cao et al., 2009) and has been described to have anti-inflammatory functions (Closa et al., 2007). The incubation of mucosal tissue from active Crohn's disease patients with Reg3β/PAP reduced the secretion of pro-inflammatory cytokines and prevented TNF-α dependent NF-κB activation in monocytic and epithelial cells (Gironella et al., 2005). Furthermore, Reg3β/PAP has been shown *in vitro* to induce the aggregation of bacteria, implicating a function in host defense (Iovanna et al., 1991). Therefore, the reduced expression of this protein in colonic epithelial cells of Stat3 knock-out animals could also play an

important role in the impaired termination of the inflammatory response after DSS exposure. The differences in tumor formation between Stat3 proficient and deficient animals, as well as the differences in the resolution of inflammation could be theoretically caused by differences in the recruitment of inflammatory cells into the lamina propria after DSS exposure. We could show that the composition of the main inflammatory cell types macrophages, dendritic cells and T-cells in the lamina propria remained largely unchanged between the two groups, as well as the recruitment of regulatory T-cells. Only the mRNA encoding for the neutrophil surface marker Gr1 showed a significant reduction in the mucosa of Stat3 deficient animals. It was shown previously that IL6/Stat3 signaling constitutes an important pathway during the clearance of neutrophil assimilation which leads to the resolution of inflammation. The mRNA coding for IL-6 is highly upregulated in the lamina propria of $Stat3^{\Delta IEC}$ animals. This could be an explanation for the observed decrease in neutrophil number (Fielding et al., 2008). Along with the wound-healing defect in these animals, they also show a defect in the resolution of inflammation, as pro-inflammatory cytokines remain high in the lamina propria for a prolonged time period after short term treatment with DSS. Interestingly, we still observed a reduction in the epithelial proliferation compared to wildtype animals despite the higher level of proliferation-inducing cytokines. This underlines the importance for epithelial Stat3 activation during cell cycle progression. Although the preneoplastic lesions found in Stat3 knock-out animals exhibit activating β-Catenin mutations to the same extent as the tumors in Stat3 proficient mice, these lesions show an accumulation of the M-phase cell-cycle marker phospho-Histone H3. This suggests a cell cycle arrest in these cells rendering them incapable of progressing into adenomas. These findings imply that the canonical Wnt signaling and the Stat3 pathway intersect on common molecular targets and are required to be induced together to initiate the expression of their target genes above the threshold required for cell cycle progression. This finding is consistent with previous work showing a reduction in tumor load in $APC^{Min}/IL\text{-}6^{-/-}$ animals (Baltgalvis et al., 2008).

5.1.3 Stat3 is induced by IL-6 family cytokines in the CAC model

Stat3 signaling is induced by a plethora of cytokines and growth factor, but the main cytokine implicated in driving hyperactivation of this pathway in IBD and colorectal cancer is IL-6 (Mitsuyama et al., 2006; Becker et al., 2004). Deletion of IL-6 signaling in the CAC model resulted in a significant reduction in tumor number (Grivennikov et al., 2009), this is consistent with findings that $Socs3^{\Delta IEC}$ animals exhibit an increase in tumor burden (Rigby et al., 2007), while inhibition of IL-6 trans signaling reduces mucosal proliferation (Becker et al., 2004). Nevertheless, lack of IL-6 signaling did not completely abolish phosphorylation of Stat3 in colonic epithelial cells in response to treatment with DSS (Grivennikov et al., 2009), suggesting additional cytokines to be involved in the activation of the pathway in this setting. Pickert and colleagues (2009) suggested an important role for IL-22 in the induction of Stat3 signaling in this model, interestingly in this study the authors did not observe any differences in Stat3 phosphorylation level in $Il\text{-}6^{-/-}$ animals after induction of colitis. This finding is controversial to the findings by Grivennikov and colleagues (2009), who show a significant reduction in Stat3 phosphorylation in $Il\text{-}6^{-/-}$ animals in response to DSS treatment. In gastric tumorigenesis, it was shown previously that Stat3 signaling plays a driving role, induced by IL-11 (Ernst et al., 2008). This led us to the hypothesis that IL-11 could as well play an important role in inducing the hyperproliferation in response to DSS treatment. Indeed, $gp130^{Y757F}/Il\text{-}11r^{-/-}/Il\text{-}6^{-/-}$ mutant mice show a significant reduction in the hyperproliferative response observable in $gp130^{Y757F}$ single mutant mice. Interestingly, ablation of each of the cytokines alone was not sufficient to obtain a significant reduction in hyperproliferation, indicating a collaborative role for IL-6 and IL-11 in the induction of the Stat3 pathway in response to DSS treatment. Stat3 signaling as well plays an important role in the intrinsic regulation of different inflammatory cells as mentioned previously. Therefore, we performed bone marrow transplantation, and could verify that the hyperproliferation in the $gp130^{Y757F}$ mice is dependent on epithelial Stat3 signaling and not resulting from a hyperactivation of the pathway in the haematopoietic fraction.

IL-6 has been shown to be secreted by myeloid cells and neutrophils in response to acute DSS treatment in a NF-κB dependent manner (Greten et al., 2004) (see Figure 5.1), depending on the time point of the model it is additionally secreted by dendritic cells and activated T-cells (Grivennikov et al., 2009; Becker et al., 2004). The source of IL-11 secretion in the colonic lamina propria remained to be defined. We could identify

CD11c^{+}-cells as a major source of IL-11 secretion as the mRNA encoding for this cytokine was greatly reduced in mice challenged with DSS and depleted of CD11c^{+} cells. Consistent with the finding by Grivennikov and colleagues, IL-6 is in part secreted by dendritic cells, but is as well expressed by other cell types, therefore depletion of CD11c^{+} cells only partly reduces the expression of its mRNA.
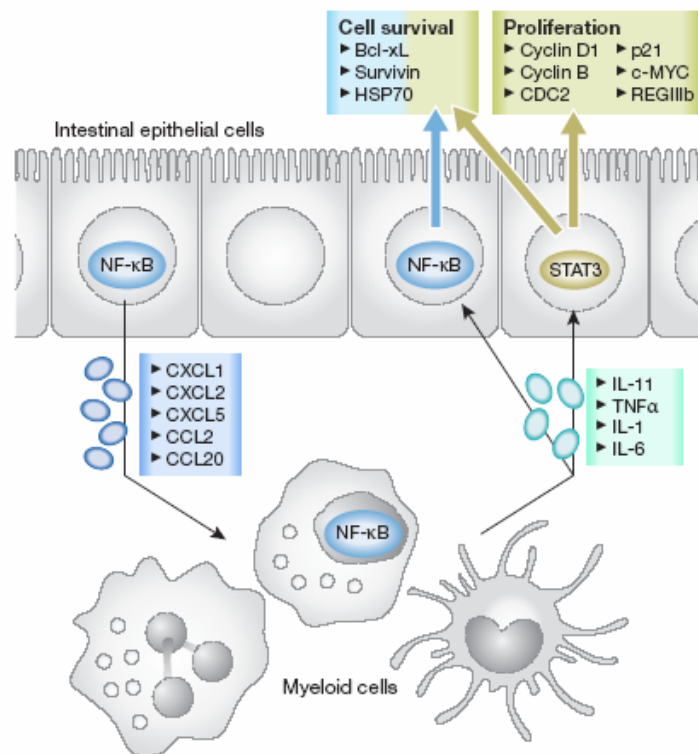

Figure 5.1.: **NF-κB activation in IEC during CAC leads to recruitment and activation of myeloid cells which in turn secrete pro-inflammatory cytokines which fuel NF-κB activation and Stat3 activation in IEC. This ensures the expression of pro-survival and pro-proliferative genes in IEC. (taken from Bollrath and Greten, 2009)**

These results suggest that dendritic cells contribute to Stat3 activation, although IL-6 production by macrophages constitutes probably the main factor in driving Stat3 activation in this model, as IKKβ deletion in myeloid cells as well significantly reduces tumor number and size (Greten et al., 2004).

5.2 Stat3 in sporadic intestinal carcinogenesis

In the model of sporadic intestinal carcinogenesis, we observed a prolongation of survival in *β-cat^{c.a}Stat3^{ΔIEC}* animals compared to *β-cat^{c.a}* animals. We could show that this survival advantage did not depend on cell-autonomous differences in genes regulating proliferation or apoptosis, but on the differential activation of immune cells.

5.2.1 In a model of sporadic intestinal carcinogenesis, Stat3 signaling does not control proliferation, but induction of apoptosis

In accordance with our previous findings, we noted an increase in epithelial cell apoptosis in our model of early tumor promotion during sporadic intestinal carcinogenesis. Interestingly, we could not demonstrate a significant regulation of the proteins presumably responsible for the induction of IEC apoptosis in our CAC model Bcl-x$_L$ or Hsp70, only Survivin showed a moderately decreased expression in our sporadic model. In sharp contrast to our data in the CAC model, we could not show any impact on IEC proliferation in our sporadic model. This constitutes an interesting finding as *APC^{Min/+}/IL6^{-/-}* show a reduction in tumor number and size (Baltgalvis et al., 2008). Curiously, tumors arising in *APC^{Min/+}/Stat3^{ΔIEC}* are supposed to show a higher proliferation rate as well as tumor invasiveness resulting in a reduced survival time in male mice, although a reduction in tumor number compared to *APC^{Min/+}* single mutant mice was observed. The authors of this publication claim that the increase in tumor proliferation and invasiveness is due to the loss of the cell adhesion protein Ceacam1 in *APC^{Min/+}/Stat3^{ΔIEC}* mice (Musteanu et al., 2009), which has been shown to modulate Wnt signaling (Leung et al., 2008). Interestingly, Leung and colleagues demonstrate as well an increase in tumor size and invasiveness in *APC^{1638N/+}/Ceacam^{-/-}* (as shown for the *APC^{Min/+}Stat3^{ΔIEC}*), but they as well show an increase in tumor number and do not observe changes in IEC proliferation, but account the changes in tumor size and number to a decrease in IEC specific apoptosis rate. Stunningly, in our hands *APC^{Min/+}/Stat3^{ΔIEC}* mice exhibited a significant increase in survival compared to *APC^{Min/+}* single mutant mice (data not shown). Our results exhibit only limited validity as we could only obtain a total of 8 *APC^{Min/+}/Stat3^{ΔIEC}* animals due to breeding problems of these mice, but still raises the questions for the reasons of these very contradictory findings. A possible explanation could be that the intestinal microflora has a deep impact on tumor formation and differs distinctly between the two animal facilities.

5.2.2 Survival advantages in β-cat$^{c.a}$Stat3$^{\Delta IEC}$ depend on activated immune cells

Although we observed a significant increases in apoptosis rate, we could not explain this by major changes in the expression of previously identified Stat3 target genes regulating cell survival in colonocytes during CAC. Therefore, we wished to further elucidate the mechanisms behind the increase in apoptosis and in survival observed in β-cat$^{c.a}$Stat3$^{\Delta IEC}$ animals. RNA microarray analysis revealed a significant upregulation in IFNγ induced genes and in genes involved in antigen presentation. An increase in the expression level of IFNγ and IL-6 could be verified by mRNA expression analysis of total tissue of β-cat$^{c.a}$Stat3$^{\Delta IEC}$ animals. IFNγ can be expressed by activated cytotoxic CD8$^+$, Th1-activated CD4$^+$ cells or natural killer cells (Bach et al., 1997; Young and Hardy, 1990). Recently, a secretion by antigen presenting cells has been described (Frucht et al., 2001). We could show that lack in IFNγ signaling reverses the survival advantage in β-cat$^{c.a}$Stat3$^{\Delta IEC}$ animals, although the animal number in this experiment was insufficient to draw a final conclusion out of it.

Of course, we wished to address which cell type is responsible for the expression of IFNγ in the lamina propria of β-cat$^{c.a}$Stat3$^{\Delta IEC}$ animals. We could show a high number of CD3$^+$ cells infiltrating the lamina propria as well as the villus epithelium of β-cat$^{c.a}$Stat3$^{\Delta IEC}$ animals. FACS analysis revealed a significant increase in IFNγ secretion by CD8$^+$ positive cells after stimulation in mesenteric lymph nodes of β-cat$^{c.a}$Stat3$^{\Delta IEC}$ on day 15. This hints at CD8$^+$ cells to be the main player in IFNγ expression, although in contrast to this, depletion of both CD4$^+$ as well as CD8$^+$ T-cells reverses the survival advantage observed in β-cat$^{c.a}$Stat3$^{\Delta IEC}$ animals. This finding can be interpreted in two ways: firstly, long-term administration of both antibodies also depletes the other cell type as both cell types arise from a common precursor which initially co-expresses CD4 and CD8 (Haynes et al., 1988), secondly, even if the CD8$^+$ cells are the effector cells responsible for IFNγ secretion, CD4$^+$ cells are needed for the efficient activation of CD8$^+$ cells. The immune response observed was also dependent on NK cells, as depletion of NK cells with a specific antibody also reverses the survival advantage. Curiously, depletion of NK cells in β-cat$^{c.a}$ single mutant mice leads to a prolongation of survival. This could hint towards a dual role for NK cells depending on their activation status as it has been described for macrophages (Mantovani et al., 2002) and neutrophils (Fridlender et al., 2009). NK and CD8$^+$ cells can either be directly activated by MHC class-I activation by epithelial cells (Huang et al., 2007b) or CD8$^+$ cells can be

activated via MHC class-I on professional antigen presenting cells and are capable of co-activating NK cells (Sabel et al., 2007). To check if the effect observed here depends on antigen presenting cells, we depleted CD11c$^+$ cells. CD11c is a marker for dendritic cells, the cell type believed to be the most potent antigen-presenting cell type. In this experiment we could as well show a reversal of the survival advantage.

Together these results imply that epithelial cell specific deletion of Stat3 in *β-cat$^{c.a}$* animals does not change cell-autonomously proliferation or apoptosis, as depletion of T-cells completely reverses the survival advantage, but leads to activation and recruitment of immune cells which secrete IFNγ. These activated immune cells - presumably mainly cytotoxic T-cells, although an equally important role for NK-cells and T-helper could not be ruled out by our experiments- then probably induce apoptosis in epithelial cells via direct killing of these. Interferons were initially described to be involved in defense against viral infections, but are now known to play additional roles in the immune response to bacterial infections and tumors. IFNγ has multiple functions, it is able to induce antigen presentation on MHC class-1 as well as MHC class-2, it induces the secretion of different other cytokines such as IL-12 to activate different immune cell subsets and possibly inhibits proliferation by suppression of c-Myc and induction of p21 and p27 expression (Schroder et al., 2004). Interestingly, in our model we were not able to show differences in epithelial cell proliferation despite the significant upregulation of IFNγ. Either the stabilization of the β-Catenin protein leads to such a dominant hyperproliferative response that the effect of IFNγ is insufficient to modulate epithelial cell proliferation or the level of IFNγ expression does not reach the threshold to modulate the proliferation rate.

5.2.3 Why does immune cell activation occur in *Stat3^{ΔIEC}* mice?

It has been reported that IL-10 knock-out animals exhibit a barrier defect which could lead to microbial translocation and activation of the immune system (Rennick et al., 1995), this could also hold true for animals lacking Stat3 in IEC. As the immune activation as well takes place to some extent in *Stat3^{ΔIEC}* animals, we sought to determine the time point of this activation and found a significant increase in IFNγ secretion by CD8$^+$ cells in MLN on day 6 after ablation of full-length *Stat3* gene by tamoxifen gavage. This effect vanished already on day 8 and was not observable on day 15 any more. We found an insignificant increase in CD11c$^+$ IL-12 producing cells at

this time point. Therefore we checked for the serum LPS levels on day 6 as a marker for an enhanced bacterial translocation across the epithelial barrier, but could not observe any increase in serum LPS-level. This finding argues against a barrier defect as the causing factor for the observed immune activation, on the other hand our experimental set-up could be too insensitive to show a minor barrier defect. Furthermore, ablation of Stat3 signaling in the colon carcinoma cell line CT26 has been shown to induce IL-6, IFN-β, IP10 and Rantes expression (Wang et al., 2004), which could have an activating function on the cells of the immune system. The authors of this publication could show that cell culture supernatants from B16 cells expressing a dominant negative form of Stat3 lead to an increase of IL-12 secretion by DC, and enhanced antigen presentation. In our model, we could not identify any significant regulation for IFN-β, IP10 and Rantes by mRNA analysis (data not shown), although we found IL-6 to be significantly upregulated in total tissue of β-cat$^{c.a}$Stat3$^{\Delta IEC}$ animals.

From our microarray data, we found several genes to be significantly upregulated in β-cat$^{c.a}$Stat3$^{\Delta IEC}$ animals. Among them was the gene encoding Mannose-binding lectin (Mbl2), a protein predominantly known for its role in the innate immune response by activating the complement system or acting as an opsonin (Anders et al., 1994; Ip et al., 2009). Over the past years, it has been shown that it can also target apoptotic cells for removal by phagocytic cells (Pittoni and Valesini, 2002), and this can lead especially in macrophages and DC to a secretion of pro-inflammatory cytokines by these cells *in vitro* (Nauta et al., 2004). As we could prove overexpression of Mbl2 in *Stat3*$^{\Delta IEC}$ and β-cat$^{c.a}$Stat3$^{\Delta IEC}$ animals, we hypothesized that this could lead to antigen presentation of epithelial antigen by DC in response to an apoptotic trigger. Furthermore, we thought that a short-lived apoptotic response could be induced by the sudden loss of full-length Stat3 protein. This could be verified on day 3 in *Stat3*$^{\Delta IEC}$ animals, 3 days before the observation of CD8$^+$ cell activation by FACS analysis.

Summing up, as a possible mechanism for the immune activation observed in *Stat3*$^{\Delta IEC}$ and β-cat$^{c.a}$Stat3$^{\Delta IEC}$ animals, as well as for the survival advantage in β-cat$^{c.a}$Stat3$^{\Delta IEC}$ animals, we propose that an early apoptotic trigger during our model constitutes an immunogenic event in these mice and leads to priming of immune cells. At later time points reactivation of these immune cells occurs leading to CD8$^+$ and NK-cell activation, IFNγ secretion and induction of apoptosis in epithelial cells.

5.2.4 What drives Stat3 signaling in this model?

Interestingly, in our sporadic model of intestinal carcinogenesis, $IL\text{-}6^{-/-}$ animals did not show any survival advantage compared to single mutant mice. This suggests that in this model, activation of the Stat3 signaling pathway is not driven by IL-6, on the contrary ablation of IL-6 signaling even leads to a small but significant reduction in survival. IL-6 plays an important regulatory role in the cells of the tumor microenvironment. It suppresses the *de novo* development of adaptive regulatory T-cells (Dominitzki et al., 2007) and is an important factor for the induction of Th17 cells (Bettelli et al., 2006), furthermore it represses dendritic cell maturation while enhancing monocyte differentiation towards the macrophage lineage (Gottfried et al., 2008) and is able to activate B-cell activity. Some of these functions could account for the reduction in survival in $\beta\text{-}cat^{c.a.}IL6^{-/-}$ animals. In the CAC model, crossing of the $gp^{130Y757F}$ to $IL6^{-/-}$ animals alone also did not significantly reduce hyperproliferation in response to DSS treatment, only double mutants for IL-6 and IL-11 receptor together showed a significant reduction in hyperproliferation. This could imply that Stat3 signaling in the β-Catenin mouse model of intestinal tumorigenesis is also activated by a mixture of different ligands in such a way that ablation of one of these ligands is not sufficient to significantly alter the degree of protein phosphorylation. The finding that $\beta\text{-}cat^{c.a.}Socs3^{\Delta IEC\text{-}}$ do not show any reduction in survival opposes this hypothesis and implies that Stat3 activation in this model does not occur via the gp130 receptor. Cytokines signaling independently of the gp130 receptor include IL-10 family cytokines as well as different growth factors, additionally the pathway can be activated by Src-family kinases (Yu et al., 2007) which are commonly hyperactivated in different cancers types, including colon cancer (Silva, 2004; Sirvent et al., 2010). Therefore other activating cytokines and growth factors such as EGF should be tested, if they hold responsible for the activation of the pathway in this model.

5.3 Stat3 signaling in IEC is a key factor in intestinal carcinogenesis

We could show that in IECs activation of the Stat3 signaling pathway is an important factor during carcinogenesis. In the CAC model, Stat3 mainly regulates cell survival and proliferation (Figure 5.2).
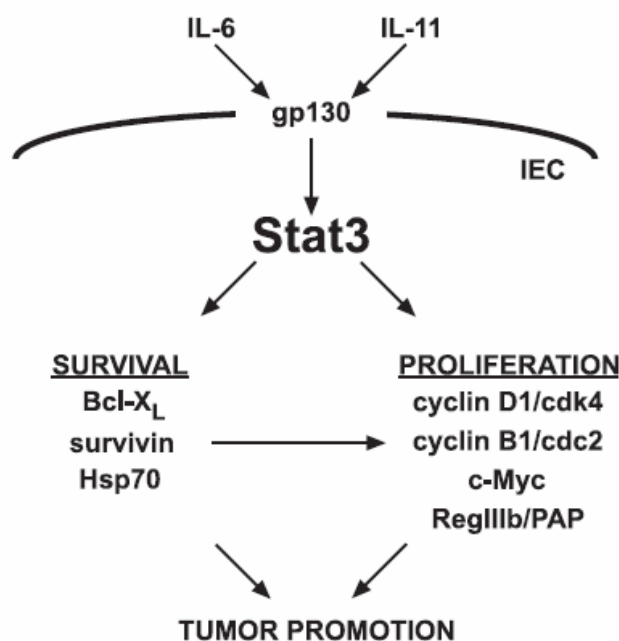

Figure 5.2.: IL-6 and IL-11 induced Stat3 activation controls cell survival and proliferation in IEC during CAC thereby modulating tumor promotion.

In our model of sporadic intestinal tumorigenesis, Stat3 ablation modified tumor development by a completely different mechanism. In this model of early tumor promotion, it seems that ablation of Stat3 signaling mainly leads to a prolongation in survival by inducing an anti-tumor immune response. This immune response is probably caused by an early apoptotic event leading to priming of immune cells with epithelial antigen and resulting in IFNγ secretion mainly by CD8$^+$ cells.

The reasons for these different findings in both models remain elusive. In both models tumor initiation occurs via activating mutations in the *Ctnnb* gene which leads to hyperactivation of the Wnt-signaling pathway. In our model of CAC, the mutations in the *Ctnnb* gene and other genes occur randomly, while the mutation in the sporadic model of one allele of the *Ctnnb* gene is well defined. One reason for the differences could be that our sporadic model constitutes an early model of tumor initiation. The step of tumor initiation was not found to be modulated in the CAC model. Animals in the sporadic model succumb within approximately 30 days, this pevents polyp formation

from taking place. In the β-Catenin model, initiated cells lead to an uncontrolled expansion of crypt cells. In the CAC model, adenomas have 12 weeks time to develop. Additionally, in our sporadic model every single cell carries the mutated protein leading to hyperproliferation. This probably distinctly changes the epithelial microenvironment. Furthermore, in the CAC model tumor formation occurs in the colon, while in the sporadic model hyperproliferation is mainly restricted to the proximal small intestine. On the other hand, $APC^{Min/+}/IL\text{-}6^{-/-}$ mice do show a reduction in epithelial proliferation and tumor number (Baltgalvis et al., 2008). This finding makes it unlikely that the mechanisms for tumor modulation in CAC and sporadic tumorigenesis are completely unrelated and implies that in a longer sporadic model Stat3 would as well modulate proliferation and apoptosis, our data derived from $APC^{Min/+}/Stat3^{\Delta IEC}$ support this hypothesis. The question if in the CAC model Stat3 ablation also leads to a hyperactivation of the immune system which would contribute to modulation of tumor development remains unanswered. An upregulation in IFNγ secretion in the lamina propria was not observed after short term treatment with DSS, this makes a distinct shift of the immune response towards IFNγ secretion unlikely. On the other hand, animals lacking Stat3 signaling do exhibit a higher and longer inflammatory response in the CAC model. Possibly the cytokine profile in the CAC model is already shaped in a very defined way leading to hyperactivation of all immune cell types, which could suppress T-cell activation by any other factor.

6. Summary

Inappropriate activation of Stat3 has been shown in a wide range of human cancers. Although no activating mutations could be identified for this gene, hyperactivation results from overproduction of activating cytokines and growth factors, such as IL-6, IL-11 and EGF. So far the importance of the activation of this signaling pathways during colorectal carcinogenesis has not been demonstrated. In order to analyze the role of Stat3 signaling during colorectal carcinogenesis, we employed two different mouse models and compared tumor growth and/or survival in wild-type mice and mice lacking Stat3 signaling specifically in intestinal epithelial cells (IEC).

In a mouse model of colitis-associated carcinogenesis comprising of mutagen injections (azoxymethane) followed by induction of chronic inflammation by administration of dextrane sodium sulfate (DSS) in the drinking water, the mice lacking Stat3 signaling in IEC were almost completely protected from tumor formation while wild-type mice developed 2-6 tumors in the distal colon. Consistently a distinct increase in tumor size and number could be observed in a gain-of-function model represented by mice carrying a mutated subunit of the cytokine receptor gp130 in all cell types which cannot bind the negative regulator Socs3 thus leading to hyperactivation of Stat3 and Stat1. We could show that during early tumor promotion Stat3 suppresses apoptosis by upregulation of the anti-apoptotic proteins Bcl-x_L, Survivin and Hsp70 in IEC. Furthermore, activation of epithelial Stat3 leads to an increase in IEC-proliferation by induction of cell cycle regulating genes encoding Cyclin D1, Cdk4, Cyclin B1 and Cdc2 and a downregulation of the Cdk inhibitor p21, as well as upregulation of regeneration-associated protein RegIIIb/PAP. These Stat3 mediated effects are triggered by both IL-6 and IL-11.

To assess the role of Stat3 signaling during sporadic colorectal carcinogenesis, we crossed $Stat3^{\Delta IEC}$ mice to mice carrying an inducible mutation of the $Ctnnb$ gene as a model for early tumor promotion during sporadic carcinogenesis. Expression of the truncated β-catenin protein in epithelial cells leads to hyperactivation and expansion of crypt stem cells. In this model ablation of Stat3 signaling mediated an increased survival compared to control animals which was accompanied by an increased IEC-apoptosis, although this increase in apoptosis could not be related to distinct expression changes in apoptosis regulating genes. Interestingly, in this model ablation of Stat3 signaling in IEC led to priming of immune cells and an anti-tumor immune response

driven by CD11c$^+$-, CD4$^+$, CD8$^+$- and natural killer cells. This activation of immune cells resulted in secretion of Interferon-γ and induction of IEC-apoptosis, thereby prolonging survival of these animals compared to control animals. Priming of immune cells presumably occurs by an early apoptotic event in IEC during the model in conjunction with the overexpression of the C-type lectin protein Mannose-binding lectin (Mbl2) in IEC of *Stat3^{ΔIEC}*-mice.

Collectively the results obtained here show that Stat3 represents an important regulatory pathway during initiation and tumor promotion steps during colorectal carcinogenesis.

7. References

A

Abraham, C. and Cho, J.H. (2009) Inflammatory bowel disease. *N Engl J Med*, **361**, 2066-2078.

Aggarwal, B.B., Kunnumakkara, A.B., Harikumar, K.B., Gupta, S.R., Tharakan, S.T., Koca, C., Dey, S. and Sung, B. (2009a) Signal transducer and activator of transcription-3, inflammation, and cancer: how intimate is the relationship? *Ann N Y Acad Sci*, **1171**, 59-76.

Aggarwal, B.B., Vijayalekshmi, R.V. and Sung, B. (2009b) Targeting inflammatory pathways for prevention and therapy of cancer: short-term friend, long-term foe. *Clin Cancer Res*, **15**, 425-430.

Algul, H., Treiber, M., Lesina, M., Nakhai, H., Saur, D., Geisler, F., Pfeifer, A., Paxian, S. and Schmid, R.M. (2007) Pancreas-specific RelA/p65 truncation increases susceptibility of acini to inflammation-associated cell death following cerulein pancreatitis. *J Clin Invest*, **117**, 1490-1501.

Alonzi, T., Newton, I.P., Bryce, P.J., Di Carlo, E., Lattanzio, G., Tripodi, M., Musiani, P. and Poli, V. (2004) Induced somatic inactivation of STAT3 in mice triggers the development of a fulminant form of enterocolitis. *Cytokine*, **26**, 45-56.

Altieri, D.C. (2008) Survivin, cancer networks and pathway-directed drug discovery. *Nat Rev Cancer*, **8**, 61-70.

Alvarez, J.V., Febbo, P.G., Ramaswamy, S., Loda, M., Richardson, A. and Frank, D.A. (2005) Identification of a genetic signature of activated signal transducer and activator of transcription 3 in human tumors. *Cancer Res*, **65**, 5054-5062.

Alvarez, J. V., and Frank, D. A. (2004). Genome-wide analysis of STAT target genes: elucidating the mechanism of STAT-mediated oncogenesis. *Cancer biology & therapy* **3**, 1045-1050.

Anders, E.M., Hartley, C.A., Reading, P.C. and Ezekowitz, R.A. (1994) Complement-dependent neutralization of influenza virus by a serum mannose-binding lectin. *J Gen Virol*, **75 (Pt 3)**, 615-622.

Arias, A.M., Brown, A.M. and Brennan, K. (1999) Wnt signalling: pathway or network? *Curr Opin Genet Dev*, **9**, 447-454.

Aust, D.E., Terdiman, J.P., Willenbucher, R.F., Chew, K., Ferrell, L., Florendo, C., Molinaro-Clark, A., Baretton, G.B., Lohrs, U. and Waldman, F.M. (2001) Altered distribution of beta-catenin, and its binding proteins E-cadherin and APC, in ulcerative colitis-related colorectal cancers. *Mod Pathol*, **14**, 29-39.

Axelrod, J.D., Miller, J.R., Shulman, J.M., Moon, R.T. and Perrimon, N. (1998) Differential recruitment of Dishevelled provides signaling specificity in the planar cell polarity and Wingless signaling pathways. *Genes Dev*, **12**, 2610-2622.

Aziz, M.H., Manoharan, H.T., Church, D.R., Dreckschmidt, N.E., Zhong, W., Oberley, T.D., Wilding, G. and Verma, A.K. (2007) Protein kinase Cepsilon interacts with signal transducers and activators of transcription 3 (Stat3), phosphorylates Stat3Ser727, and regulates its constitutive activation in prostate cancer. *Cancer Res*, **67**, 8828-8838.

_____

B

Bach, E.A., Aguet, M. and Schreiber, R.D. (1997) The IFN gamma receptor: a paradigm for cytokine receptor signaling. *Annu Rev Immunol*, **15**, 563-591.

Backstrom, E., Kristensson, K. and Ljunggren, H.G. (2004) Activation of natural killer cells: underlying molecular mechanisms revealed. *Scand J Immunol*, **60**, 14-22.

Balkwill, F. (2004) Cancer and the chemokine network. *Nat Rev Cancer*, **4**, 540-550.

Baltgalvis, K.A., Berger, F.G., Pena, M.M., Davis, J.M., Muga, S.J. and Carson, J.A. (2008) Interleukin-6 and cachexia in ApcMin/+ mice. *Am J Physiol Regul Integr Comp Physiol*, **294**, R393-401.

Baumgart, D.C. (2009) The diagnosis and treatment of Crohn's disease and ulcerative colitis. *Dtsch Arztebl Int*, **106**, 123-133.

Baumgart, D.C. and Carding, S.R. (2007) Inflammatory bowel disease: cause and immunobiology. *Lancet*, **369**, 1627-1640.

Becker, C., Fantini, M.C., Schramm, C., Lehr, H.A., Wirtz, S., Nikolaev, A., Burg, J., Strand, S., Kiesslich, R., Huber, S., Ito, H., Nishimoto, N., Yoshizaki, K., Kishimoto, T., Galle, P.R., Blessing, M., Rose-John, S. and Neurath, M.F. (2004) TGF-beta suppresses tumor progression in colon cancer by inhibition of IL-6 trans-signaling. *Immunity*, **21**, 491-501.

Behrens, J. (2005) The role of the Wnt signalling pathway in colorectal tumorigenesis. *Biochem Soc Trans*, **33**, 672-675.

Behrens, J., von Kries, J.P., Kuhl, M., Bruhn, L., Wedlich, D., Grosschedl, R. and Birchmeier, W. (1996) Functional interaction of beta-catenin with the transcription factor LEF-1. *Nature*, **382**, 638-642.

Berg, D.J., Davidson, N., Kuhn, R., Muller, W., Menon, S., Holland, G., Thompson-Snipes, L., Leach, M.W. and Rennick, D. (1996) Enterocolitis and colon cancer in interleukin-10-deficient mice are associated with aberrant cytokine production and CD4(+) TH1-like responses. *J Clin Invest*, **98**, 1010-1020.

Bettelli, E., Carrier, Y., Gao, W., Korn, T., Strom, T.B., Oukka, M., Weiner, H.L. and Kuchroo, V.K. (2006) Reciprocal developmental pathways for the generation of pathogenic effector TH17 and regulatory T cells. *Nature*, **441**, 235-238.

Bollrath, J., and Greten, F. R. (2009). IKK/NF-kappaB and STAT3 pathways: central signalling hubs in inflammation-mediated tumour promotion and metastasis. *EMBO reports* **10**, 1314-1319.

Bowman, T., Broome, M.A., Sinibaldi, D., Wharton, W., Pledger, W.J., Sedivy, J.M., Irby, R., Yeatman, T., Courtneidge, S.A. and Jove, R. (2001) Stat3-mediated Myc expression is required for Src transformation and PDGF-induced mitogenesis. *Proc Natl Acad Sci U S A*, **98**, 7319-7324.

Brand, S. (2009) Crohn's disease: Th1, Th17 or both? The change of a paradigm: new immunological and genetic insights implicate Th17 cells in the pathogenesis of Crohn's disease. *Gut*, **58**, 1152-1167.

Bromberg, J.F., Wrzeszczynska, M.H., Devgan, G., Zhao, Y., Pestell, R.G., Albanese, C. and Darnell, J.E., Jr. (1999) Stat3 as an oncogene. *Cell*, **98**, 295-303.

_____

C

Cao, G., Ma, J., Zhang, Y., Liu, B. and Li, F. (2009) Pancreatitis-associated protein is related closely to neoplastic proliferative activity in patients with colorectal carcinoma. *Anat Rec (Hoboken)*, **292**, 249-253.

Center, M.M., Jemal, A., Smith, R.A. and Ward, E. (2009) Worldwide variations in colorectal cancer. *CA Cancer J Clin*, **59**, 366-378.

Chan, C.W. and Housseau, F. (2008) The 'kiss of death' by dendritic cells to cancer cells. *Cell Death Differ*, **15**, 58-69.

Chao, C. and Hellmich, M.R. (2010) Gastrin, inflammation, and carcinogenesis. *Curr Opin Endocrinol Diabetes Obes*, **17**, 33-39.

Chaput, N., Conforti, R., Viaud, S., Spatz, A. and Zitvogel, L. (2008) The Janus face of dendritic cells in cancer. *Oncogene*, **27**, 5920-5931.

Chomarat, P., Banchereau, J., Davoust, J. and Palucka, A.K. (2000) IL-6 switches the differentiation of monocytes from dendritic cells to macrophages. *Nat Immunol*, **1**, 510-514.

Chu, F.F., Esworthy, R.S., Chu, P.G., Longmate, J.A., Huycke, M.M., Wilczynski, S. and Doroshow, J.H. (2004) Bacteria-induced intestinal cancer in mice with disrupted Gpx1 and Gpx2 genes. *Cancer Res*, **64**, 962-968.

Chung, Y.C. and Chang, Y.F. (2003) Serum interleukin-6 levels reflect the disease status of colorectal cancer. *J Surg Oncol*, **83**, 222-226.

Clapper, M.L., Cooper, H.S. and Chang, W.C. (2007) Dextran sulfate sodium-induced colitis-associated neoplasia: a promising model for the development of chemopreventive interventions. *Acta Pharmacol Sin*, **28**, 1450-1459.

Closa, D., Motoo, Y. and Iovanna, J.L. (2007) Pancreatitis-associated protein: from a lectin to an anti-inflammatory cytokine. *World J Gastroenterol*, **13**, 170-174.

Colotta, F., Allavena, P., Sica, A., Garlanda, C. and Mantovani, A. (2009) Cancer-related inflammation, the seventh hallmark of cancer: links to genetic instability. *Carcinogenesis*, **30**, 1073-1081.

D

Dalton, D.K., Pitts-Meek, S., Keshav, S., Figari, I.S., Bradley, A. and Stewart, T.A. (1993) Multiple defects of immune cell function in mice with disrupted interferon-gamma genes. *Science*, **259**, 1739-1742.

de Visser, K.E., Eichten, A. and Coussens, L.M. (2006) Paradoxical roles of the immune system during cancer development. *Nat Rev Cancer*, **6**, 24-37.

Dechow, T.N., Pedranzini, L., Leitch, A., Leslie, K., Gerald, W.L., Linkov, I. and Bromberg, J.F. (2004) Requirement of matrix metalloproteinase-9 for the transformation of human mammary epithelial cells by Stat3-C. *Proc Natl Acad Sci U S A*, **101**, 10602-10607.

Deng, L., Zhou, J.F., Sellers, R.S., Li, J.F., Nguyen, A.V., Wang, Y., Orlofsky, A., Liu, Q., Hume, D.A., Pollard, J.W., Augenlicht, L. and Lin, E.Y. (2010) A novel mouse model of inflammatory bowel disease links mammalian target of rapamycin-dependent hyperproliferation of colonic epithelium to inflammation-associated tumorigenesis. *Am J Pathol*, **176**, 952-967.

Dominitzki, S., Fantini, M.C., Neufert, C., Nikolaev, A., Galle, P.R., Scheller, J., Monteleone, G., Rose-John, S., Neurath, M.F. and Becker, C. (2007) Cutting edge: trans-signaling via the soluble IL-6R abrogates the induction of FoxP3 in naive CD4+CD25 T cells. *J Immunol*, **179**, 2041-2045.

E

Eaden, J.A., Abrams, K.R. and Mayberry, J.F. (2001) The risk of colorectal cancer in ulcerative colitis: a meta-analysis. *Gut*, **48**, 526-535.

Eckmann, L., Nebelsiek, T., Fingerle, A.A., Dann, S.M., Mages, J., Lang, R., Robine, S., Kagnoff, M.F., Schmid, R.M., Karin, M., Arkan, M.C. and Greten, F.R. (2008) Opposing functions of IKKbeta during acute and chronic intestinal inflammation. *Proc Natl Acad Sci U S A*, **105**, 15058-15063.

el Marjou, F., Janssen, K.P., Chang, B.H., Li, M., Hindie, V., Chan, L., Louvard, D., Chambon, P., Metzger, D. and Robine, S. (2004) Tissue-specific and inducible Cre-mediated recombination in the gut epithelium. *Genesis*, **39**, 186-193.

Ernst, M., Najdovska, M., Grail, D., Lundgren-May, T., Buchert, M., Tye, H., Matthews, V.B., Armes, J., Bhathal, P.S., Hughes, N.R., Marcusson, E.G., Karras, J.G., Na, S., Sedgwick, J.D., Hertzog, P.J. and Jenkins, B.J. (2008) STAT3 and STAT1 mediate IL-11-dependent and inflammation-associated gastric tumorigenesis in gp130 receptor mutant mice. *J Clin Invest*, **118**, 1727-1738.

F

Fielding, C.A., McLoughlin, R.M., McLeod, L., Colmont, C.S., Najdovska, M., Grail, D., Ernst, M., Jones, S.A., Topley, N. and Jenkins, B.J. (2008) IL-6 regulates neutrophil trafficking during acute inflammation via STAT3. *J Immunol*, **181**, 2189-2195.

Frank, D.A. (2007) STAT3 as a central mediator of neoplastic cellular transformation. *Cancer Lett*, **251**, 199-210.

Franke, A., Balschun, T., Sina, C., Ellinghaus, D., Hasler, R., Mayr, G., Albrecht, M., Wittig, M., Buchert, E., Nikolaus, S.*, et al.* (2010) Genome-wide association study for ulcerative colitis identifies risk loci at 7q22 and 22q13 (IL17REL). *Nature genetics* **42**, 292-294.

Fridlender, Z.G., Sun, J., Kim, S., Kapoor, V., Cheng, G., Ling, L., Worthen, G.S. and Albelda, S.M. (2009) Polarization of tumor-associated neutrophil phenotype by TGF-beta: "N1" versus "N2" TAN. *Cancer Cell*, **16**, 183-194.

Frucht, D.M., Fukao, T., Bogdan, C., Schindler, H., O'Shea, J.J. and Koyasu, S. (2001) IFN-gamma production by antigen-presenting cells: mechanisms emerge. *Trends Immunol*, **22**, 556-560.

Fujii, S., Fujimori, T. and Kashida, H. (2002) Ulcerative colitis-associated neoplasia. *Pathol Int*, **52**, 195-203.

Fujino, S., Andoh, A., Bamba, S., Ogawa, A., Hata, K., Araki, Y., Bamba, T. and Fujiyama, Y. (2003) Increased expression of interleukin 17 in inflammatory bowel disease. *Gut*, **52**, 65-70.

Funayama, N., Fagotto, F., McCrea, P. and Gumbiner, B.M. (1995) Embryonic axis induction by the armadillo repeat domain of beta-catenin: evidence for intracellular signaling. *J Cell Biol*, **128**, 959-968.

_____

G

Galm, O., Yoshikawa, H., Esteller, M., Osieka, R. and Herman, J.G. (2003) SOCS-1, a negative regulator of cytokine signaling, is frequently silenced by methylation in multiple myeloma. *Blood*, **101**, 2784-2788.

Garcia, R., Bowman, T.L., Niu, G., Yu, H., Minton, S., Muro-Cacho, C.A., Cox, C.E., Falcone, R., Fairclough, R., Parsons, S., Laudano, A., Gazit, A., Levitzki, A., Kraker, A. and Jove, R. (2001) Constitutive activation of Stat3 by the Src and JAK tyrosine kinases participates in growth regulation of human breast carcinoma cells. *Oncogene*, **20**, 2499-2513.

Gijsbers, K., Gouwy, M., Struyf, S., Wuyts, A., Proost, P., Opdenakker, G., Penninckx, F., Ectors, N., Geboes, K. and Van Damme, J. (2005) GCP-2/CXCL6 synergizes with other endothelial cell-derived chemokines in neutrophil mobilization and is associated with angiogenesis in gastrointestinal tumors. *Exp Cell Res*, **303**, 331-342.

Gironella, M., Iovanna, J.L., Sans, M., Gil, F., Penalva, M., Closa, D., Miquel, R., Pique, J.M. and Panes, J. (2005) Anti-inflammatory effects of pancreatitis associated protein in inflammatory bowel disease. *Gut*, **54**, 1244-1253.

Gottfried, E., Kreutz, M. and Mackensen, A. (2008) Tumor-induced modulation of dendritic cell function. *Cytokine Growth Factor Rev*, **19**, 65-77.

Greenwald, B.D., Harpaz, N., Yin, J., Huang, Y., Tong, Y., Brown, V.L., McDaniel, T., Newkirk, C., Resau, J.H. and Meltzer, S.J. (1992) Loss of heterozygosity affecting the p53, Rb, and mcc/apc tumor suppressor gene loci in dysplastic and cancerous ulcerative colitis. *Cancer Res*, **52**, 741-745.

Greten, F.R., Eckmann, L., Greten, T.F., Park, J.M., Li, Z.W., Egan, L.J., Kagnoff, M.F. and Karin, M. (2004) IKKbeta links inflammation and tumorigenesis in a mouse model of colitis-associated cancer. *Cell*, **118**, 285-296.

Grivennikov, S., Karin, E., Terzic, J., Mucida, D., Yu, G.Y., Vallabhapurapu, S., Scheller, J., Rose-John, S., Cheroutre, H., Eckmann, L. and Karin, M. (2009) IL-6 and Stat3 are required for survival of intestinal epithelial cells and development of colitis-associated cancer. *Cancer Cell*, **15**, 103-113.

Grivennikov, S.I., Greten, F.R. and Karin, M. (2010) Immunity, inflammation, and cancer. *Cell*, **140**, 883-899.

Groner, B., Lucks, P. and Borghouts, C. (2008) The function of Stat3 in tumor cells and their microenvironment. *Semin Cell Dev Biol*, **19**, 341-350.

H

Hanahan, D. and Weinberg, R.A. (2000) The hallmarks of cancer. *Cell*, **100**, 57-70.

Harada, N., Tamai, Y., Ishikawa, T., Sauer, B., Takaku, K., Oshima, M. and Taketo, M.M. (1999) Intestinal polyposis in mice with a dominant stable mutation of the beta-catenin gene. *Embo J*, **18**, 5931-5942.

Haybaeck, J., Zeller, N., Wolf, M.J., Weber, A., Wagner, U., Kurrer, M.O., Bremer, J., Iezzi, G., Graf, R., Clavien, P.A., Thimme, R., Blum, H., Nedospasov, S.A., Zatloukal, K., Ramzan, M., Ciesek, S., Pietschmann, T., Marche, P.N., Karin, M., Kopf, M., Browning, J.L., Aguzzi, A. and Heikenwalder, M. (2009) A lymphotoxin-driven pathway to hepatocellular carcinoma. *Cancer Cell*, **16**, 295-308.

Haynes, B.F., Martin, M.E., Kay, H.H. and Kurtzberg, J. (1988) Early events in human T cell ontogeny. Phenotypic characterization and immunohistologic localization of T cell precursors in early human fetal tissues. *J Exp Med*, **168**, 1061-1080.

He, B., You, L., Uematsu, K., Zang, K., Xu, Z., Lee, A.Y., Costello, J.F., McCormick, F. and Jablons, D.M. (2003) SOCS-3 is frequently silenced by hypermethylation and suppresses cell growth in human lung cancer. *Proc Natl Acad Sci U S A*, **100**, 14133-14138.

Heinrich, P.C., Behrmann, I., Haan, S., Hermanns, H.M., Muller-Newen, G. and Schaper, F. (2003) Principles of interleukin (IL)-6-type cytokine signalling and its regulation. *Biochem J*, **374**, 1-20.

Hinoi, T., Akyol, A., Theisen, B.K., Ferguson, D.O., Greenson, J.K., Williams, B.O., Cho, K.R. and Fearon, E.R. (2007) Mouse model of colonic adenoma-carcinoma progression based on somatic Apc inactivation. *Cancer Res*, **67**, 9721-9730.

Hosui, A., Ohkawa, K., Ishida, H., Sato, A., Nakanishi, F., Ueda, K., Takehara, T., Kasahara, A., Sasaki, Y., Hori, M. and Hayashi, N. (2003) Hepatitis C virus core protein differently regulates the JAK-STAT signaling pathway under interleukin-6 and interferon-gamma stimuli. *J Biol Chem*, **278**, 28562-28571.

Huang, J., Edwards, L.J., Evavold, B.D. and Zhu, C. (2007a) Kinetics of MHC-CD8 interaction at the T cell membrane. *J Immunol*, **179**, 7653-7662.

Huang, Y., Shah, S. and Qiao, L. (2007b) Tumor resistance to CD8+ T cell-based therapeutic vaccination. *Arch Immunol Ther Exp (Warsz)*, **55**, 205-217.

I

Ilaria, R.L., Jr. and Van Etten, R.A. (1996) P210 and P190(BCR/ABL) induce the tyrosine phosphorylation and DNA binding activity of multiple specific STAT family members. *J Biol Chem*, **271**, 31704-31710.

Iovanna, J., Orelle, B., Keim, V. and Dagorn, J.C. (1991) Messenger RNA sequence and expression of rat pancreatitis-associated protein, a lectin-related protein overexpressed during acute experimental pancreatitis. *J Biol Chem*, **266**, 24664-24669.

Ip, W.K., Takahashi, K., Ezekowitz, R.A. and Stuart, L.M. (2009) Mannose-binding lectin and innate immunity. *Immunol Rev*, **230**, 9-21.

Itzkowitz, S.H. and Yio, X. (2004) Inflammation and cancer IV. Colorectal cancer in inflammatory bowel disease: the role of inflammation. *Am J Physiol Gastrointest Liver Physiol*, **287**, G7-17.

J

Jain, N., Zhang, T., Kee, W.H., Li, W. and Cao, X. (1999) Protein kinase C delta associates with and phosphorylates Stat3 in an interleukin-6-dependent manner. *J Biol Chem*, **274**, 24392-24400.

Janssen, E.M., Lemmens, E.E., Gour, N., Reboulet, R.A., Green, D.R., Schoenberger, S.P. and Pinkoski, M.J. (2010) Distinct roles of cytolytic effector molecules for antigen-restricted killing by CTL in vivo. *Immunol Cell Biol*.

Jemal, A., Siegel, R., Ward, E., Hao, Y., Xu, J. and Thun, M.J. (2009) Cancer statistics, 2009. *CA Cancer J Clin*, **59**, 225-249.

_____

Jenkins, B.J., Grail, D., Nheu, T., Najdovska, M., Wang, B., Waring, P., Inglese, M., McLoughlin, R.M., Jones, S.A., Topley, N., Baumann, H., Judd, L.M., Giraud, A.S., Boussioutas, A., Zhu, H.J. and Ernst, M. (2005) Hyperactivation of Stat3 in gp130 mutant mice promotes gastric hyperproliferation and desensitizes TGF-beta signaling. *Nat Med*, **11**, 845-852.

Jones, S.A., Horiuchi, S., Topley, N., Yamamoto, N. and Fuller, G.M. (2001) The soluble interleukin 6 receptor: mechanisms of production and implications in disease. *Faseb J*, **15**, 43-58.

Jung, S., Unutmaz, D., Wong, P., Sano, G., De los Santos, K., Sparwasser, T., Wu, S., Vuthoori, S., Ko, K., Zavala, F., Pamer, E.G., Littman, D.R. and Lang, R.A. (2002) In vivo depletion of CD11c(+) dendritic cells abrogates priming of CD8(+) T cells by exogenous cell-associated antigens. *Immunity*, **17**, 211-220.

K

Karin, M. and Greten, F.R. (2005) NF-kappaB: linking inflammation and immunity to cancer development and progression. *Nat Rev Immunol*, **5**, 749-759.

Kiuchi, N., Nakajima, K., Ichiba, M., Fukada, T., Narimatsu, M., Mizuno, K., Hibi, M. and Hirano, T. (1999) STAT3 is required for the gp130-mediated full activation of the c-myc gene. *J Exp Med*, **189**, 63-73.

Kobayashi, T., Okamoto, S., Hisamatsu, T., Kamada, N., Chinen, H., Saito, R., Kitazume, M.T., Nakazawa, A., Sugita, A., Koganei, K., Isobe, K. and Hibi, T. (2008) IL23 differentially regulates the Th1/Th17 balance in ulcerative colitis and Crohn's disease. *Gut*, **57**, 1682-1689.

Kolligs, F.T., Bommer, G. and Goke, B. (2002) Wnt/beta-catenin/tcf signaling: a critical pathway in gastrointestinal tumorigenesis. *Digestion*, **66**, 131-144.

Kopf, M., Baumann, H., Freer, G., Freudenberg, M., Lamers, M., Kishimoto, T., Zinkernagel, R., Bluethmann, H. and Kohler, G. (1994) Impaired immune and acute-phase responses in interleukin-6-deficient mice. *Nature*, **368**, 339-342.

Kortylewski, M., Xin, H., Kujawski, M., Lee, H., Liu, Y., Harris, T., Drake, C., Pardoll, D. and Yu, H. (2009) Regulation of the IL-23 and IL-12 balance by Stat3 signaling in the tumor microenvironment. *Cancer Cell*, **15**, 114-123.

Kuhn, R., Lohler, J., Rennick, D., Rajewsky, K. and Muller, W. (1993) Interleukin-10-deficient mice develop chronic enterocolitis. *Cell*, **75**, 263-274.

L

Lang, R., Pauleau, A.L., Parganas, E., Takahashi, Y., Mages, J., Ihle, J.N., Rutschman, R. and Murray, P.J. (2003) SOCS3 regulates the plasticity of gp130 signaling. *Nat Immunol*, **4**, 546-550.

Lee, J.S., Ishimoto, A. and Yanagawa, S. (1999) Characterization of mouse dishevelled (Dvl) proteins in Wnt/Wingless signaling pathway. *J Biol Chem*, **274**, 21464-21470.

Leung, N., Turbide, C., Balachandra, B., Marcus, V. and Beauchemin, N. (2008) Intestinal tumor progression is promoted by decreased apoptosis and dysregulated Wnt signaling in Ceacam1-/- mice. *Oncogene*, **27**, 4943-4953.

Li, F., Ambrosini, G., Chu, E.Y., Plescia, J., Tognin, S., Marchisio, P.C. and Altieri, D.C. (1998) Control of apoptosis and mitotic spindle checkpoint by survivin. *Nature*, **396**, 580-584.

_____

Lin, W.W. and Karin, M. (2007) A cytokine-mediated link between innate immunity, inflammation, and cancer. *J Clin Invest*, **117**, 1175-1183.

Liu, T., Zhang, M., Zhang, H., Sun, C. and Deng, Y. (2008) Inhibitory effects of cucurbitacin B on laryngeal squamous cell carcinoma. *Eur Arch Otorhinolaryngol*, **265**, 1225-1232.

M

Macadam, R.C., Sarela, A.I., Farmery, S.M., Robinson, P.A., Markham, A.F. and Guillou, P.J. (2000) Death from early colorectal cancer is predicted by the presence of transcripts of the REG gene family. *Br J Cancer*, **83**, 188-195.

Madison, B.B., Dunbar, L., Qiao, X.T., Braunstein, K., Braunstein, E. and Gumucio, D.L. (2002) Cis elements of the villin gene control expression in restricted domains of the vertical (crypt) and horizontal (duodenum, cecum) axes of the intestine. *J Biol Chem*, **277**, 33275-33283.

Mantovani, A., Schioppa, T., Porta, C., Allavena, P. and Sica, A. (2006) Role of tumor-associated macrophages in tumor progression and invasion. *Cancer Metastasis Rev*, **25**, 315-322.

Mantovani, A., Sozzani, S., Locati, M., Allavena, P. and Sica, A. (2002) Macrophage polarization: tumor-associated macrophages as a paradigm for polarized M2 mononuclear phagocytes. *Trends Immunol*, **23**, 549-555.

Masuda, M., Suzui, M., Yasumatu, R., Nakashima, T., Kuratomi, Y., Azuma, K., Tomita, K., Komiyama, S. and Weinstein, I.B. (2002) Constitutive activation of signal transducers and activators of transcription 3 correlates with cyclin D1 overexpression and may provide a novel prognostic marker in head and neck squamous cell carcinoma. *Cancer Res*, **62**, 3351-3355.

Melillo, J.A., Song, L., Bhagat, G., Blazquez, A.B., Plumlee, C.R., Lee, C., Berin, C., Reizis, B. and Schindler, C. (2010) Dendritic cell (DC)-specific targeting reveals Stat3 as a negative regulator of DC function. *J Immunol*, **184**, 2638-2645.

Mirabelli-Primdahl, L., Gryfe, R., Kim, H., Millar, A., Luceri, C., Dale, D., Holowaty, E., Bapat, B., Gallinger, S. and Redston, M. (1999) Beta-catenin mutations are specific for colorectal carcinomas with microsatellite instability but occur in endometrial carcinomas irrespective of mutator pathway. *Cancer Res*, **59**, 3346-3351.

Mitsuyama, K., Sata, M. and Rose-John, S. (2006) Interleukin-6 trans-signaling in inflammatory bowel disease. *Cytokine Growth Factor Rev*, **17**, 451-461.

Moolenbeek, C., and Ruitenberg, E. J. (1981). The "Swiss roll": a simple technique for histological studies of the rodent intestine. *Laboratory animals* **15**, 57-59.

Murdoch, C., Muthana, M., Coffelt, S.B. and Lewis, C.E. (2008) The role of myeloid cells in the promotion of tumour angiogenesis. *Nat Rev Cancer*, **8**, 618-631.

Musteanu, M., Blaas, L., Mair, M., Schlederer, M., Bilban, M., Tauber, S., Esterbauer, H., Mueller, M., Casanova, E., Kenner, L., Poli, V. and Eferl, R. (2010) Stat3 is a negative regulator of intestinal tumor progression in Apc(Min) mice. *Gastroenterology*, **138**, 1003-1011 e1001-1005.

_____

N

Naugler, W.E. and Karin, M. (2008) The wolf in sheep's clothing: the role of interleukin-6 in immunity, inflammation and cancer. *Trends Mol Med*, **14**, 109-119.

Naugler, W.E., Sakurai, T., Kim, S., Maeda, S., Kim, K., Elsharkawy, A.M. and Karin, M. (2007) Gender disparity in liver cancer due to sex differences in MyD88-dependent IL-6 production. *Science*, **317**, 121-124.

Nauta, A.J., Castellano, G., Xu, W., Woltman, A.M., Borrias, M.C., Daha, M.R., van Kooten, C. and Roos, A. (2004) Opsonization with C1q and mannose-binding lectin targets apoptotic cells to dendritic cells. *J Immunol*, **173**, 3044-3050.

Neurath, M.F. and Finotto, S. (2009) Translating inflammatory bowel disease research into clinical medicine. *Immunity*, **31**, 357-361.

Nishihara, M., Ogura, H., Ueda, N., Tsuruoka, M., Kitabayashi, C., Tsuji, F., Aono, H., Ishihara, K., Huseby, E., Betz, U.A., Murakami, M. and Hirano, T. (2007) IL-6-gp130-STAT3 in T cells directs the development of IL-17+ Th with a minimum effect on that of Treg in the steady state. *Int Immunol*, **19**, 695-702.

Niu, G., Wright, K.L., Huang, M., Song, L., Haura, E., Turkson, J., Zhang, S., Wang, T., Sinibaldi, D., Coppola, D., Heller, R., Ellis, L.M., Karras, J., Bromberg, J., Pardoll, D., Jove, R. and Yu, H. (2002) Constitutive Stat3 activity up-regulates VEGF expression and tumor angiogenesis. *Oncogene*, **21**, 2000-2008.

O

O'Connor, D.S., Grossman, D., Plescia, J., Li, F., Zhang, H., Villa, A., Tognin, S., Marchisio, P.C. and Altieri, D.C. (2000) Regulation of apoptosis at cell division by p34cdc2 phosphorylation of survivin. *Proc Natl Acad Sci U S A*, **97**, 13103-13107.

Oshima, H., Oshima, M., Kobayashi, M., Tsutsumi, M. and Taketo, M.M. (1997) Morphological and molecular processes of polyp formation in Apc(delta716) knockout mice. *Cancer Res*, **57**, 1644-1649.

Ostman, A. and Augsten, M. (2009) Cancer-associated fibroblasts and tumor growth--bystanders turning into key players. *Curr Opin Genet Dev*, **19**, 67-73.

P

Park, E.J., Lee, J.H., Yu, G.Y., He, G., Ali, S.R., Holzer, R.G., Osterreicher, C.H., Takahashi, H. and Karin, M. (2010) Dietary and genetic obesity promote liver inflammation and tumorigenesis by enhancing IL-6 and TNF expression. *Cell*, **140**, 197-208.

Pickert, G., Neufert, C., Leppkes, M., Zheng, Y., Wittkopf, N., Warntjen, M., Lehr, H.A., Hirth, S., Weigmann, B., Wirtz, S., Ouyang, W., Neurath, M.F. and Becker, C. (2009) STAT3 links IL-22 signaling in intestinal epithelial cells to mucosal wound healing. *J Exp Med*, **206**, 1465-1472.

Pikarsky, E., Porat, R.M., Stein, I., Abramovitch, R., Amit, S., Kasem, S., Gutkovich-Pyest, E., Urieli-Shoval, S., Galun, E. and Ben-Neriah, Y. (2004) NF-kappaB functions as a tumour promoter in inflammation-associated cancer. *Nature*, **431**, 461-466.

Pittoni, V. and Valesini, G. (2002) The clearance of apoptotic cells: implications for autoimmunity. *Autoimmun Rev*, **1**, 154-161.

Polakis, P. (2000) Wnt signaling and cancer. *Genes Dev*, **14**, 1837-1851.

Pollard, J.W. (2004) Tumour-educated macrophages promote tumour progression and metastasis. *Nat Rev Cancer*, **4**, 71-78.

_____

Powell, S.M., Zilz, N., Beazer-Barclay, Y., Bryan, T.M., Hamilton, S.R., Thibodeau, S.N., Vogelstein, B. and Kinzler, K.W. (1992) APC mutations occur early during colorectal tumorigenesis. *Nature*, **359**, 235-237.

Purdy, A.K. and Campbell, K.S. (2009) Natural killer cells and cancer: regulation by the killer cell Ig-like receptors (KIR). *Cancer Biol Ther*, **8**, 2211-2220.

R

Radaeva, S., Sun, R., Pan, H.N., Hong, F. and Gao, B. (2004) Interleukin 22 (IL-22) plays a protective role in T cell-mediated murine hepatitis: IL-22 is a survival factor for hepatocytes via STAT3 activation. *Hepatology*, **39**, 1332-1342.

Rakoff-Nahoum, S. and Medzhitov, R. (2007) Regulation of spontaneous intestinal tumorigenesis through the adaptor protein MyD88. *Science*, **317**, 124-127.

Rebouissou, S., Amessou, M., Couchy, G., Poussin, K., Imbeaud, S., Pilati, C., Izard, T., Balabaud, C., Bioulac-Sage, P. and Zucman-Rossi, J. (2009) Frequent in-frame somatic deletions activate gp130 in inflammatory hepatocellular tumours. *Nature*, **457**, 200-204.

Rennick, D., Davidson, N. and Berg, D. (1995) Interleukin-10 gene knock-out mice: a model of chronic inflammation. *Clin Immunol Immunopathol*, **76**, S174-178.

Rigby, R.J., Simmons, J.G., Greenhalgh, C.J., Alexander, W.S. and Lund, P.K. (2007) Suppressor of cytokine signaling 3 (SOCS3) limits damage-induced crypt hyper-proliferation and inflammation-associated tumorigenesis in the colon. *Oncogene*, **26**, 4833-4841.

Rodel, F., Hoffmann, J., Distel, L., Herrmann, M., Noisternig, T., Papadopoulos, T., Sauer, R. and Rodel, C. (2005) Survivin as a radioresistance factor, and prognostic and therapeutic target for radiotherapy in rectal cancer. *Cancer Res*, **65**, 4881-4887.

S

Sabel, M.S., Arora, A., Su, G., Mathiowitz, E., Reineke, J.J. and Chang, A.E. (2007) Synergistic effect of intratumoral IL-12 and TNF-alpha microspheres: systemic anti-tumor immunity is mediated by both CD8+ CTL and NK cells. *Surgery*, **142**, 749-760.

Sansom, O.J., Meniel, V.S., Muncan, V., Phesse, T.J., Wilkins, J.A., Reed, K.R., Vass, J.K., Athineos, D., Clevers, H. and Clarke, A.R. (2007) Myc deletion rescues Apc deficiency in the small intestine. *Nature*, **446**, 676-679.

Schaper, F., Gendo, C., Eck, M., Schmitz, J., Grimm, C., Anhuf, D., Kerr, I.M. and Heinrich, P.C. (1998) Activation of the protein tyrosine phosphatase SHP2 via the interleukin-6 signal transducing receptor protein gp130 requires tyrosine kinase Jak1 and limits acute-phase protein expression. *Biochem J*, **335 (Pt 3)**, 557-565.

Schroder, K., Hertzog, P.J., Ravasi, T. and Hume, D.A. (2004) Interferon-gamma: an overview of signals, mechanisms and functions. *J Leukoc Biol*, **75**, 163-189.

Schutte, K., Bornschein, J. and Malfertheiner, P. (2009) Hepatocellular carcinoma--epidemiological trends and risk factors. *Dig Dis*, **27**, 80-92.

Seidelin, J.B., Bjerrum, J.T., Coskun, M., Widjaya, B., Vainer, B. and Nielsen, O.H.(2010) IL-33 is upregulated in colonocytes of ulcerative colitis. *Immunol Lett*, **128**, 80-85.

Sica, A., Allavena, P. and Mantovani, A. (2008) Cancer related inflammation: the macrophage connection. *Cancer Lett*, **267**, 204-215.

Sikora, A. and Grzesiuk, E. (2007) Heat shock response in gastrointestinal tract. *J Physiol Pharmacol*, **58 Suppl 3**, 43-62.

Silva, C.M. (2004) Role of STATs as downstream signal transducers in Src family kinase-mediated tumorigenesis. *Oncogene*, **23**, 8017-8023.

Silzle, T., Randolph, G.J., Kreutz, M. and Kunz-Schughart, L.A. (2004) The fibroblast: sentinel cell and local immune modulator in tumor tissue. *Int J Cancer*, **108**, 173-180.

Sinibaldi, D., Wharton, W., Turkson, J., Bowman, T., Pledger, W.J. and Jove, R. (2000) Induction of p21WAF1/CIP1 and cyclin D1 expression by the Src oncoprotein in mouse fibroblasts: role of activated STAT3 signaling. *Oncogene*, **19**, 5419-5427.

Sirvent, A., Benistant, C., Pannequin, J., Veracini, L., Simon, V., Bourgaux, J.F., Hollande, F., Cruzalegui, F. and Roche, S.(2010) Src family tyrosine kinases-driven colon cancer cell invasion is induced by Csk membrane delocalization. *Oncogene*, **29**, 1303-1315.

Siveen, K.S. and Kuttan, G. (2009) Role of macrophages in tumour progression. *Immunol Lett*, **123**, 97-102.

Smits, R., Kartheuser, A., Jagmohan-Changur, S., Leblanc, V., Breukel, C., de Vries, A., van Kranen, H., van Krieken, J.H., Williamson, S., Edelmann, W., Kucherlapati, R., KhanPm and Fodde, R. (1997) Loss of Apc and the entire chromosome 18 but absence of mutations at the Ras and Tp53 genes in intestinal tumors from Apc1638N, a mouse model for Apc-driven carcinogenesis. *Carcinogenesis*, **18**, 321-327.

Solinas, G., Germano, G., Mantovani, A. and Allavena, P. (2009) Tumor-associated macrophages (TAM) as major players of the cancer-related inflammation. *J Leukoc Biol*, **86**, 1065-1073.

Spaeth, E.L., Dembinski, J.L., Sasser, A.K., Watson, K., Klopp, A., Hall, B., Andreeff, M. and Marini, F. (2009) Mesenchymal stem cell transition to tumor-associated fibroblasts contributes to fibrovascular network expansion and tumor progression. *PLoS One*, **4**, e4992.

Stassen, M., Fondel, S., Bopp, T., Richter, C., Muller, C., Kubach, J., Becker, C., Knop, J., Enk, A.H., Schmitt, S., Schmitt, E. and Jonuleit, H. (2004) Human CD25+ regulatory T cells: two subsets defined by the integrins alpha 4 beta 7 or alpha 4 beta 1 confer distinct suppressive properties upon CD4+ T helper cells. *Eur J Immunol*, **34**, 1303-1311.

Steinbrink, K., Jonuleit, H., Muller, G., Schuler, G., Knop, J. and Enk, A.H. (1999) Interleukin-10-treated human dendritic cells induce a melanoma-antigen-specific anergy in CD8(+) T cells resulting in a failure to lyse tumor cells. *Blood*, **93**, 1634-1642.

Strober, W., Kitani, A., Fuss, I., Asano, N., and Watanabe, T. (2008). The molecular basis of NOD2 susceptibility mutations in Crohn's disease. *Mucosal immunology* **1 Suppl 1**, S5-9.

Su, Y., Li, G., Zhang, X., Gu, J., Zhang, C., Tian, Z. and Zhang, J. (2008) JSI-124 inhibits glioblastoma multiforme cell proliferation through G(2)/M cell cycle arrest and apoptosis augment. *Cancer Biol Ther*, **7**, 1243-1249.

_____

T

Taieb, J., Chaput, N., Menard, C., Apetoh, L., Ullrich, E., Bonmort, M., Pequignot, M., Casares, N., Terme, M., Flament, C., Opolon, P., Lecluse, Y., Metivier, D., Tomasello, E., Vivier, E., Ghiringhelli, F., Martin, F., Klatzmann, D., Poynard, T., Tursz, T., Raposo, G., Yagita, H., Ryffel, B., Kroemer, G. and Zitvogel, L. (2006) A novel dendritic cell subset involved in tumor immunosurveillance. *Nat Med*, **12**, 214-219.

Takeda, K., Clausen, B.E., Kaisho, T., Tsujimura, T., Terada, N., Forster, I. and Akira, S. (1999) Enhanced Th1 activity and development of chronic enterocolitis in mice devoid of Stat3 in macrophages and neutrophils. *Immunity*, **10**, 39-49.

Takeda, K., Kaisho, T., Yoshida, N., Takeda, J., Kishimoto, T. and Akira, S. (1998) Stat3 activation is responsible for IL-6-dependent T cell proliferation through preventing apoptosis: generation and characterization of T cell-specific Stat3-deficient mice. *J Immunol*, **161**, 4652-4660.

Taketo, M.M. and Edelmann, W. (2009) Mouse models of colon cancer. *Gastroenterology*, **136**, 780-798.

Tanaka, K., Namba, T., Arai, Y., Fujimoto, M., Adachi, H., Sobue, G., Takeuchi, K., Nakai, A. and Mizushima, T. (2007) Genetic evidence for a protective role for heat shock factor 1 and heat shock protein 70 against colitis. *J Biol Chem*, **282**, 23240-23252.

Tazzyman, S., Lewis, C.E. and Murdoch, C. (2009) Neutrophils: key mediators of tumour angiogenesis. *Int J Exp Pathol*, **90**, 222-231.

te Velde, A.A., de Kort, F., Sterrenburg, E., Pronk, I., ten Kate, F.J., Hommes, D.W. and van Deventer, S.J. (2007) Comparative analysis of colonic gene expression of three experimental colitis models mimicking inflammatory bowel disease. *Inflamm Bowel Dis*, **13**, 325-330.

Tebbutt, N.C., Giraud, A.S., Inglese, M., Jenkins, B., Waring, P., Clay, F.J., Malki, S., Alderman, B.M., Grail, D., Hollande, F., Heath, J.K. and Ernst, M. (2002) Reciprocal regulation of gastrointestinal homeostasis by SHP2 and STAT-mediated trefoil gene activation in gp130 mutant mice. *Nat Med*, **8**, 1089-1097.

Trimboli, A.J., Cantemir-Stone, C.Z., Li, F., Wallace, J.A., Merchant, A., Creasap, N., Thompson, J.C., Caserta, E., Wang, H., Chong, J.L., Naidu, S., Wei, G., Sharma, S.M., Stephens, J.A., Fernandez, S.A., Gurcan, M.N., Weinstein, M.B., Barsky, S.H., Yee, L., Rosol, T.J., Stromberg, P.C., Robinson, M.L., Pepin, F., Hallett, M., Park, M., Ostrowski, M.C. and Leone, G. (2009) Pten in stromal fibroblasts suppresses mammary epithelial tumours. *Nature*, **461**, 1084-1091.

Tsujino, T., Seshimo, I., Yamamoto, H., Ngan, C.Y., Ezumi, K., Takemasa, I., Ikeda, M., Sekimoto, M., Matsuura, N. and Monden, M. (2007) Stromal myofibroblasts predict disease recurrence for colorectal cancer. *Clin Cancer Res*, **13**, 2082-2090.

U

Ullrich, E., Menard, C., Flament, C., Terme, M., Mignot, G., Bonmort, M., Plumas, J., Chaperot, L., Chaput, N. and Zitvogel, L. (2008) Dendritic cells and innate defense against tumor cells. *Cytokine Growth Factor Rev*, **19**, 79-92.

V

Van Limbergen, J., Wilson, D.C. and Satsangi, J. (2009) The genetics of Crohn's disease. *Annu Rev Genomics Hum Genet*, **10**, 89-116.

Vogelstein, B., Fearon, E.R., Hamilton, S.R., Kern, S.E., Preisinger, A.C., Leppert, M., Nakamura, Y., White, R., Smits, A.M. and Bos, J.L. (1988) Genetic alterations during colorectal-tumor development. *N Engl J Med*, **319**, 525-532.

W

Wan, Y.Y. and Flavell, R.A. (2009) How diverse--CD4 effector T cells and their functions. *J Mol Cell Biol*, **1**, 20-36.

Wang, L., Yi, T., Kortylewski, M., Pardoll, D.M., Zeng, D. and Yu, H. (2009) IL-17 can promote tumor growth through an IL-6-Stat3 signaling pathway. *J Exp Med*, **206**, 1457-1464.

Wang, T., Niu, G., Kortylewski, M., Burdelya, L., Shain, K., Zhang, S., Bhattacharya, R., Gabrilovich, D., Heller, R., Coppola, D., Dalton, W., Jove, R., Pardoll, D. and Yu, H. (2004) Regulation of the innate and adaptive immune responses by Stat-3 signaling in tumor cells. *Nat Med*, **10**, 48-54.

Wegenka, U.M., Buschmann, J., Lutticken, C., Heinrich, P.C. and Horn, F. (1993) Acute-phase response factor, a nuclear factor binding to acute-phase response elements, is rapidly activated by interleukin-6 at the posttranslational level. *Mol Cell Biol*, **13**, 276-288.

Weiner, H.L. (2001) Induction and mechanism of action of transforming growth factor-beta-secreting Th3 regulatory cells. *Immunol Rev*, **182**, 207-214.

Willert, K. and Nusse, R. (1998) Beta-catenin: a key mediator of Wnt signaling. *Curr Opin Genet Dev*, **8**, 95-102.

Wislez, M., Philippe, C., Antoine, M., Rabbe, N., Moreau, J., Bellocq, A., Mayaud, C., Milleron, B., Soler, P. and Cadranel, J. (2004) Upregulation of bronchioloalveolar carcinoma-derived C-X-C chemokines by tumor infiltrating inflammatory cells. *Inflamm Res*, **53**, 4-12.

Wu, S., Rhee, K.J., Albesiano, E., Rabizadeh, S., Wu, X., Yen, H.R., Huso, D.L., Brancati, F.L., Wick, E., McAllister, F., Housseau, F., Pardoll, D.M. and Sears, C.L. (2009) A human colonic commensal promotes colon tumorigenesis via activation of T helper type 17 T cell responses. *Nat Med*, **15**, 1016-1022.

X

Xie, K. (2001) Interleukin-8 and human cancer biology. *Cytokine Growth Factor Rev*, **12**, 375-391.

Xie, T.X., Wei, D., Liu, M., Gao, A.C., Ali-Osman, F., Sawaya, R. and Huang, S. (2004) Stat3 activation regulates the expression of matrix metalloproteinase-2 and tumor invasion and metastasis. *Oncogene*, **23**, 3550-3560.

Y

Yasukawa, H., Ohishi, M., Mori, H., Murakami, M., Chinen, T., Aki, D., Hanada, T., Takeda, K., Akira, S., Hoshijima, M., Hirano, T., Chien, K.R. and Yoshimura, A. (2003) IL-6 induces an anti-inflammatory response in the absence of SOCS3 in macrophages. *Nat Immunol*, **4**, 551-556.

Yokogami, K., Wakisaka, S., Avruch, J. and Reeves, S.A. (2000) Serine phosphorylation and maximal activation of STAT3 during CNTF signaling is mediated by the rapamycin target mTOR. *Curr Biol*, **10**, 47-50.

Yoshikawa, H., Matsubara, K., Qian, G.S., Jackson, P., Groopman, J.D., Manning, J.E., Harris, C.C. and Herman, J.G. (2001) SOCS-1, a negative regulator of the JAK/STAT pathway, is silenced by methylation in human hepatocellular carcinoma and shows growth-suppression activity. *Nat Genet*, **28**, 29-35.

Young, H.A. and Hardy, K.J. (1990) Interferon-gamma: producer cells, activation stimuli, and molecular genetic regulation. *Pharmacol Ther*, **45**, 137-151.

Yu, C.L., Meyer, D.J., Campbell, G.S., Larner, A.C., Carter-Su, C., Schwartz, J. and Jove, R. (1995) Enhanced DNA-binding activity of a Stat3-related protein in cells transformed by the Src oncoprotein. *Science*, **269**, 81-83.

Yu, D., Berlin, J.A., Penning, T.M. and Field, J. (2002) Reactive oxygen species generated by PAH o-quinones cause change-in-function mutations in p53. *Chem Res Toxicol*, **15**, 832-842.

Yu, H. and Jove, R. (2004) The STATs of cancer--new molecular targets come of age. *Nat Rev Cancer*, **4**, 97-105.

Yu, H., Kortylewski, M. and Pardoll, D. (2007) Crosstalk between cancer and immune cells: role of STAT3 in the tumour microenvironment. *Nat Rev Immunol*, **7**, 41-51.

Z

Zhong, Z., Wen, Z. and Darnell, J.E., Jr. (1994) Stat3: a STAT family member activated by tyrosine phosphorylation in response to epidermal growth factor and interleukin-6. *Science*, **264**, 95-98.

8. Abbreviations

AOM	azoxymethane
APC	adenomatous polyposis coli
Bcl	B cell lymphoma
BrdU	bromodesoxyuridine
CAC	colitis-associated carcinogenesis
CCL	chemokine ligand C-C motif
CD	Crohn's disease
CD	cluster of differentiation
CIN	chromosomal instability
CK	cytokeratin
CNTF	ciliary neutrophic factor
CRC	colorectal cancer
CTL	cytotoxic T-lymphocytes
CXCL	chemokine ligand C-X-C motif
DAPI	4',6-diamidino-2-phenylindole
DC	dendritic cell
DNA	deoxyribonucleic acid
dNTP	deoxynucleotide triphosphate
DSS	dextrane sulfate sodium
DTR	diphtheria toxin receptor
ECM	extra-cellular matrix
EGF	endothelial growth factor
FACS	fluorescence activated cell sorting
FAP	familial adenomatous polyposis
FCS	fetal calf serum
FGF	fibroblast growth factor
Gpx	glutathione peroxidase
gp130	glycoprotein 130
h	hour
H&E	haematoxylin & eosin
HCC	hepatocellular carinogenesis
HGF	hepatocyte growth factor
HNPCC	hereditary nonpolyposis colorectal cancer
HRP	horseradish peroxidase
K-RAS	Kirsten-Ras

IBD	inflammatory bowel disease
IEC	intestinal epithelial cell
IFN	interferon
IHC	immunohistochemistry
IKK	I kappa B kinase
IL	interleukin
i.p.	intra-peritoneal
Jak	janus-associated kinase
LIF	leukemia inhibitory factor
Mcl-1	myeloid cell leukemia sequence 1
MHC	major histocompatibility complex
min	minute
MMP	matrix-metalloproteinase
MMR	mismatch repair
MSI	microsatellite instability
Myd88	myeloid differentiation primary response gene 88
NF-κB	nuclear factor kappa B
NK	natural killer
OSM	oncostatin M
PBS	phosphate buffered saline
PCR	polymerase chain reaction
PDGF	platelet derived growth factor
PFA	paraformaldehyde
PIAS	protein inhibitor of activated Stat3
RNA	ribonucleic acid
s	second
SDS	sodium dodecyl sulfate
SEM	standard error of the mean
SH2	src-homology 2
Socs	suppressor of cytokine signaling
Src	sarcoma kinase
Stat	signal transducer and activator of transcription
TAM	tumor associated macrophages
TGF	transforming growth factor
Th	T helper
TIMP	tissue inhibitors of metalloproteinase
TLR	toll-like receptor
TNF	tumor necrosis factor
TRAIL	TNF related apoptosis induced ligand
TUNEL	TdT-mediated dUTP-biotin nick end labeling

UC	ulcerative colitis
UV	ultra-violett
VEGF	vascular endothelial growth factor
Wnt	mouse homolog of wingless